ANALYSIS AND SYNTHESIS OF PARALLEL MANIPULATORS

A Thesis Submitted to
the Graduate School of Engineering and Sciences of
İzmir Institute of Technology
in Partial Fulfillment of the Requirements for the Degree of

DOCTOR OF PHILOSOPHY

in Mechanical Engineering

by
Fatih Cemal CAN

December 2008
İZMİR

We approve the thesis of **Fatih Cemal CAN**

_____

Prof. Dr. Tech. Sci. Rasim ALİZADE
Supervisor

_____

Prof. Dr. Math. Sci. Refail ALİZADE
Committee Member

_____

Prof. Dr. Hira KARAGÜLLE
Committee Member

_____

Assoc. Prof. Dr. Bülent YARDIMOĞLU
Committee Member

_____

Asst. Prof. Dr. H. Seçil ALTUNDAĞ ARTEM
Committee Member

15 December 2008

_____   _____
Assoc. Prof. Dr. Metin TANOĞLU   **Prof. Dr. Hasan BÖKE**
Head of Mechanical Engineering Department   Dean of the Graduate of School of
                                                              Engineering and Science

ACKNOWLEDGEMENTS

ABSTRACT

ANALYSIS AND SYNTHESIS OF PARALLEL MANIPULATORS

In this study, novel parallel manipulators are introduced for industrial and medical applications. New methods are developed for the structural synthesis of Euclidean platform robot-manipulators with variable general constraints (EPRM). New mechanical structures such as serial, parallel and serial-parallel EPRM are designed along with proposed method. A new dimensional synthesis method of two DoF planar and spherical seven link mechanisms is presented. Interpolation and least square approximations are used to design the mechanism. In the solution of dimensional synthesis problems, nonlinear equations are converted to system of linear equations. The motion generation problem of a 3 DoF platform robot manipulator is solved for three, four and five precision poses. It is shown that the synthesis problem can be solved analytically for three prescribed poses. However, the solution is achieved by using a numerical method for four and five poses. The result, which is obtained from three prescribed poses, is used as an initial guess for four and five poses. Kinematic analysis of the manipulators is investigated. After the derivation of vector-loop equations, inverse and direct position analyses of the manipulators are presented. Constant orientation workspace of a three DoF spatial parallel manipulator is presented. The mechanical elements which are necessary for the construction of manipulators are introduced. The information about the motors which is needed for actuation of manipulators is given. Three DoF parallel manipulator is constructed for a industrial packaging system. Assembly of manufactured parts and mechanical elements are shown.

ÖZET

PARALEL MANİPÜLATÖRLERİN ANALİZİ VE SENTEZİ

Bu çalışmada, yeni paralel manipülatörler endüstriyel ve sağlık alanındaki uygulamalar için sunulmuştur. Genel değişken kısıtlamalı Euclidean platform robot-manipulatörlerin (EPRM) yapısal sentezi için yeni metodlar geliştirilmiştir. Seri, paralel ve seri-paralel EPRM olmak üzere yeni mekanik yapılar önerilen metodla tasarlanmıştır. İki serbestlik dereceli düzlemsel ve küresel yedi link mekanizmalarının yeni bir boyutsal sentez metodu sunulmuştur. Mekanizmayı dizayn etmek için interpolasyon ve en küçük kare yaklaşımları kullanılmıştır. Problemlerin çözümünde doğrusal olmayan denklemler doğrusal denklemlere dönüştürülmüştür. Üç serbestlik dereceli bir uzaysal robot manipülatörün haraket üretim problemi üç, dört ve beş hassas pozlar için çözülmüştür. Tanımlanmış üç poz için sentez probleminin analitik olarak çözülebildiği gösterilmiştir. Fakat, dört ve beş pozları için çözüme numerik bir metod kullanılarak ulaşılmıştır. Üç poz için elde edilen sonuçlar dört ve beş pozları için başlangıç tahminleri olarak kullanılmıştır. Manipulatörlerin kinematik analizi incelenemiştir. Vektör-kapanım denklemlerinin türetilmesinden sonra manipülatörlerin doğru ve ters pozisyon analizleri sunulmuştur. Üç serbestlik dereceli bir uzaysal manipülatörün sabit oryantasyon çalışma alanı sunulmuştur. Manipülatörlerin yapımı için gerekli olan makina elemanları tanıtılmıştır. Manipülatörlerin hareketi için ihtiyaç duyulan motorlar hakkında bilgi verilmiştir. Bir endüstriyel paketleme sistemi için üç serbestlik dereceli paralel manipulator yapılmıştır. Üretilen parçaların ve mekanik parçaların montajı gösterilmiştir.

To My Parents and My Sisters

TABLE OF CONTENTS

LIST OF FIGURES

LIST OF TABLES

CHAPTER I

INTRODUCTION

A parallel manipulator consists of a moving platform that is connected to the base by several legs. Another definition is given by (Merlet 2006): a generalized parallel manipulator is a closed-loop kinematic chain mechanism whose end-effector is linked to the base by several independent kinematic chains. Parallel manipulators are sometimes called platform manipulators. They have specific advantages against to serial manipulators. The most important advantage is that parallel manipulators can carry heavy loads due to the fact that they have several legs which shares external loads. Another one is that parallel manipulators can work very precisely. In industry and scientific facilities, parallel manipulators are widely used for different areas such as flight simulations, earthquake simulations, high speed and high precision machining center, pointing devices, medical applications, mining machines, walking machines, adjustable articulated trusses and etc.

Application is vital in every problem of every engineering discipline. Therefore, we firstly review parallel manipulators with respect to their applications.

1.1 Classification of parallel manipulators

- **Parallel manipulators are used as simulators**.

Patent of the first flight simulator shown in Figure 1.1 was granted by Klaus Cappel in 1964. When the patent was filed, Mr. Cappel was unaware of Gough's invention (or of Stewart's paper which was not yet published). Three rotations and three translations are sufficient to simulate a flying object in space. In order to describe these motions, six legs constructed by pneumatic cylinders are used in Gough platform. Furthermore, one of the earthquake simulators is constructed by creating novel mechanical architecture (Cassino Parallel manipulator Figure 1.2.a). A single platform connected to base with three identical legs is utilized to describe vibration of the ground of real world. Another example of

earthquake simulator is investigated in Laboratory in University of Nevada. The shake table is given to this kind of parallel manipulators. (Figure 1.2.b)
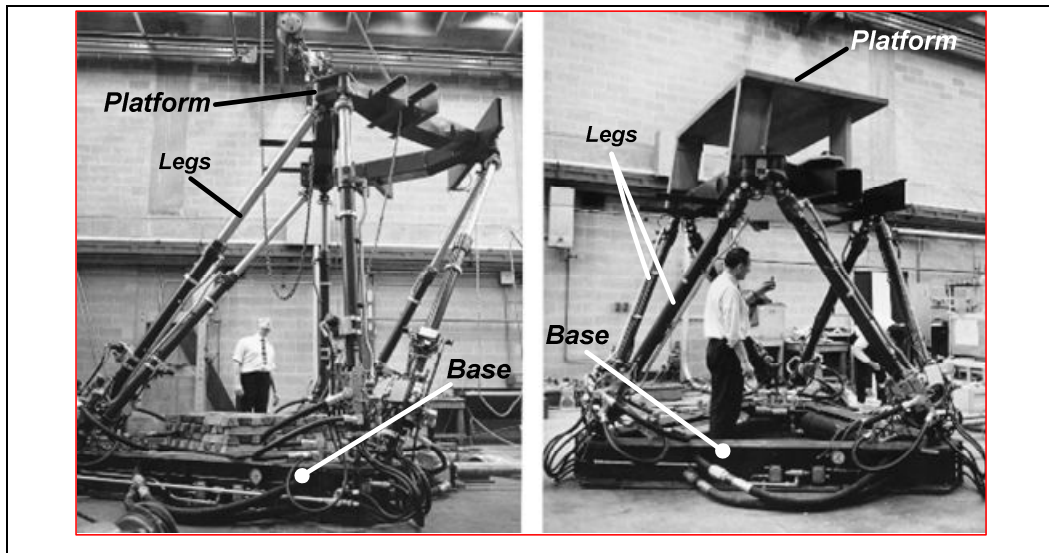
Figure 1.1. The first flight simulator based on an octahedral hexapod as in the mid 1960s
(Source: courtesy of Klaus Cappel)
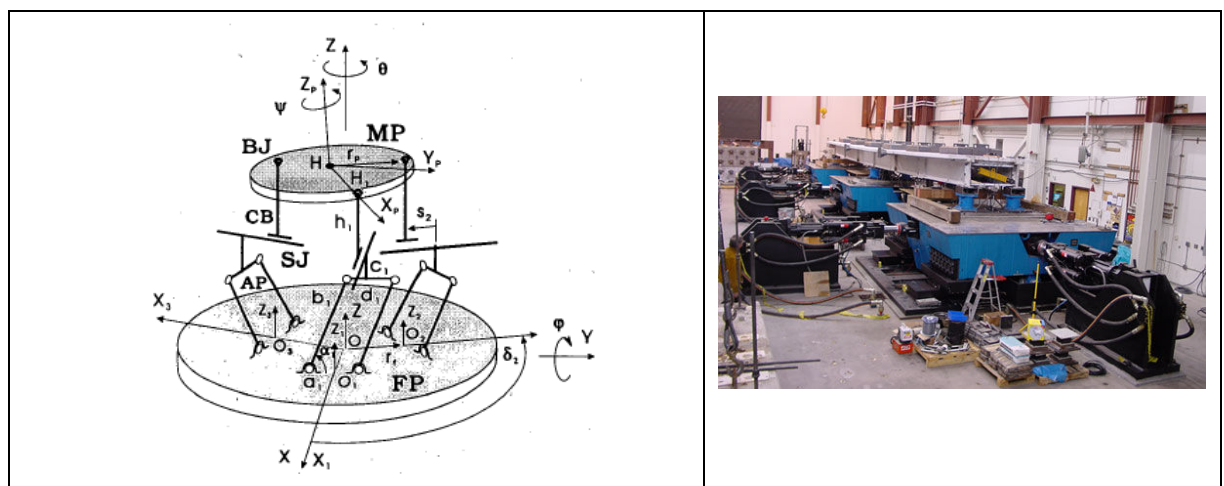
Figure 1.2. Earthquake simulations (a) Cassino Parallel Manipulator (Source: Ceccarelli et. al., 2002), (b) The multiple shake table in University of Nevada (Source: Labortary in University of Nevada 2008)

- **Parallel manipulators are used as medical devices**.

Parallel manipulators are becoming increasingly popular in medical area due to their precision and high stiffness. As a result, there are several companies producing robotic devices in medical market. One product is microdex alpha prototype shown in Figure 1.3. Some special operations such as brain tumors, certain aneurysms, cervical spine problems require high precision. Therefore, the high precision and user friendly mechanical systems have to be developed both for doctor and patient. This kind of manipulators are fully controlled by a doctor to help surgery process. But, development in artificial intelligence can make these systems fully autonomous in the future.

Figure 1.3. MicroDex Alpha Prototype
(Source: Advanced Robotics for Medicine and Industry 2008)

Another product, Mazor shown in Figure 1.4, is manufactured to make the surgical environment safer and more accurate. The system includes both open and close kinematic chain. A serial manipulator is placed on a known parallel mechanical structure. The prototype robot, shown in Figure 1.5, has been constructed for testing in medical tasks such as manipulating a laparoscope and an orthroscope in Orthroscopic knee surgery.

Figure 1.4. Cutting-edge technology to the development of SmartAssist (Mazor)

(Source: SmartAssist 2008)
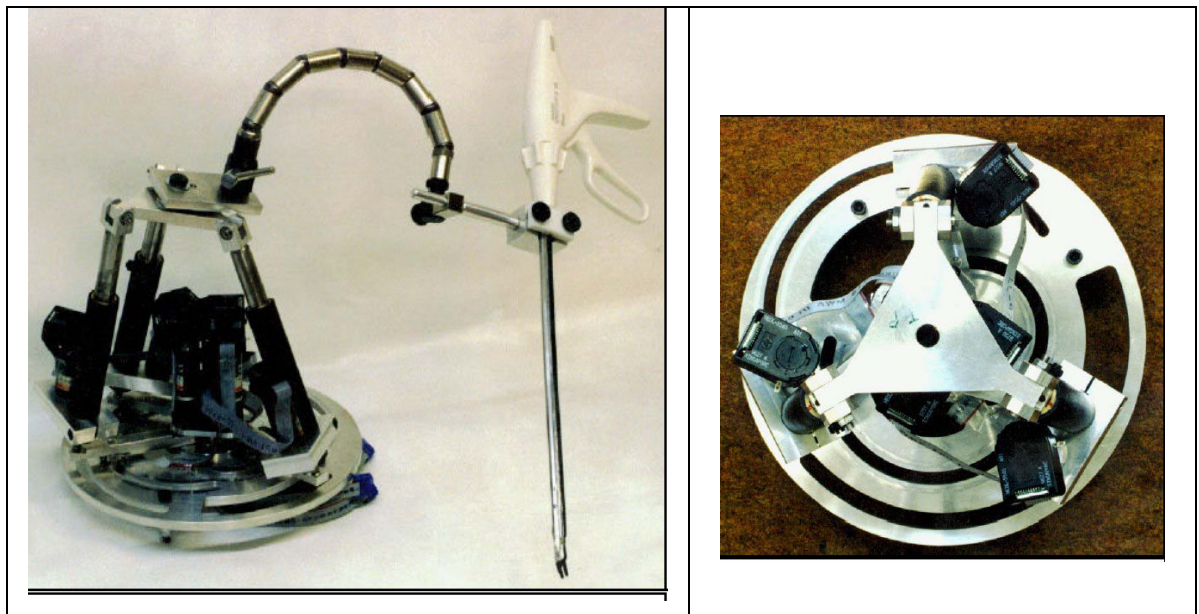
Figure 1.5. The prototype robot for Orthroscopic knee surgery,

(Source: Master Study of Nabil Simaan 1999)

Parallel manipulators are used not only in surgery but also in scanning operations. Headfix is one example of these scanning machines (Figure 1.6). This system is specifically designed to overcome the drawbacks of conventional invasive fixation and non-invasive thermoplastic masks. Surgiscope is created for scanning brain or neurology in medical area (Figure 1.7). The structure is constructed on three identical limbs to create necessary motions. As seen from figure, camera is placed on the moving platform and manipulator is mounted downward.

Figure 1.6. HeadFIX
(Source: Medical Intelligence 2008)
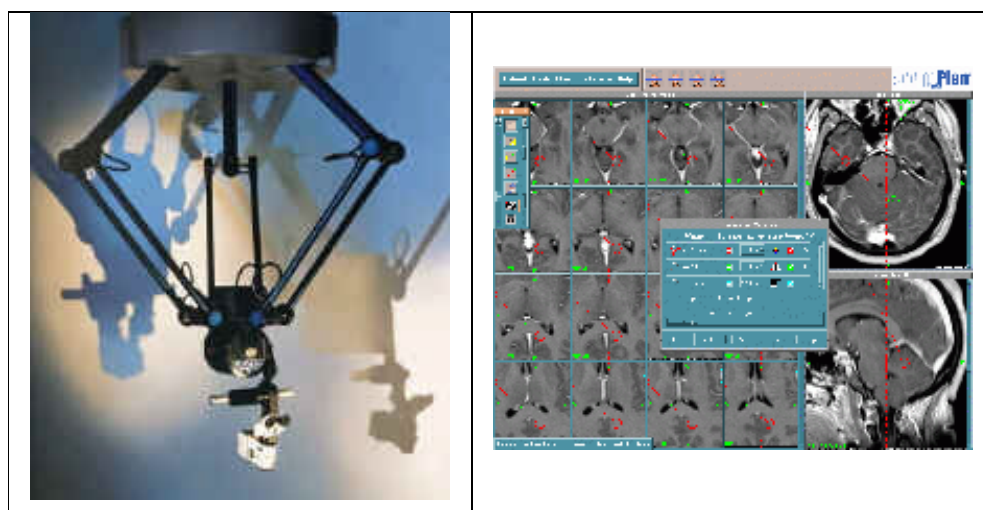
Figure 1.7. The SurgiScope® is a ceiling mounted robotized tool-holder device
(Source: iSiS 2008)

- **Parallel manipulators are used as machine tools**.

A three DoF parallel manipulator has been developed to measure the quality of the manufactured parts of a machine. (Figure 1.8)
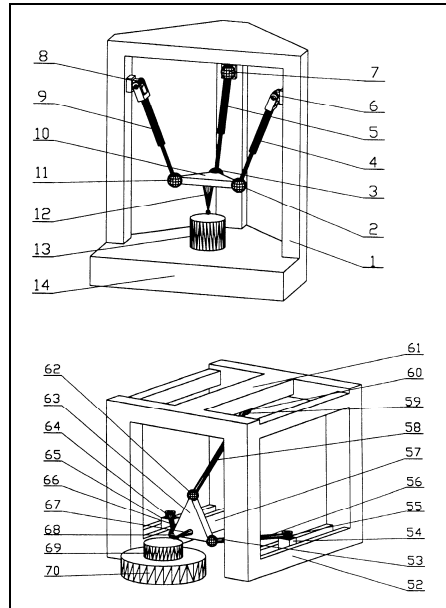
Figure 1.8. Parallel structure of a spatial 3-axis machine tool with three degrees-of-freedom.(Source: United States Patent No 6575676)

Main studies on parallel manipulators can be ordered as follows,

- Structural Synthesis: Structural synthesis is to create open and closed chains for new mechanical architectures. Number of joints, type of joints and classification of manipulator are determined by knowing DoF, shape of platform and number of legs, branch loops and number of hinges. Different structures can be obtained by using exchangeability of kinematic pairs. For instance, three intersecting revolute joints can be represented by a spherical pair.

6

- Dimensional Synthesis: The geometric dimension of the known structures is designed for the desired motion of the gripper. Objective function is defined by representing closure equations of manipulator geometry. There are three common tasks in dimensional synthesis: function generation, path generation and motion generation.

- Kinematic Analysis: Structure and geometric shape of parallel manipulator must be known in order to perform kinematic analysis. Two possible analyses are inverse and forward analyses. One investigates position of end effector with known joint variables in forward analysis. But, joint variables are calculated by knowing position of end effector. Forward analysis is harder than inverse analysis for a parallel manipulator. Kinematic analysis of a mechanism-manipulator includes position, velocity and acceleration analyses, respectively.

- Dynamic Synthesis: Objective of dynamical synthesis is to make shaking force and moments zero or as near as possible to zero. In most cases, making shaking force and moment zero is impossible but decreasing shaking force and moment is very good for manipulator service life. In order to reach this objective, mass and mass moment of inertia of the manipulator's links should be designed.

- Dynamical Analysis: Performing dynamical analysis is only possible after completing mentioned synthesis and kinematic analysis. Reaction and actuator forces can be calculated by writing necessary Newton-Euler equations. Lagrange equation of motion is another method to determine these forces-moments.

- Vibration and stability analysis: Final mechanical analysis is to make vibration analysis of the manipulator. Here, natural frequency of actuated links is important.

- Control and simulations: Simulations can be used in every step of design and analysis. But final simulation is most desirable to observe whether manipulator fulfill necessary conditions or not. Control method or algorithm can be created after performing all design and analysis steps.

7

1.2. Background

Study of structural synthesis always be in a state of development during the last centuries. Due to this development, many investigations on this subject are discussed in literature. Detailed and recent review about kinematic structure of mechanisms was introduced by (Mruthyunjaya 2003). In his review, pattern of growth of literature on kinematic structure over four decades is shown. (Gogu 2005) introduced a mobility analysis of translational parallel robot manipulators, which is different from previous mobility analyses. After this study, (Alizade, et al. 2006) reviewed the history of degrees of freedom analysis and structural synthesis formulations in a table that also includes the names of authors, publication dates and commentaries. Furthermore, a new structural synthesis formulation of Cartesian robot manipulators is presented in the same investigation. The structural synthesis of new serial and parallel manipulators is introduced (Alizade, et al. 2007). The Euclidean platform robot manipulators with variable general constraints are firstly presented by (Alizade, et al. 2008).

(Denavit and Hartenberg 1955, Sheth, et al. 1971, Khalil, et al. 1985) introduced the link and joint parameters, which allow the mathematical modeling of robotic mechanical systems. Methodological structural synthesis of serial parallel manipulators is introduced by (Alizade and Bayram 2004). Creation of CAD structural system by using topological description method of kinematic chains and classification of robotic systems was done by (Roth 1975). Graph theory of structural synthesis and analysis of mechanisms have been investigated by using the method of intuition and inspection, (Crossley 1964) and (Woo 1967), by using the concept of transformation of binary chains for the structural synthesis of kinematic chains with up to 10 links and 3 DoF, (Mruthyunjaya 1979, Mruthyunjaya 1984), by using the development of structural Assur groups, (Manolescu 1979, Manolescu 1987), by using robotic system application, (Merlet 1990) and by using CAD strucutural synthesis of planar kinematic chains, (Hwang, et al. 1992). Topological structure, description and classification of industrial robots of different levels have been presented by (Mitrouchev, 2001) by using the number of closed loops. Method on the concept of loop formation, which obviates the necessity of the test for isomorphism, is presented by (Rao, et al. 2001) . (Zhao, et al. 2004) proposed new concept of configuration

degrees of freedom (CDoF) that can form a theoretical base for analyzing the mobility, singularity and stability of mechanisms.

(Huang and Li 2002) proposed a general methodology for type synthesis of lower mobility parallel manipulators by using screw theory. By the help of proposed method, they presented three novel lower mobility parallel manipulators with 3, 4 and 5 DoF. In the light of well known Tricept robot, (Huang, et. al. 2005) designed a new hybrid robot manipulator named Trivariant. They also compared their design with Tricept robot according to cost and kinematic performance. The new parallel manipulator family, where at least one leg contains a planar four-bar parallelogram has been presented by (Liu, et. al 2005). Some fully parallel mechanisms with two to six DoFs, where at least one leg consits of a planar four-bar parallelogram are intended for pure translation in planar, high or improved rotational capability and better stiffness (Liu and Wang 2003). (Fang and Tsai 2002) developed a systematic approach of structural synthesis by using screw theory. They enumerated limb structures for constructing 4-DoF or 5-DoF parallel manipulators according to reciprocity of limb twist system and wrench system. The Lie group of rigid body displacements is represented by operator including screw or twist. The screw system has a Lie algebraic structure that represents all possible displacements. In the study of (Herve 1999), it is shown that mathematical representation of the connection between any pair of bodies obtained through two operations, the composition and the intersection of mechanical bonds. New manipulator with 3 DoF motions of a platform where three limbs generates subsets of possible displacements, Lie subgroup of Schoenflies motions, is illustrated.

The main problem in construction of the robots is how to design it. Study of kinematic structure is the first problem of the design. The problem of kinematic structure includes the selection of actuations, DoF, link number, joint numbers, and direction of joints' axes. The second problem of design, named as dimensional synthesis, is to determine the dimension between joints for the desired motion of the end effector. Dimensional synthesis includes three common tasks which are function, path, and motion generation. These three tasks are applied to different closed and open chains by academicians, engineers and designers. A general method for computer aided optimum kinematic synthesis of planar and spatial multibody systems is proposed by presenting a

new computationally efficient formulation (Jiminéz, et. al. 1997). A neural network is applied to path generation synthesis of a four-bar mechanism (Vasiliu and Yannou 1997). Circle path generation synthesis algorithms of four-bar mechanism has been proposed to achieve the design of the Chebyshev set (Ceccarelli and Vinciguerra 2000). Moreover, new mechanisms with analogous characteristics are presented by introducing new algorithms. Graphical and analytical methods for synthesis of four bar mechanism are explained along practical examples (Reifschneider 2005). Planar path generation synthesis of single DoF coupled serial chain mechanism is introduced by using Fourier series (Nie and Krovi 2005). Furthermore, physical prototype of a reconfigurable 3-link single DoF coupled serial chain mechanism is designed by the help of their method. In order to obtain design equation (input-output displacement equation) for function generation problem of planar and spatial linkages, a new analytical method based on the symbolic representation and the Piogram symbolic operation rule is presented (Wu and Chen 1997). A general method for function, path and motion generation problem of planar linkages is proposed by the help of exact determination of gradient (Sancibrian, et. al. 2006). Three examples are given to illustrate the method: path generation of a four bar, rigid-body guidance in a Stephenson III six-bar linkage, function generation using a Watt II six-bar linkage. Rigid body guidance synthesis of a planar four bar mechanism is presented by optimizing and combining two planar dyads (Yao and Angeles 2000). Moreover, all real roots of a system of polynomial equations are calculated by using contour method during the optimization of planar dyads. The motion generation synthesis of a RPS serial chain is examined with ten dimensional parameters (Su and McCharty 2005). The solution of ten quartic polynomials in ten unknown dimensional parameters is carried out by using polynomial continuation method and then it is implied that the number of roots can be maximum 1024. A planar 3 DoF six bar mechanism is reduced to one DoF mechanism by adding two cam-pairs to two selected link of the mechanism (Gatti and Mundo 2007). Motion generation synthesis of new one DoF mechanism is performed by using inverse kinematics of six bar mechanism. The design equations for three poses of a Bennett linkage's motion generation synthesis are formulated by studying the spatial RR chain with geometric properties of the cylindroid (Perez and McCarthy 2003). Motion generation synthesis of adjustable RRSS mechanisms is presented for the first time by using method based upon modified R-R and S-S dyad constraint

equation (Russell and Sodhi 2001). Planar mechanisms, which are designed for many applications such as furniture and car hoods, are synthesized for prescribed motion by means of an analytical approach (Crocesi and Pennestrı 2005).

A lot of studies are introduced for function generation synthesis of planar and spherical mechanisms in literature. However, the recent ones give sufficient information of the problem's background. Motion and path generation tasks are presented for planar five-bar mechanism with variable topology (Balli and Chand 2002). Furthermore, authors use transmission angle, which is considered for the effective force motion transmission by a mechanism, to reduce the solution space for the design of five-bar mechanism with variable topology. In similar way, dimensional synthesis of a planar seven-link mechanism with variable topology is proposed by keeping some link temporarily fixed (Balli and Chand 2002). Analytical solution of function generating spherical four-bar mechanism is introduced for the five precision points by using superposition methods (Alizade and Kilit 2005). In order to obtain design equation (input-output displacement equation) for function generation problem of planar and spatial linkages, a new analytical method based on the symbolic representation and the Piogram symbolic operation rule is presented (Wu and Chen 1997). A general method for function, path and motion generation problem of planar linkages is proposed by the help of exact determination of gradient (Sancibrian, et al. 2006). Function generation synthesis problem of several types Watt II mechanisms is solved analytically (Simionescu and Smith, 2000). A fourth order T1 motion theory is applied to synthesis of a four bar mechanism for both motion and function generation problems (Goehler, et. al. 2004). Ant-gradient search method is applied to the exact-approximate synthesis problem of planar mechanisms (Diab and Smaili 2008).

Two mathematical models are possible to investigate relations between actuated joint variables and location of end-effector for a specified geometry of parallel manipulator. The first one, inverse kinematics is to find actuated joint variables for a specified location of end-effector. The second one, direct kinematics is to determine the location of end-effector for specified actuated joint variables. Inverse kinematics is generally easier than direct kinematics for closed-loop mechanical system such as a parallel manipulator.

Kinematic analysis of manipulators is very attractive topic in Mechanism and Machine Theory. Researches and scientists have been studied on this topic for a very long

time. Kinematics of parallel robots are solved by using numerical and analytical methods. In most cases, inverse kinematics of parallel robots can be solved analytically. On the other hand, in direct kinematics of parallel robots, numerical methods such as Newton-Raphson, genetic algorithms have to be utilized due to nonlinearity of the problem. Inverse and direct kinematics of a 3-RPS parallel platform manipulator is presented (Fang and Huang 1996). The forward and the inverse kinematics and dynamics of a parallel manipulator actuated by a planar motor is studied (Ben-Horin et al 1998). This manipulator has very simple design along with much larger work volume than commonly-used parallel robot manipulators. The inverse kinematics of two DoF and three DoF planar parallel manipulators are computed and velocity equations are derived to investigate singularity analysis (Gosselin and Wang 1997). The inverse and direct kinematics of planar 5R symmetrical parallel manipulator is presented to determine the workspace and assembly modes (Liu, et al. 2006). Inverse kinematics and kinetostatic model of a parallel mechanism made up of 3-PRS kinematic chains are presented in detail (Zhanga 2006). Inverse, forward kinematics and error modelling of a three degree of freedom parallel robots are introduced by using a very effective Jacobian approximation method (Cui, et al. 2005). The analytical solution of assembly modes of SR-PS-RS structure is presented to compute the forward position analysis of three-legged parallel manipulators which generates SR-PS-RS structure when actuator is locked (Gregorio 2006). By using reciprocal screw, kinematics of a special 3 DoF parallel manipulator which has three UPU limbs and generates 3D translational motion is studied (Huang 2004). Inverse kinematics of a variable geometry body, which is attached to the Stewart platform, is introduced (Wang 2005).

Although the direct kinematics of a parallel robot is hard due to nonlinearity, the direct kinematic problem of a serial robot is recursive and solved easily. A new and efficient algorithm to compute inverse kinematics of 6R serial kinematic chain is proposed by using classical multidimensional geometry (Husty, et al. 2007). Furthermore, in order to simplify kinematic equations, they broke 6R in the middle to form two open 3R chains. In order to solve the inverse kinematics problem of serial robot faster and more accurately, a recursive algorithm is introduced (Martins and Guenther 2003). The algorithm is applied to two serial robots known as SCARA and PUMA in literature. The forward and inverse kinematic problems of a parallel-serial manipulator are presented by obtaining closed-form

solutions (Tanev 2000). A velocity equation by using Jocabian formulation is introduced to develop general-purpose software of any mechanism topology (Altuzarra et al. 2006). The variable geometry parallel manipulator (VGPM) is designed by combining the Stewart platform as a driving mechanism and a number of spatial RSRR kinematic chains. In order to solve inverse kinematic problem of VGPM, approximate distribution is developed.

Workspace is the reachable volume, 3D surface for the end effector of a spatial manipulators or the reachable area for the end effector of a planar manipulators. Workspace of one spatial parallel manipulator made up of 3-PUU kinematic chains and one planar four bar manipulator is investigated by using planar symmetry, rotational axis symmetry and point symmetry (Zhao 2006). The compatible orientation workspace of 6 DoF Stewart-Gough parallel manipulators is developed through boundary curves on two-dimensional cross-sections (Tsai and Lin 2006). Moreover, the orientation workspace is represented by three parameters such as the Euler angles, and by using constant geometric parameters of manipulator, the boundary of workspace is a two-dimensional surface.

In this thesis, new methods are developed to investigate analysis and synthesis problems of parallel manipulators. New type of parallel manipulators, named as Euclidean Parallel Robot Manipulators, are presented for both medical and industrial applications. Kinematic equations in analysis and dimensional synthesis problems are obtained by using known mathematical models. But, the approach in steps of solution of the equations is different. A hybrid manipulator is developed for an industrial application. This manipulator has two layers such that the first layer is a parallel structure whereas the second one is a serial chain.

CHAPTER 2

STRUCTURAL DESIGN OF
PARALLEL ROBOT MANIPULATORS

2.1. Introduction to Structural Synthesis of Manipulators

Structural synthesis of mechanisms is one of the main branches of the fundamental Mechanisms and Machine Science. Structural synthesis is a methodology that is used to generate all structures with desired kinematic performance.

The investigations on structural synthesis of mechanisms are generally studied in sub-categories as: geometrical and kinematic structural synthesis. The purpose of geometrical structural synthesis is to create data foundation to discover particular geometrical features and optimum structures by

- Further development theory of degrees of freedom of mechanisms with variable general constraints and motion of platforms.
- Generating kinematic chains for hinges, branch-loops, and legs of platforms to create simple structural groups.
- Linking simple structural groups to the actuators of manipulators.
- Linking simple structural groups with variable general constraint parameters to the moving platform and ground or actuators of parallel Cartesian robot- manipulators.
- Creating new EPRM with variable general constraints in space or subspaces.
- Creating modular systems with multi-mobility using successive layers of serial trees and parallel manipulators.
- Computer aided structural synthesis.

On the other hand, Kinematic structural synthesis focuses on the following problems:

- Generation of the branches and legs of parallel manipulators by describing the axis of kinematic pairs and links, also joint and link construction parameters.
- Identifying angular and linear conditions for over constraint mechanisms.

- Rearranging the leg configurations of parallel manipulators in such a way that it will be easier to carry out the forward and the inverse tasks.

2.2. Structural Synthesis of Euclidean Robot Manipulators

In this chapter, new parallel manipulators classified as parallel Euclidean platform robot manipulators are introduced. After structural synthesis preliminaries, Euclidean motions are explained to describe new EPRM. New structural formulas of parallel and serial platform Euclidean robot manipulators with variable general constraints are introduced. Furthermore, parallel multiplatform Euclidean robot manipulators and their structural classification with variable general constraints of branch loops are presented. Also, structural parameters, kinematic structures, motion of platforms and 3D drawings of new manipulators are depicted in tables.

2.2.1. Structural Synthesis of Euclidean Platform Robot Manipulators with variable general constraints

Serial robots are limited in the number of possible mechanical structures; however, there is a variety of possible parallel robots that are constructed from the branch loops with variable general constraints, multiple platforms, hinges and legs. Note that, the overall performance of these robots can be affected by the topology of their structures.

2.2.1.1. Motion in Euclidean Planes

In this study, Euclidean planes are utilized to obtain Euclidean motions. Euclidean motion of $\mathbb{R}^2$ is an affine transformation whose linear part is orthogonal (Gray, 1993). Examples of affine transformation can be given as geometric contractions, expansions, dilations, reflections, rotations, shears, similarity transformations, spiral similarities, translations and their combinations. However, rotations and translations are enough for our study due to rigid links and platforms of the manipulators. The new proposed Euclidean

manipulators have several legs, which create Euclidean motions on their own Euclidean planes.

In order to obtain Euclidean plane motion in the design, legs of manipulators are selected as dyads. These dyads can be RR, PR, RP and PP chains as shown in Figure 2.1. Note that, point G of each leg is connected to the platform by spherical or spherical-torus pairs. Position of point G with respect to the fixed reference frame (Figure 2.1.) defines the curve of one point of the platform in the reference Euclidean plane. The motion of the platform can be defined by minimum three independent curves of three platform points moving on three Euclidean reference planes.

Trajectory of point G	Trajectory of point G	Trajectory of point G	Trajectory of point G
$G = \begin{bmatrix} l_1 c\,\theta_1 + l_2 c\,\theta_2 \\ 0 \\ l_1 s\,\theta_1 + l_2 s\,\theta_2 \end{bmatrix}$	$G = \begin{bmatrix} -s_1 + l_2 c\,\theta_2 \\ 0 \\ l_1 + l_2 s\,\theta_2 \end{bmatrix}$	$G = \begin{bmatrix} l_1 c\,\theta_1 + s_2 c\,\theta_2 \\ 0 \\ l_1 s\,\theta_1 + s_2 s\,\theta_2 \end{bmatrix}$	$G = \begin{bmatrix} -s_1 + s_2 c\,\theta_2 \\ 0 \\ l_1 + s_2 s\,\theta_2 \end{bmatrix}$
RR chain	PR chain	RP chain	PP chain
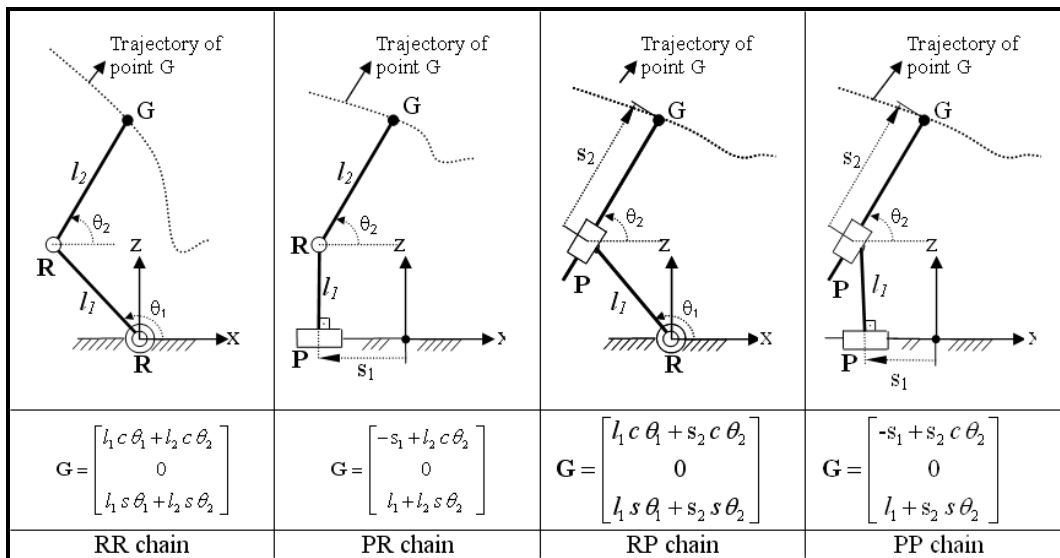
Figure 2.1. Four possible dyads for the legs of EPRM

Note that a kinematic pair with 4 DoF is also introduced as spherical torus pair (S_t) which consists of three rotations and one circular translation (Figure 2.2). The name of the kinematic pair comes from its torus workspace that is drawn by using Mathematica computer software after the kinematic analysis of the pair by Denavit-Hartenberg convention.
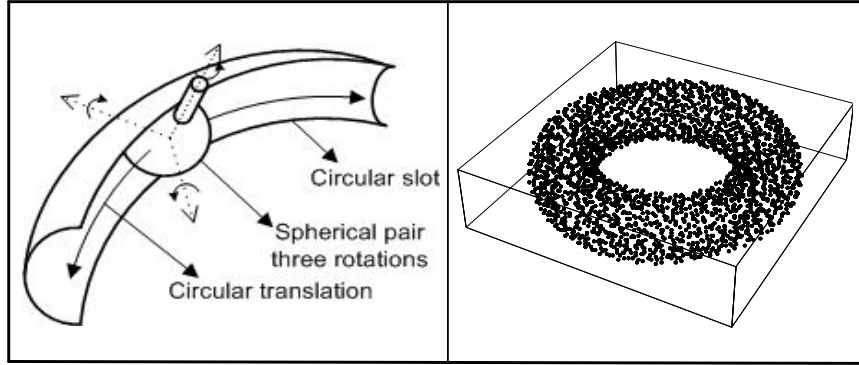
Figure 2.2. Spherical-torus (S_t) kinematic pair and its workspace

2.2.1.2. Structural formula of parallel and serial Euclidean platform robot manipulators

It is clear that freely moving platform in three dimensional space has six degrees of freedom. This DoF is related to the location of the platform in space with respect to the reference frame. Location of the platform defines both position and orientation of the moving coordinate system, which is attached to the moving platform, with respect to the fixed frame as shown in Figure 2.3.a, where u,v and w are the axes of the moving frame and define the independent direction cosines of the moving frame that consists of three rotations and ρ has three translational component (ρ_x, ρ_y, ρ_z) which indicates the origin of the moving frame with respect to the fixed frame. If two moving platforms are connected by hinge (revolute pair), DoF of the serial moving platforms is increased to seven (Figure 2.3.b). If the number of hinges between the platforms is more than one (Figure 2.3.c), DoF of the serial moving platforms can be calculated as,

$$M_{SP} = \lambda + j_h \tag{2.1}$$

where λ is the number of independent parameters describing the positions and orientations of any rigid body in space or subspaces and j_h is the number of hinges between platforms.
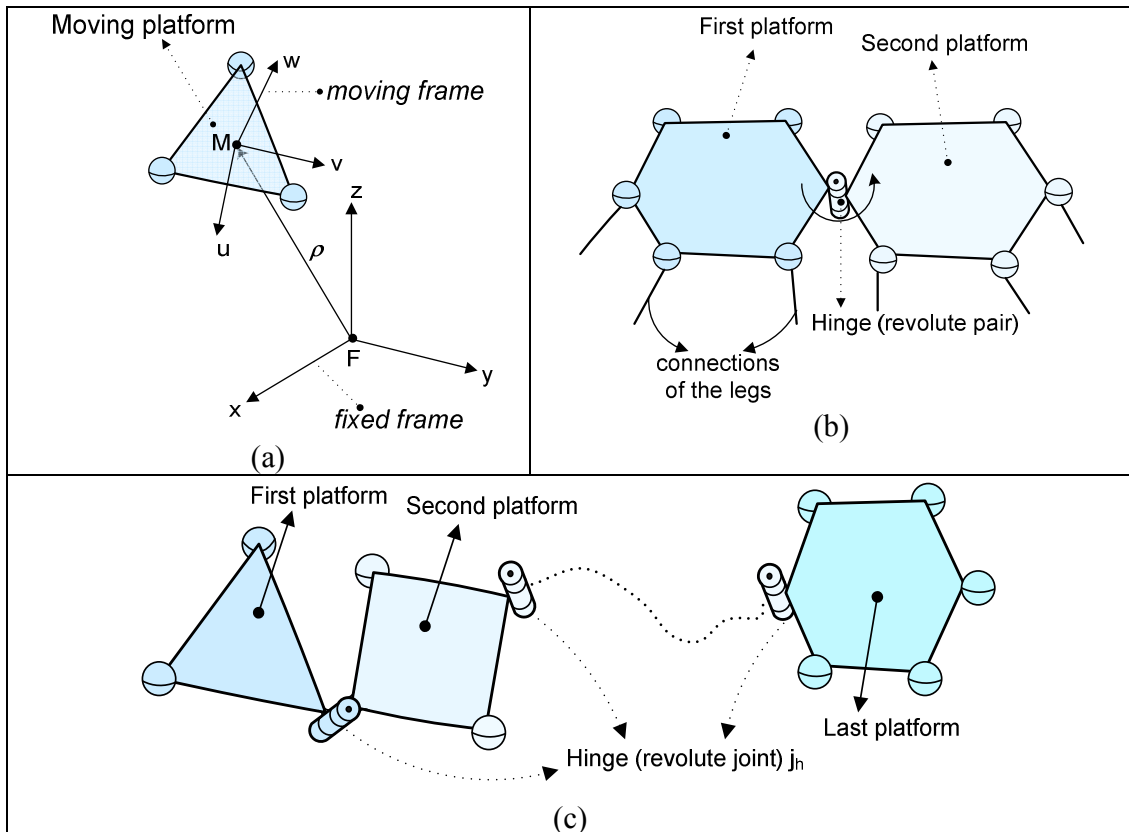
Figure 2.3. (a) 6 independent quantities of the moving platform (b) Two platform connected by hinge (revolute pair) (c) Several numbers of serial moving platforms

If the entire legs of the serial platform manipulators are connected to the moving serial platforms and to the ground, mobility of the kinematic chains of the legs can be defined as,

$$M_l = \sum_{l=1}^{c_l} \left(f_l - \lambda_l \right) \tag{2.2}$$

where $\sum\limits_{l=1}^{c_l} f_l$ is the total DoF of all the kinematic pairs on the legs c_l, and λ_l is the general constraint of each leg ($\lambda_l = 2, ..., 6$).

The combination of Eqs. (2.1) and (2.2) results in the general structural formula of serial platform robot manipulators as,

$$M = \lambda + j_h + \sum_{l=1}^{c_l}(f_l - \lambda_l) \tag{2.3}$$

If the number of moving platforms is unity in space ($\lambda = 6$, $j_h = 0$), Eq. (2.3) will be reduced to the structural formula of parallel manipulators as,

$$M = 6 + \sum_{l=1}^{c_l}(f_l - \lambda_l) \tag{2.4}$$

The motion of one platform on the parallel robot manipulators can be described by,

$$m_p = \lambda + c_l + \sum_{l=1}^{c_l}(d_l - D) \tag{2.5}$$

where D is the number of dimensions of vectors in the reference frame *(D is three for space ($\mathbb{R}^3$), and two for plane ($\mathbb{R}^2$))*, and d_l is the number of dimensions of vectors in subspaces of the legs. Also motion of two or more serial platforms can be formulated as,

$$m = \lambda + c_l + \sum_{l=1}^{c_l}(d_l - D) + j_h \tag{2.6}$$

19

Using the structural formulas, Eqs. (2.3) and (2.4), we can calculate the mobility of parallel or serial Euclidean robot manipulators, while Eqs. (2.5) and (2.6) can be used to describe the motions of platforms relate to them.

Example 1. Design a parallel Euclidean robot manipulator with $c_l = 5$, $M = 5$, and $\lambda_l = 6$. Find both the number and kind of kinematic pairs on each leg by solving the problem of structural synthesis.

By using Eq. (2.4), total DoF of kinematic pairs of the legs can be calculated as, $\sum_{l=1}^{c_l} f_l = M + \sum_{l=1}^{c_l} \lambda_l - 6 = 5 + 30 - 6 = 29$. So that, in the designed manipulator, one leg will consist of five kinematic pairs and the remaining legs will consist of six kinematic pairs with one degrees of freedom, $j_l = c_l^{-1} \sum_{l=1}^{5} f_l = 5(4)$. Using exchangeability of kinematic pairs and conditions of Euclidean robot manipulators, the design can be improved for the mentioned purpose. Kinematic structure, structural parameters and structural bonding of this robot manipulator can be seen in Table 2.1.b.

By using the same procedure of structural synthesis, parallel manipulators with different structural parameters can be generated. Some of these new manipulators are shown in Table 2.1. Elements of structural bonds are illustrated as:
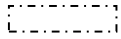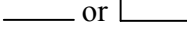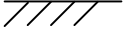
(dashed rectangle) describes general platforms of moving kinematic chains

(dash and point rectangle) platforms on the legs

_____ or └──── Connection of the pairs on platforms to the remaining pairs of legs

////// Fixed frame

Table 2.1. New Parallel Euclidean Platform Robot Manipulators

Structural bonding	Illustration						
	Motion of Platform	λ_l	c_l	$\sum f_l$	d_l	m_p	M
1	2	3	4	5	6	7	8
RR—[St S St S]—RR (with RR above and RR below)	R_x, R_y, P_y, P_z	6	4	22	2, 1, 2, 1	4	4
(a)							
1	2	3	4	5	6	7	8
RR—[St St St St S]—RR (with RR above and RR below)	R_x, R_y, R_z, P_x, P_z	6	5	29	2, 2, 2, 2, 1	5	5
(b)							

Table 2.1 (cont.). New Parallel Euclidean Platform Robot Manipulators

1	2	3	4	5	6	7	8
RR—RR— RR— / RR—S_t S_t S_t S_t S_t S_t—RR / —RR— —RR—	R_x, R_y, R_z P_x, P_y, P_z	6	6	36	2, 2, 2, 2, 2, 2	6	6
(c)							

1	2	3	4	5	6	7	8
RR—S S S—PR / PR	R_x, R_y, P_z	6	3	15	1, 1, 1	3	3
(d)							

Table 2.1 (cont.). New Parallel Euclidean Platform Robot Manipulators

1	2	3	4	5	6	7	8
RR—S—S_t—S—RR R—RR R—R	$R_x, R_y, R_z,$ P_z	6, 3	3, 2	19	1, 2, 1	4	4
(e)							

1	2	3	4	5	6	7	8
RR R—RRS_t—S—S_tRR—R RR RR	R_x, R_y, R_z P_y, P_z	6, 3, 3	3, 2, 2	23	2, 2, 1	5	5
(f)							

Example 2. Design a serial Euclidian robot manipulator with c_l=6, M=6, and $\lambda_l = 6$. By using these parameters, just two serial platform manipulators with two rectangular platforms or with one triangular and pentagonal platforms can be designed. Now let us take the first one into consideration.

Using Eq. (2.3), total number of kinematic pairs on the legs can be found as,

$\sum_{l=1}^{c_l} f_l = M + \sum_{l=1}^{c_l} \lambda_l - \lambda - j_h = 6 + 6 \cdot 6 - 6 - 1 = 35$. Each leg will consist of 5 pairs and the

remaining five pairs can be placed to any leg, $j_l = c_l^{-1} \sum_{l=1}^{6} f_l = 5(5)$. Kinematic structure of

this robot manipulator is shown in Table 2.2.a. Kinematic structure and the structural bonding of the serial Euclidean platform robot manipulator with (c_l=4, M=4, j_h=1 and λ_l=6) are shown in Table 2.2.b.

Table 2.2. New Serial Euclidean Platform Robot Manipulators that include a hinge

Structural bonding	Illustration						
	Motion of Platform	λ_l	c_l	$\sum f_l$	d_l	m	M
1	*2*	*3*	*4*	*5*	*6*	*7*	*8*
	R_x, R_y, R_z P_x, P_y, P_z	6	6	35	2, 2, 2, 2, 2, 1	6	6
(a)							

Table 2.2 (cont.). New Serial Euclidean Platform Robot Manipulators that include a hinge

1	*2*	*3*	*4*	*5*	*6*	*7*	*8*
RR RR S_t S R S S RR RR	R_x, R_y, R_z,P_z	6	4	21	2,1,1,1	4	4
(b)							

2.2.1.3 Structural formula of Euclidean platform robot manipulators that include branch-loops with variable general constraints

As mentioned in previous section, a moving platform has six DoF in space (Figure 2.4.a). If two or more platforms are connected by a loop, total DoF of platforms is affected by subspace of loop and number of kinematic pairs of loop. For example, two platforms are connected by planar loop (it means subspace is three) consisting of four revolute joints (Figure 2.4.b). The total DoF of platforms is seven due to the fact that planar loop gives only one DoF to the system. If several number of platforms are connected by several loops in different subspaces (Figure 2.4.c), the total DoF of platforms can be calculated as follows,

$$M_{MP} = \lambda + \sum_{L=1}^{n}\left(f_L - \lambda_L\right) \tag{2.7}$$

The mobility of all legs was defined in Eq. (2.2). Therefore, DoF of manipulator can be calculated by using the following structural synthesis formula:

$$M = \lambda + \sum_{L=1}^{n}\left(f_L - \lambda_L\right) + \sum_{l=1}^{c_l}\left(f_l - \lambda_l\right) \tag{2.8}$$

The motion of two or more platforms with relative motions created by loops between platforms is formulated as follows,

$$m = \lambda + c_l + \sum_{l=1}^{c_l}\left(d_l - D\right) + \sum_{l=1}^{c_l}\left(f_l - \lambda_l\right) \tag{2.9}$$
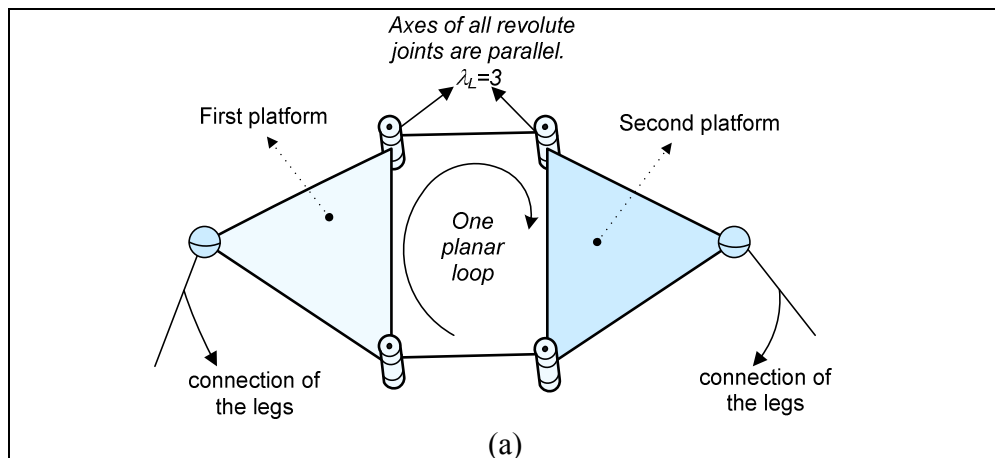
Figure 2.4. (a) Two platforms connected by a planar loop (b) Several number of loops

First platform

Second platform

Third platform

First planar loop $\lambda_1=3$

Second loop $\lambda_2=5$

connection of the legs

(b)
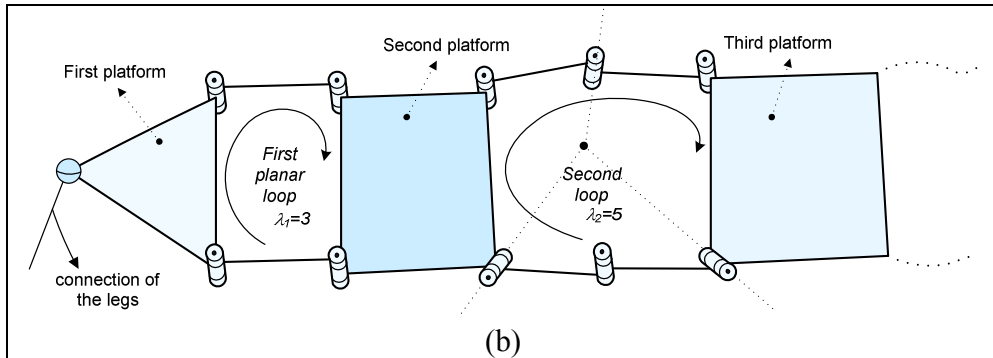
Figure 2.4 (cont.) (a) Two platforms connected by a planar loop (b) Several number of loops

Example 3. Design a serial Euclidean robot manipulators with number of legs $c_l = 6$, mobility $M = 6$, subspace for legs $\lambda_l = 6$, number of loops $L = 2$ and subspace for two loops $\lambda_L = 6$. Assume that kinematic pairs of the loops are shown in Figure 2.5. Find kinematic pairs on each legs.

S: spherical joint
P: prismatic joint
U: universal joint
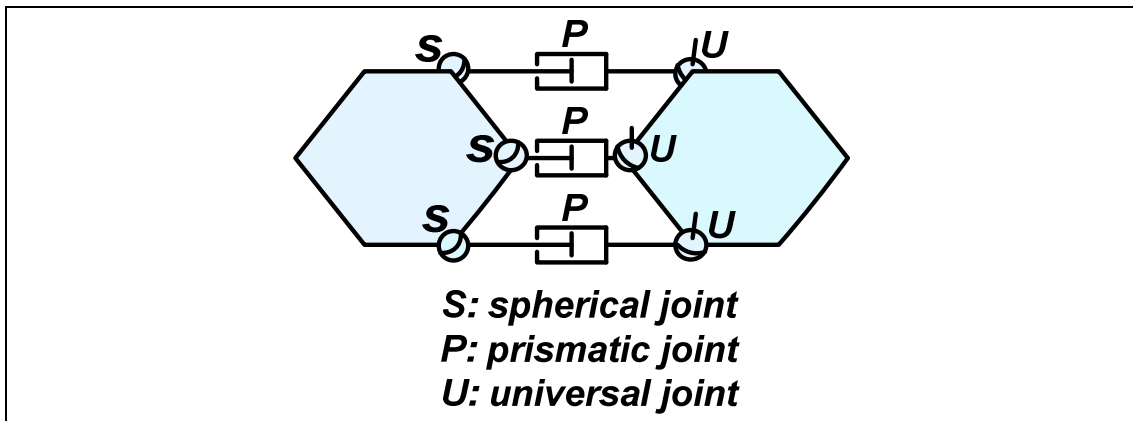
Figure 2.5. Two platforms connected by two loops

By using Eq. (2.8), all kinematic pairs on the legs can be calculated as follows,

$$\sum_{l=1}^{c_l} f_l = M - \lambda - \sum_{L=1}^{n}\left(f_L - \lambda_L\right) + \sum_{l=1}^{c_l} \lambda_l$$

$$\sum_{l=1}^{6} f_l = 6 - 6 - \left(18 - 12\right) + 6 \cdot 6 = 30$$

27

Kinematic pair on each legs is found by dividing the number of all kinematic pairs to the number of legs

$$f = \frac{\sum_{l=1}^{6} f_l}{c_l} = \frac{30}{6} = 5$$

Then, structural bonding of designed manipulator is drawn as,

RR—S S—P—U S—RR
RR—S S—P—U S—RR
RR—S S—P—U S—RR
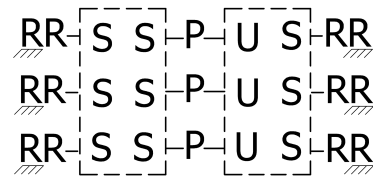
Table 2.3. New Parallel Euclidean Platform Robot Manipulator that includes two branch-loops

Structural bonding	Illustration						
	λ_L	λ_l	c_l	$\sum f_l$	d_l	m	M
RR—S U—P—S S—RR RR—S U—P—S S—RR RR—S U—P—S S—RR	6	6	6	30	1,1,1, 1,1,1	6	6

2.2.1.4. Structural formula of serial-parallel Euclidean platform robot manipulators that include hinges, legs and branch-loops with variable general constraints

As mentioned before, one platform has six DoF in space. If this platform connected to another platform by a hinge, total DoF for two platforms will be seven. If two platforms connected by a loop which has four parallel revolute pairs, total DoF for three platforms will be eight (Figure 2.6). The mobility of legs was given in Eq. (2.2). Consequently, structural formula can be constructed by summing all parameters. Final DoF equation of manipulator shown in Figure 2.6 will be sum of eight and DoF of legs.

three platforms connected by a hinge and a loop.
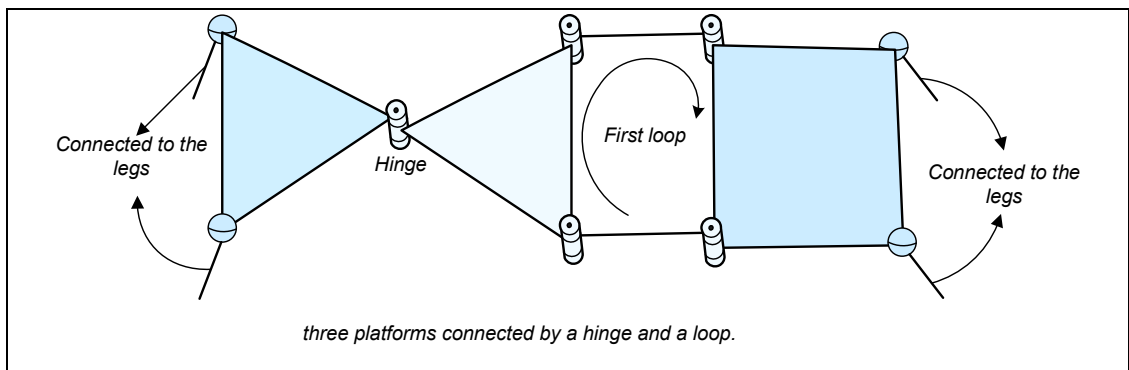
Figure 2.6. Serial Euclidean robot manipulator connected by a hinge and a loop

By combining Eqs. (2.3) and (2.8), the general structural formula of serial Euclidean robot manipulator connected by several hinges and loops can be defined as follows,

$$M = \lambda + j_h + \sum_{L=1}^{n} \left(f_L - \lambda_L \right) + \sum_{l=1}^{c_l} \left(f_l - \lambda_l \right) \qquad (2.10)$$

The general formula of motion of manipulators with relative motions created by loops and hinges is given in the following form:

$$m = \lambda + c_l + \sum_{l=1}^{c_l}(d_l - D) + j_h + \sum_{L=1}^{n}(f_L - \lambda_L) \qquad (2.11)$$

Example 4. Design a serial Euclidean robot manipulator with $c_l = 4$, $M = 4$, $\lambda_l = 6$, $n = 1, \lambda_L = 3$ and $j_h = 1$. Assume that kinematic pairs of the loop and hinge are configured as kinematic chain in Figure 2.7. Find the number of kinematic pairs on each leg.
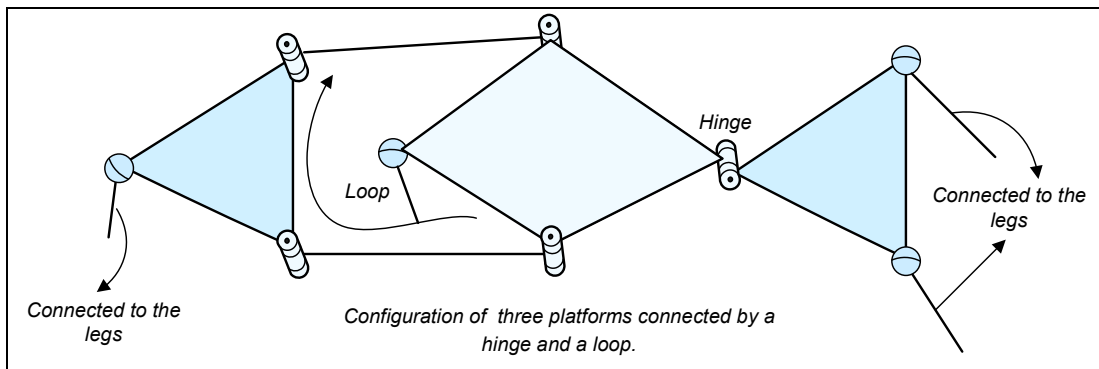
Figure 2.7. Configuration of kinematic pairs of the branch-loop and hinge

By using Eq.(2.10), the total degrees of freedom of the legs can be found as, $\sum_{l=1}^{c_l} f_l = M - \lambda - j_h - \sum_{L=1}^{n}(f_L - \lambda_L) + \lambda_l \cdot c_l = 4 - 6 - 1 - 1 + 6 \cdot 4 = 20$, and the number of kinematic pairs on each leg will be $j_l = c_l^{-1}\sum_{l=1}^{4} f_l = 5$. Using exchangeability of kinematic pairs the new Euclidean serial-parallel manipulator can be designed as shown in Table 2.4.

The motion of platforms can be calculated by using Eq.(2.11) as,

$$m = \lambda + c_l + \sum_{l=1}^{c_l}(d_l - D) + j_h + \sum_{L=1}^{n}(f_L - \lambda_L) = 6 + 4 + (1-3) + (1-3) + (1-3) + (1-3) + 1 + (4-3) = 4.$$

Table 2.4. New Serial-Parallel Euclidean Platform Robot Manipulator with one loop and hinge

Structural bonding	Illustration						
	λ_L	λ_l	c_l	$\sum f_l$	d_l	m	M
	3	6	4	20	1,1,1,1	4	4

A lot of new serial-parallel EPRMs can be generated by combining one DoF branch loops that are depicted in Table 2.5. For instance, a new advanced serial-parallel EPRM (Table 2.6) is constructed by selecting three branch loops as $\lambda_L = 3$, $\lambda_L = 4$ and $\lambda_L = 5$. The variation of structures is very much when two or more DoF branch loops in different subspaces are considered. As a conclusion of this chapter, all formulations for generating new EPRMs are tabulated in Table 2.7.

Table 2.5. One DoF Branch Loops with Variable General Constraints
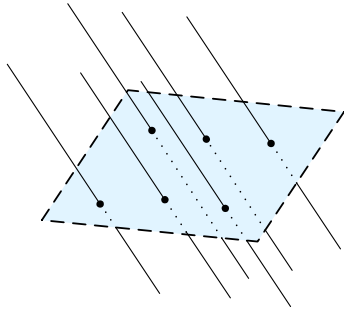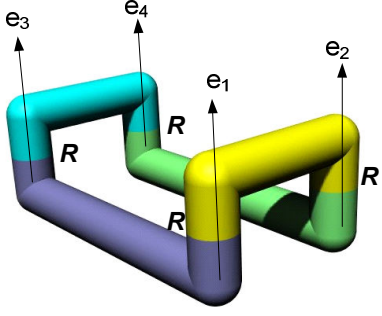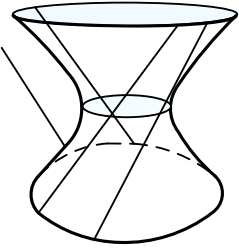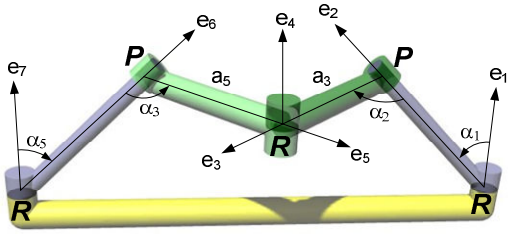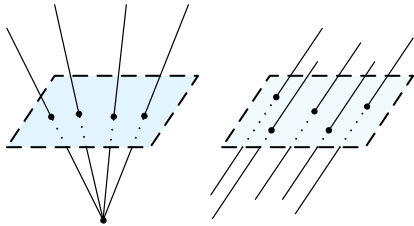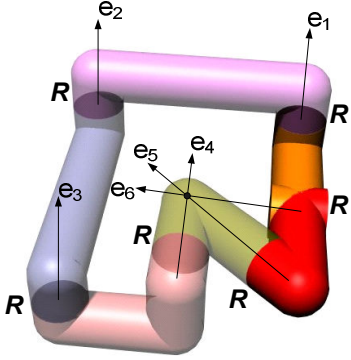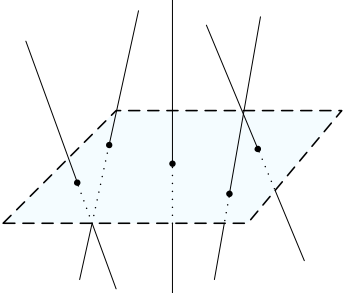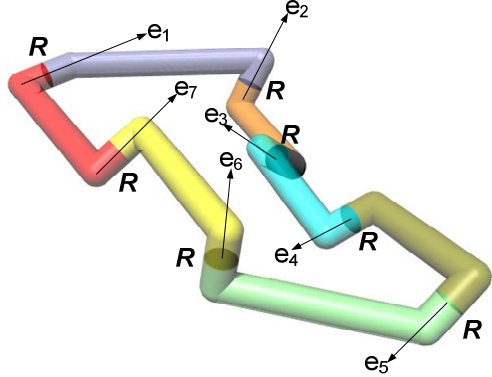
#	λ	Geometrical interpretations	One DoF branch loops
1	$\lambda_L = 3$	All axes are parallel	$e_1 /\!/ e_2 /\!/ e_3 /\!/ e_4$
2	$\lambda_L = 4$	Linear and angular constraints	$a_3 = a_5,\ \alpha_1 = \alpha_5,\ \alpha_2 = \alpha_3$
3	$\lambda_L = 5$	some axes are intersect in one point and some are parallel to each other	axes e_1, e_2, e_3 are parallel to each other and e_4, e_5, e_6 are intersect in one point
4	$\lambda_L = 6$	All axes have arbitrary direction	

Table 2.6. New Advanced Serial-Parallel Euclidean Platform Robot Manipulator

Structural bonding	Illustration						
	λ_L	λ_l	c_l	$\sum f_l$	d_l	m	M
	3, 4, 5	6	4	19	1,1,1,1	5	4

Table 2.7. New mobility formulations(1. parallel EPRM , 2. serial EPRM, 3. Parallel EPRM with branch-loops, 4. serial-parallel EPRM)

	Mobility of legs M_l	Mobility of single platform M_P	Mobility of hinges M_H	Mobility of branch-loops M_{BL}	Mobility equation $M = M_l + M_p + M_H + M_{BL}$
1	$\sum\limits_{l=1}^{c_l}\left(f_l - \lambda_l\right)$	λ	-	-	$M = \lambda + \sum\limits_{l=1}^{c_l}\left(f_l - \lambda_l\right)$
2	$\sum\limits_{l=1}^{c_l}\left(f_l - \lambda_l\right)$	λ	j_h	-	$M = \lambda + j_h + \sum\limits_{l=1}^{c_l}\left(f_l - \lambda_l\right)$
3	$\sum\limits_{l=1}^{c_l}\left(f_l - \lambda_l\right)$	λ	-	$\sum\limits_{L=1}^{n}\left(f_L - \lambda_L\right)$	$M = \lambda + \sum\limits_{L=1}^{n}\left(f_L - \lambda_L\right) + \sum\limits_{l=1}^{c_l}\left(f_l - \lambda_l\right)$
4	$\sum\limits_{l=1}^{c_l}\left(f_l - \lambda_l\right)$	λ	j_h	$\sum\limits_{L=1}^{n}\left(f_L - \lambda_L\right)$	$M = \lambda + j_h + \sum\limits_{L=1}^{n}\left(f_L - \lambda_L\right) + \sum\limits_{l=1}^{c_l}\left(f_l - \lambda_l\right)$

CHAPTER 3

GEOMETRIC DESIGN OF PARALLEL ROBOT MANIPULATORS

3.1. Introduction to Geometric Design of Manipulators

Objective of geometric design is to determine the dimensions of all construction parameters of manipulator's link and joint that can satisfy a desired task. Dimensional synthesis is a part of the geometric design of mechanism. Although geometric design of mechanism begins generation of desired motion, it continues with design of cross-sections of links. The first is related to kinematics of mechanism whereas the second one is related to dynamics. Dimensional synthesis includes three common tasks which are function, path, and motion generation. Function generation task is to design dimensions of a mechanism or a robot, which satisfies a specified function between the motion of input and output link. In path generation task, the position of the end effector's tip point, whose motion creates a path, is correlated to the given input. In motion generation task, a specified motion is generated by a body, which is generally end link of the serial robots or the platform of the parallel robots. Necessary equations for both synthesis and analysis problems are same but different parameters of the same mechanism are calculated. Therefore, kinematic equations are derived by using same methods. Methods for kinematic equations can be found in Chapter 4.

Precision points-poses: Continuous desired task is described discretely by using precision points-poses. Our aim is to reach these points- poses by calculating link and joint parameters in synthesis problem. Function and path generation problems are solved with precision points whereas motion generation problem is solved with precision poses. In function generation synthesis, precision points are calculated by using given function $F(x)$ for a selected input value x (Figure 3.1.a). On the other hand, precision points for

path generation are selected on a given trajectory. In Figure 3.1.b, five precision points can be described by vectors $\mathbf{r_1}, \mathbf{r_2}$...and $\mathbf{r_5}$. From basic kinematics, the vectors are written as $\mathbf{r}_i = x_i\,\mathbf{i} + y_i\,\mathbf{j}$ where $i = 1,...,5$. In order to define the desired motion, some precision poses are depicted in Figure 3.1.c. The coordinate system $O_1x_1y_1$ defines the first pose. There are three independent parameters for the coordinate system: position of origin O_1 and direction of axis x or y.
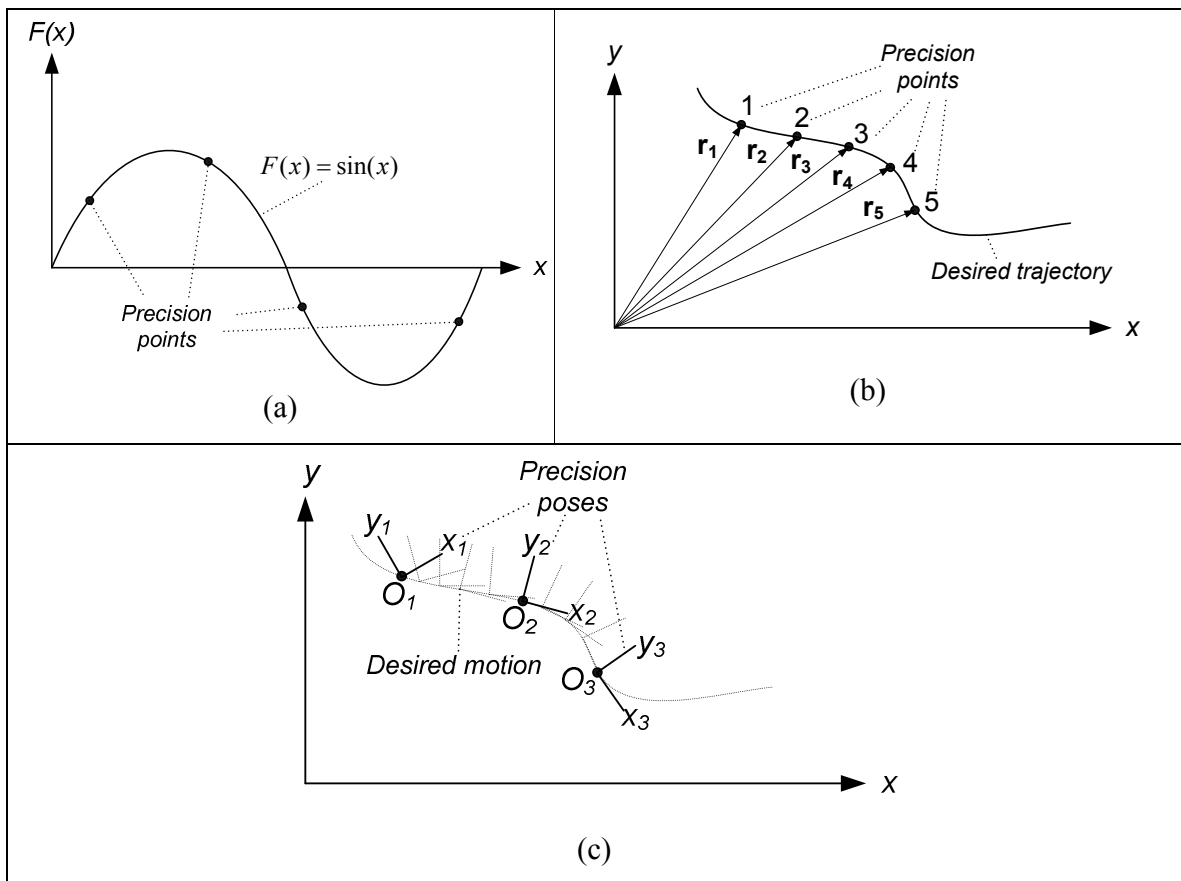
Figure 3.1. Precision points for (a) function generation (b) path generation (c) motion generation

Exact Synthesis: If the number of construction parameters of manipulator–mechanism are equal to the number of given precision points or poses, and then synthesis is called exact synthesis due to the fact that precision points or poses are exactly reached by designed manipulator-mechanism. However, points between precision points are unpredictable. Interpolation solution method is an exact synthesis due to equality of parameters and precision points.

Approximation Synthesis: When the number of construction parameters of manipulator–mechanism are less than the number of given precision points or poses, the synthesis is called approximation synthesis. The precision points or poses are approximated by designed manipulator-mechanism. However, precision points have some errors in this synthesis. The ultimate purpose is to optimize these errors by varying design parameters. The well known approximation techniques are least square and Chebsevy's approximation. Genetic algorithm or neural network is non-algebraic methods or in other words soft computing techniques. But, nowadays, they are very popular techniques because technology of personal computers is developing very fast.

Function generation synthesis: It is generally applied to mechanism. Mechanism construction parameters are designed in such a way that motion of input and output variables of the mechanism are adjusted with a given function. For example, variation of output variable is described as a function of variation of input variable in Figure 3.2.
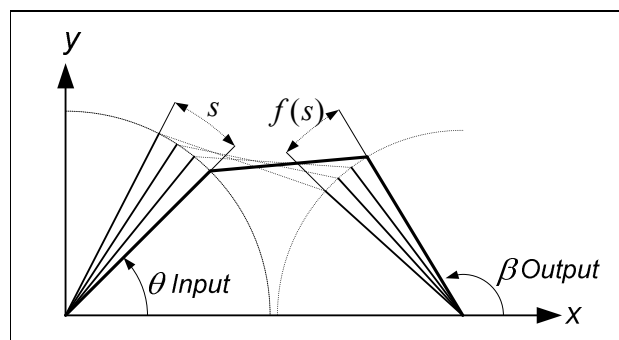
Figure 3.2. Function generating four-bar mechanism

Path generation synthesis: Desired trajectory that passes through some precision points must be generated by construction parameters of mechanism-manipulator for the specified input values (Figure 3.3).
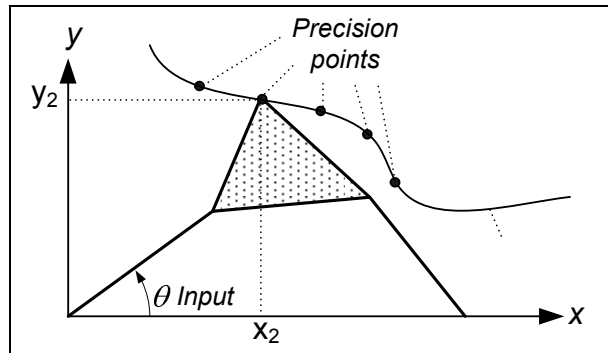
Figure 3.3. Path generating four-bar mechanism

Motion generation synthesis: A specified coordinate system attached to a rigid body of mechanism-manipulator must pass through a set of precision poses after designing construction parameters. For instance, coordinate system $O_M x_M y_M$ must be aligned to firstly $O_1 x_1 y_1$ pose and then $O_2 x_2 y_2$ pose (Figure 3.4).
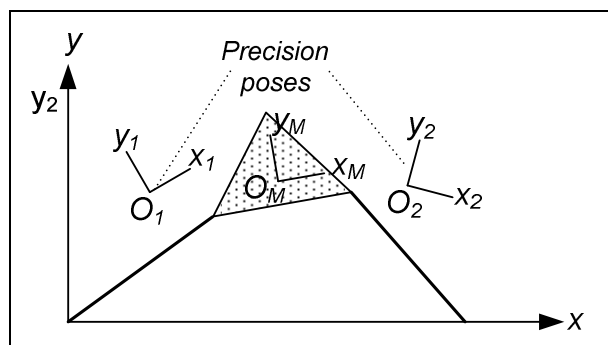
Figure 3.4. Motion generating four-bar mechanism

3.2. Function Generation Synthesis of Planar Seven Link Mechanism

The planar seven link mechanism consists of three planar RR dyads. In Figure 3.5 , points (A D P), (B E P) and (C F P) defines the position of planar dyads. The end point of all dyads must be at point P for every motion of mechanism. Therefore, loop equation for each dyad will be as follows,

$$P_x = A_x + L_1 \cos(\theta_1) + L_2 \cos(\theta_2)$$
$$P_y = A_y + L_1 \sin(\theta_1) + L_2 \sin(\theta_2)$$

(3.1a)

$$P_x = B_x + L_3 \cos(\beta_1) + L_4 \cos(\beta_2)$$
$$P_y = B_y + L_3 \sin(\beta_1) + L_4 \sin(\beta_2)$$

(3.1b)

$$P_x = C_x + L_5 \cos(\psi_1) + L_6 \cos(\psi_2)$$
$$P_y = C_y + L_5 \sin(\psi_1) + L_6 \sin(\psi_2)$$

(3.1c)
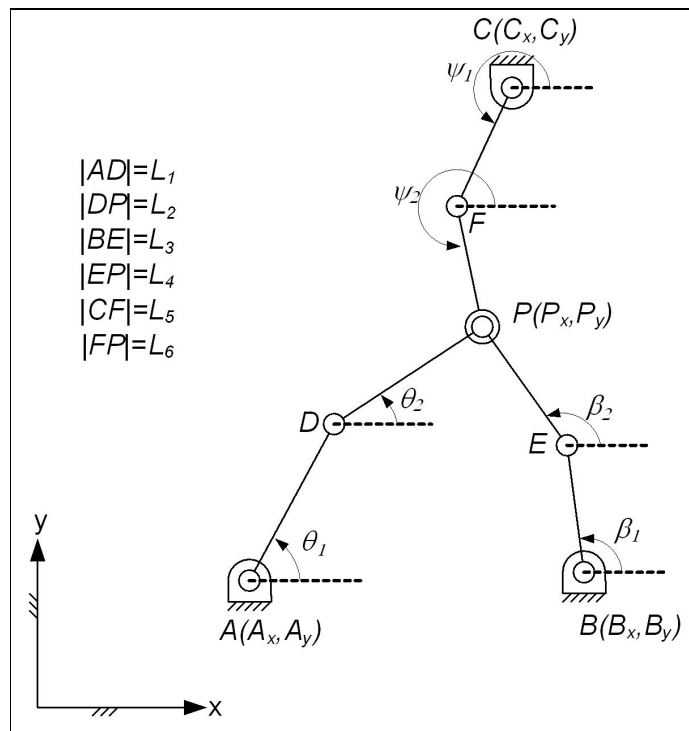
Figure 3.5. Planar seven link mechanism

3.2.1. Design Equation

The second angles of dyads θ_2, β_2 and ψ_2 must be eliminated from Eqs. (3.1a-c), respectively. In order to eliminate the angle θ_2, we rewrite Eq. (3.1a) as,

$$L_2 \cos(\theta_2) = P_x - A_x - L_1 \cos(\theta_1) \tag{3.2a}$$
$$L_2 \sin(\theta_2) = P_y - A_y - L_1 \sin(\theta_1) \tag{3.2b}$$

By summing square of Eqs. (3.2a) and (3.2b), elimination of the angle will be completed. The design equation for the first dyad (A D P) is therefore given as,

$$\begin{aligned} L_2^2 &= A_x^2 + A_y^2 + L_1^2 - 2 A_x P_x - 2 A_y P_y + 2 L_1 A_x c\theta_1 + 2 L_1 A_y s\theta_1 \\ &\quad -2 L_1 \left(P_x c\theta_1 + P_y s\theta_1 \right) + P_x^2 + P_y^2 \end{aligned} \tag{3.3}$$

The procedure of the elimination for other two angles β_2 and ψ_2 is completely same. Therefore, we have two additional design equations for the second and third dyads given in Eqs.(3.4) and (3.5), respectively.

$$\begin{aligned} L_4^2 &= B_x^2 + B_y^2 + L_3^2 - 2 B_x P_x - 2 B_y P_y + 2 L_3 B_x c\beta_1 + 2 L_3 B_y s\beta_1 \\ &\quad -2 L_3 \left(P_x c\beta_1 + P_y s\beta_1 \right) + P_x^2 + P_y^2 \end{aligned} \tag{3.4}$$

$$\begin{aligned} L_6^2 &= C_x^2 + C_y^2 + L_5^2 - 2 C_x P_x - 2 C_y P_y + 2 L_5 C_x c\psi_1 + 2 L_5 C_y s\psi_1 \\ &\quad -2 L_5 \left(P_x c\psi_1 + P_y s\psi_1 \right) + P_x^2 + P_y^2 \end{aligned} \tag{3.5}$$

3.2.2. Synthesis for four precision points

Depending on the similarity of the design equations, steps of synthesis formulation for each dyad will be exactly same. Only terms for design parameters and input angles in the formulations will change. Therefore, in this section, explanation of just one dyad's synthesis is sufficient to understand full mechanism synthesis. Interpolation approximation is used due to the fact that number of precision points is equal to number of design parameters.

Now, let's consider synthesis of the first dyad. The design equation will be written for four precision points as follows,

$$
\begin{aligned}
&A_x^2 + A_y^2 + L_1^2 - L_2^2 - 2\,A_x\,P_{xi} - 2\,A_y\,P_{yi} + 2\,L_1\,A_x\,c\theta_{1i} + 2\,L_1\,A_y\,s\theta_{1i} \\
&-2\,L_1\left(P_{xi}\,c\theta_{1i} + P_{yi}\,s\theta_{1i}\right) + P_{xi}^2 + P_{yi}^2 = 0
\end{aligned}
\qquad i = 1,\ldots,4 \qquad (3.6)
$$

Eq. (3.6) can be rewritten as,

$$
P_1\,f_{1i} + P_2\,f_{2i} + P_3\,f_{3i} + P_4\,f_{4i} + P_5\,f_{5i} + P_6\,f_{6i} - F_i = 0 \qquad (3.7)
$$

where $P_1 = A_x^2 + A_y^2 + L_1^2 - L_2^2$, $f_{1i} = 1$, $P_2 = A_x$, $f_{2i} = -2\,P_{xi}$, $P_3 = A_y$, $f_{3i} = -2\,P_{yi}$, $P_4 = L_1$, $f_{4i} = -2\left(P_{xi}\,c\theta_{1i} + P_{yi}\,s\theta_{1i}\right)$, $P_5 = P_2\,P_4$, $f_{5i} = 2\,c\theta_{1i}$, $P_6 = P_3\,P_4$, $f_{6i} = 2\,s\theta_{1i}$, $F_i = -\left(P_{xi}^2 + P_{yi}^2\right)$, and $i = 1,\ldots,4$. Two nonlinear parameters are defined as λ_1 and λ_2 in place of P_5 and P_6, respectively.

$$
P_2\,P_4 - \lambda_1 = 0 \qquad (3.8)
$$

$$
P_3\,P_4 - \lambda_2 = 0 \qquad (3.9)
$$

New form of design equation with nonlinear parameters λ_1 and λ_2 is obtained by substituting Eqs. (3.8) and (3.9) into Eq. (3.7). If F_i and nonlinear parameters (λ_1, λ_2) are collected to left side of this equation, our final design equation becomes;

$$P_1 f_{1i} + P_2 f_{2i} + P_3 f_{3i} + P_4 f_{4i} = F_i - \lambda_1 f_{5i} - \lambda_2 f_{6i} \qquad i = 1,...,4 \qquad (3.10)$$

The constructional parameters can be formulated as $P_k = l_k + \lambda_1 m_k + \lambda_2 n_k$, $k = 1,...,4$ which are linearly proportional to λ_1 and λ_2. If these construction parameters are substituted into Eq. (3.10), four equations for each pose are obtained as follows;

$$\begin{aligned}
&\left(l_1 f_{1i} + l_2 f_{2i} + l_3 f_{3i} + l_4 f_{4i} \right) + \lambda_1 \left(m_1 f_{1i} + m_2 f_{2i} + m_3 f_{3i} + m_4 f_{4i} \right) \\
&+ \lambda_2 \left(n_1 f_{1i} + n_2 f_{2i} + n_3 f_{3i} + n_4 f_{4i} \right) = F_i - \lambda_1 f_{5i} - \lambda_2 f_{6i} \qquad i = 1,...,4
\end{aligned} \qquad (3.11)$$

Note that Eq. (3.11) refers to 12 linear system of equation due to the fact that coefficients of both sides must be equal. Therefore, Eq.(3.11) can be represented in matrix form:

$$\begin{bmatrix} [A] & & 0 \\ & [A] & \\ 0 & & [A] \end{bmatrix}_{12 \times 12} \cdot \begin{pmatrix} \mathbf{L} \\ \mathbf{M} \\ \mathbf{N} \end{pmatrix}_{12 \times 1} = \begin{pmatrix} \mathbf{F} \\ \mathbf{f_5} \\ \mathbf{f_6} \end{pmatrix}_{12 \times 1} \qquad (3.12)$$

where $[A] = \begin{bmatrix} f_{11} & f_{21} & f_{31} & f_{41} \\ f_{12} & f_{22} & f_{32} & f_{42} \\ f_{13} & f_{23} & f_{33} & f_{43} \\ f_{14} & f_{24} & f_{34} & f_{44} \end{bmatrix}$, $\mathbf{L} = \begin{pmatrix} l_1 \\ l_2 \\ l_3 \\ l_4 \end{pmatrix}$, $\mathbf{M} = \begin{pmatrix} m_1 \\ m_2 \\ m_3 \\ m_4 \end{pmatrix}$, $\mathbf{N} = \begin{pmatrix} n_1 \\ n_2 \\ n_3 \\ n_4 \end{pmatrix}$, $\mathbf{F} = \begin{pmatrix} F_1 \\ F_2 \\ F_3 \\ F_4 \end{pmatrix}$,

$$\mathbf{f_5} = \begin{pmatrix} -f_{51} \\ -f_{52} \\ -f_{53} \\ -f_{54} \end{pmatrix}, \quad \mathbf{f_6} = \begin{pmatrix} -f_{61} \\ -f_{62} \\ -f_{63} \\ -f_{64} \end{pmatrix}.$$

In order to continue synthesis problem, the determinant of square matrix in Eq. (3.12) must not equal to be zero. If it is zero, vector $(\mathbf{L} \quad \mathbf{M} \quad \mathbf{N})^T$ cannot be determined. Assuming that the determinant of matrix is not zero, vector $(\mathbf{L} \quad \mathbf{M} \quad \mathbf{N})^T$ is calculated by using inverse of square matrix. Then, nonlinear parameters λ_1 and λ_2 can be computed by rewriting Eqs. (3.8) and (3.9) as,

$$P_2 = \xi\,\lambda_1 \tag{3.13}$$
$$P_3 = \xi\,\lambda_2 \tag{3.14}$$

where $\xi = 1/P_4$. Remember that the construction parameters were defined as $P_k = l_k + \lambda_1\,m_k + \lambda_2\,n_k$, $k = 1,...,4$. If P_2, P_3 and P_4 are substituted into Eqs. (3.13), (3.14) and $\xi = 1/P_4$, one can obtain three equations:

$$l_2 + \lambda_1\left(m_2 - \xi\right) + \lambda_2\,n_2 = 0 \tag{3.15}$$
$$l_3 + \lambda_1\,m_3 + \lambda_2\left(n_3 - \xi\right) = 0 \tag{3.16}$$
$$\xi\left(l_4 + m_4\,\lambda_1 + n_4\,\lambda_2\right) - 1 = 0 \tag{3.17}$$

Our purpose is to find nonlinear parameters λ_1 and λ_2 in terms of ξ. Therefore, linear systems of Eqs. (3.15) and (3.16) is represented as,

$$\begin{bmatrix} m_2 - \xi & n_2 \\ m_3 & n_3 - \xi \end{bmatrix} \begin{bmatrix} \lambda_1 \\ \lambda_2 \end{bmatrix} = \begin{bmatrix} -l_2 \\ -l_3 \end{bmatrix} \tag{3.18}$$

Solution of Eq.(3.18) gives two results for $\lambda_1 = \dfrac{\left(l_3\,n_2 - l_2\,n_3 + \xi\,l_2\right)}{\left(m_2\,n_3 - m_3\,n_2 - \xi\left(m_2 + n_3\right) + \xi^2\right)}$

and $\lambda_2 = \dfrac{\left(l_2\,m_3 - l_3\,m_2 + \xi\,l_3\right)}{\left(m_2\,n_3 - m_3\,n_2 - \xi\left(m_2 + n_3\right) + \xi^2\right)}$. Substituting λ_1 and λ_2 into Eq. (3.17), we get

a cubic equation as follows,

$$\xi^3 + a_2\,\xi^2 + a_1\,\xi + a_0 = 0 \tag{3.19}$$

where $a_2 = \left(l_3\,n_4 - l_4\,n_3 + l_2\,m_4 - l_4\,m_2 - 1\right)/l_4$,

$\quad a_1 = \left(m_2 + n_3 + \left(l_3\,m_4 - l_4\,m_3\right)n_2 + \left(l_4\,m_2 - l_2\,m_4\right)n_3 + \left(l_2\,m_3 - l_3\,m_2\right)n_4\right)/l_4$,

$\quad a_0 = \left(m_3\,n_2 - m_2\,n_3\right)/l_4$.

In the case of $l_4 = 0$, cubic equation becomes quadratic equation and two distinct solutions can be found for ξ. The cubic algebraic equation was first solved by Tartaglia but made public by Cardano in his book Ars Magna (1545). The three roots of cubic algebraic equation can be given as follows:

$$\xi_1 = -\frac{a_2}{3} + \left(s + t\right)$$

$$\xi_2 = -\frac{a_2}{3} + \frac{\sqrt{3}\,i\left(s - t\right) - \left(s + t\right)}{2}$$

$$\xi_3 = -\frac{a_2}{3} - \frac{\sqrt{3}\,i\left(s - t\right) + \left(s + t\right)}{2}$$

where $q = \left(3a_1 - a_2^2\right)/9$, $\quad r = \left(9\,a_1\,a_2 - 27\,a_0 - 2\,a_2^3\right)/54$, $\quad u = q^3 + r^2$, $\quad s = \left(r + \sqrt{u}\right)^{1/3}$ and $t = \left(r - \sqrt{u}\right)^{1/3}$.

Once ξ values are found, λ_1 and λ_2 can be computed by using Eq. (3.18). λ_1 and λ_2 are utilized to calculate P_k $\quad k = 1,...,4$. Finally, the design parameters can be found by substituting P_k values into equations $A_x = P_2$, $A_y = P_3$, $L_1 = P_4$ and $L_2 = \sqrt{A_x^2 + A_y^2 + L_1^2 - P_1}$.

Then, design parameters of other two dyads ($\{ B_x, B_y, L_3, L_4 \}$ and $\{ C_x, C_y, L_5, L_6 \}$) are calculated by using similar procedure.

3.2.3. Synthesis for any precision points

In order to design the mechanism for any precision points, least square approximation is applied to problem. For interpolation approximation, our objective function (Eq. (3.7)) will be changed as follows,

$$F\left(P_1, P_2, P_3, P_4\right) = \sum_{i=1}^{m}\left[F\left(x_i, \mathbf{c}\right) - F\left(x_i\right)\right]^2 = \sum_{i=1}^{m}\delta_i^2 \tag{3.20}$$

where $F\left(x_i, \mathbf{c}\right) = P_1\, f_{1i} + P_2\, f_{2i} + P_3\, f_{3i} + P_4\, f_{4i} + \lambda_1\, f_{5i} + \lambda_2\, f_{6i}$, $F\left(x_i\right) = F_i$. Note that δ_i^2 is error between two functions.

By taking derivatives of Eq.(3.20) with respect to P_1, P_2, P_3 and P_4, we get four equations as:

$$\frac{\partial F\left(P_1, P_2, P_3, P_4\right)}{\partial P_1} = 2\sum_{i=1}^{m} f_{1i}\left(P_1\, f_{1i} + P_2\, f_{2i} + P_3\, f_{3i} + P_4\, f_{4i} + P_5\, f_{5i} + P_6\, f_{6i} - F_i\right) \tag{3.21}$$

$$\frac{\partial F\left(P_1, P_2, P_3, P_4\right)}{\partial P_2} = 2\sum_{i=1}^{m} f_{2i}\left(P_1\, f_{1i} + P_2\, f_{2i} + P_3\, f_{3i} + P_4\, f_{4i} + P_5\, f_{5i} + P_6\, f_{6i} - F_i\right) \tag{3.22}$$

$$\frac{\partial F\left(P_1, P_2, P_3, P_4\right)}{\partial P_3} = 2\sum_{i=1}^{m} f_{3i}\left(P_1\, f_{1i} + P_2\, f_{2i} + P_3\, f_{3i} + P_4\, f_{4i} + P_5\, f_{5i} + P_6\, f_{6i} - F_i\right) \tag{3.23}$$

$$\frac{\partial F\left(P_1, P_2, P_3, P_4\right)}{\partial P_4} = 2\sum_{i=1}^{m} f_{4i}\left(P_1\, f_{1i} + P_2\, f_{2i} + P_3\, f_{3i} + P_4\, f_{4i} + P_5\, f_{5i} + P_6\, f_{6i} - F_i\right) \tag{3.24}$$

The four equations can be rearranged by using Gauss form as,

$$[f_1 \quad f_1]P_1 + [f_2 \quad f_1]P_2 + [f_3 \quad f_1]P_3 + [f_4 \quad f_1]P_4 = [F \quad f_1] - \lambda_1[f_5 \quad f_1] - \lambda_2[f_6 \quad f_1] \quad (3.25)$$

$$[f_2 \quad f_1]P_1 + [f_2 \quad f_2]P_2 + [f_3 \quad f_2]P_3 + [f_4 \quad f_2]P_4 = [F \quad f_2] - \lambda_1[f_5 \quad f_2] - \lambda_2[f_6 \quad f_2] \quad (3.26)$$

$$[f_3 \quad f_1]P_1 + [f_3 \quad f_2]P_2 + [f_3 \quad f_3]P_3 + [f_4 \quad f_3]P_4 = [F \quad f_3] - \lambda_1[f_5 \quad f_3] - \lambda_2[f_6 \quad f_3] \quad (3.27)$$

$$(3.28)$$
$$[f_4 \quad f_1]P_1 + [f_4 \quad f_2]P_2 + [f_4 \quad f_3]P_3 + [f_4 \quad f_4]P_4 = [F \quad f_4] - \lambda_1[f_5 \quad f_4] - \lambda_2[f_6 \quad f_4]$$

where $\left[f_j \quad f_k \right] = \sum_{i=1}^{m} f_{ji} f_{ki}$, $\left[F \quad f_k \right] = \sum_{i=1}^{m} F_i f_{ki}$, $j = 1,2,3,4,5,6$ and $k = 1,2,3,4$.

Eqs. (3.25-28) can be combined in matrix form as follows,

$$\begin{bmatrix} [T] & & 0 \\ & [T] & \\ 0 & & [T] \end{bmatrix}_{12 \times 12} \cdot \begin{pmatrix} \mathbf{L} \\ \mathbf{M} \\ \mathbf{N} \end{pmatrix}_{12 \times 1} = \begin{pmatrix} \mathbf{F} \\ \mathbf{f_5} \\ \mathbf{f_6} \end{pmatrix}_{12 \times 1} \quad (3.29)$$

where $[T] = \begin{bmatrix} [f_1 \ f_1] & [f_2 \ f_1] & [f_3 \ f_1] & [f_4 \ f_1] \\ [f_2 \ f_1] & [f_2 \ f_2] & [f_3 \ f_2] & [f_4 \ f_2] \\ [f_3 \ f_1] & [f_3 \ f_2] & [f_3 \ f_3] & [f_4 \ f_3] \\ [f_4 \ f_1] & [f_4 \ f_2] & [f_4 \ f_3] & [f_4 \ f_4] \end{bmatrix}$, $\mathbf{L} = \begin{pmatrix} l_1 \\ l_2 \\ l_3 \\ l_4 \end{pmatrix}$, $\mathbf{M} = \begin{pmatrix} m_1 \\ m_2 \\ m_3 \\ m_4 \end{pmatrix}$, $\mathbf{N} = \begin{pmatrix} n_1 \\ n_2 \\ n_3 \\ n_4 \end{pmatrix}$,

$$\mathbf{F} = \begin{pmatrix} [F \ f_1] \\ [F \ f_2] \\ [F \ f_3] \\ [F \ f_4] \end{pmatrix}, \quad \mathbf{f_5} = \begin{pmatrix} -[f_5 \ f_1] \\ -[f_5 \ f_2] \\ -[f_5 \ f_3] \\ -[f_5 \ f_4] \end{pmatrix}, \quad \mathbf{f_6} = \begin{pmatrix} -[f_6 \ f_1] \\ -[f_6 \ f_2] \\ -[f_6 \ f_3] \\ -[f_6 \ f_4] \end{pmatrix}.$$

Vector $(\mathbf{L} \quad \mathbf{M} \quad \mathbf{N})^T$ can be easily calculated from Eq. (3.29). Then, similar procedures in previous parts are utilized to calculate design parameters.

3.2.4. Scale of Given Function

Function of seven link mechanism is given in form of $z = f(x,y)$. In many applications, it is required to scale this function to another function $\psi = f(\theta, \beta)$. For

instance, designer may want to design seven link mechanism satisfying a differential function, $z = x - y$. Input values of function changes in the range as $x_{\min} \le x \le x_{\max}$ and

$y_{\min} \le y \le y_{\max}$. The three relations can be written $\dfrac{\theta - \theta_{\min}}{x - x_{\min}} = \dfrac{\theta_{\max} - \theta_{\min}}{x_{\max} - x_{\min}}$,

$\dfrac{\beta - \beta_{\min}}{y - y_{\min}} = \dfrac{\beta_{\max} - \beta_{\min}}{y_{\max} - y_{\min}}$ and $\dfrac{\psi - \psi_{\min}}{z - z_{\min}} = \dfrac{\psi_{\max} - \psi_{\min}}{z_{\max} - z_{\min}}$, respectively. Therefore, we can write

for the first input: $x = \left(\theta - \theta_{\min}\right)\dfrac{x_{\max} - x_{\min}}{\theta_{\max} - \theta_{\min}} + x_{\min}$, for the second input:

$y = \left(\beta - \beta_{\min}\right)\dfrac{y_{\max} - y_{\min}}{\beta_{\max} - \beta_{\min}} + y_{\min}$ and for output of the system

$\psi = \left(\dfrac{\psi_{\max} - \psi_{\min}}{z_{\max} - z_{\min}}\right)\left(f\left(x, y\right) - z_{\min}\right) + \psi_{\min}$. Finally, scale function is computed by substituting

inputs in the output function (Eq. (3.30)).

$$\psi = \left(\dfrac{\psi_{\max} - \psi_{\min}}{z_{\max} - z_{\min}}\right)\left(\left(\theta - \theta_{\min}\right)\dfrac{x_{\max} - x_{\min}}{\theta_{\max} - \theta_{\min}} + x_{\min} - \left(\beta - \beta_{\min}\right)\dfrac{y_{\max} - y_{\min}}{\beta_{\max} - \beta_{\min}} - y_{\min} - z_{\min}\right) + \psi_{\min} \qquad (3.30)$$

3.2.5. Numerical Example for four precision positions

Let's use function z=x-y for planar seven link mechanism in the range of $0 \le x \le 5$, $0 \le y \le 3$. It is also clear that variable z will change from 0 to 2 ($0 \le z \le 2$). For scaling purpose, also the range of angles are selected as $\pi/6 \le \theta \le \pi/3$, $13\pi/24 \le \beta \le 11\pi/8$ and $9\pi/8 \le \psi \le 35\pi/24$. By using Eq.(3.30), the scale function is calculated as $\psi(\theta, \beta) = \dfrac{37\pi}{60} - \dfrac{3\beta}{5} + 5\theta$. Eventually, four precision points are given in Table 3.1. Precision points are given by using functions $\theta = \theta_{\min} + k\left(\dfrac{\theta_{\max} - \theta_{\min}}{n}\right)$ and

$\beta = \beta_{\min} + k\left(\dfrac{\beta_{\max} - \beta_{\min}}{n}\right)$ for $n = 99$, $k = 25$, $k = 50$, $k = 75$ and $k = 90$.

Table 3.1. Four precision points of planar seven link mechanism

i	θ (rad)	β (rad)	ψ (rad)	P_x (mm)	P_y (mm)
1	0.655821	2.36281	3.79784	6	8
2	0.788043	3.02392	4.06318	7	8.25
3	0.920265	3.68502	4.32762	8	8.75
4	0.999598	4.08169	4.48629	9	9

The synthesis procedure is applied to the first, the second and the third dyads, respectively. Firstly, constant coefficients l_k, m_k, n_k are calculated by solving linear system in Eq.(3.12). Then, roots of cubic equation are computed and nonlinear parameters are found (λ_1 and λ_2). After defining nonlinear parameters, design coefficients P_k, $k = 1,...,4$ are determined by $P_k = l_k + \lambda_1 m_k + \lambda_2 n_k$. All coefficients and parameters are depicted in Table 3.2.

Table 3.2. Coefficients and parameters of planar seven link mechanism

# of dyad	k	(l_k, m_k, n_k)	$(\xi_1 \ \xi_2 \ \xi_3)$	$(\lambda_1 \ \lambda_2)$ for ξ_3	P_k for ξ_3
1	1	$(118.714, -3.7944, 0.579)$	$\begin{pmatrix} -0.06218 - 0.1102i \\ -0.06218 + 0.1102i \\ 0.0226 \end{pmatrix}^T$	$\begin{pmatrix} 23.2776 \\ 482.14 \end{pmatrix}^T$	309.546
	2	$(10.6769, -0.0203, -0.2008)$			0.5251
	3	$(10.702, -0.07144, 0.00381)$			10.8758
	4	$(-4.1853, -0.04275, 0.1027)$			44.3314
2	1	$(166.057, 18.8833, -11.4947)$	$\begin{pmatrix} -0.6047 - 0.6615i \\ -0.6047 + 0.6615i \\ 0.04997 \end{pmatrix}^T$	$\begin{pmatrix} 114.306 \\ 196.455 \end{pmatrix}^T$	66.3286
	2	$(8.6233, 0.129, -0.08985)$			5.712
	3	$(10.1008, 0.9795, -0.571334)$			9.817
	4	$(0.357, 0.08936, 0.04806)$			20.0116
3	1	$(96.6242, 7.2194, -2.7416)$	$\begin{pmatrix} 0.1409 - 0.2245i \\ 0.1409 + 0.2245i \\ 0.1409 \end{pmatrix}^T$	$\begin{pmatrix} 120.021 \\ 276.763 \end{pmatrix}^T$	204.329
	2	$(8.2812, 0.0963, -0.0537)$			4.9602
	3	$(7.8459, 0.2509, -0.0958)$			11.4381
	4	$(1.4674, -0.0242, 0.0926)$			24.1966

Finally, the design parameters are calculated by using P_k design coefficients for each dyad. They are tabulated in Table 3.3.

Table 3.3. Design parameters of planar seven link mechanism

# of dyad	Design parameters (mm)			
1	$A_x = 0.5251$	$A_y = 10.8758$	$L_1 = 44.3314$	$L_2 = 42.1223$
2	$B_x = 5.712$	$B_y = 9.817$	$L_3 = 20.0116$	$L_4 = 21.5206$
3	$C_x = 4.9602$	$C_y = 11.4381$	$L_5 = 24.1966$	$L_6 = 23.1642$

The designed planar seven link mechanism satisfies precision positions. However, there will be error between precision positions. This error can be defined as $\psi_{error} = \psi_{designed} - \psi_{desired}$ where $\psi_{designed}$ is output angle of designed mechanism whereas $\psi_{desired}$ is equal to $\psi(\theta, \beta) = \dfrac{37\pi}{60} - \dfrac{3\beta}{5} + 5\theta$. Note that angle $\psi_{designed}$ can be calculated by analyzing kinematics of the designed mechanism. Therefore, the error is plotted as shown in Figure 3.6.
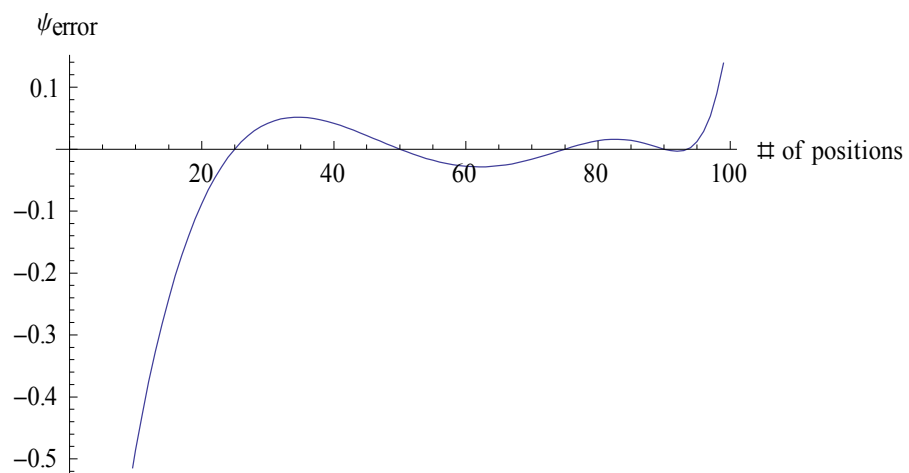
Figure 3.6. The error between $\psi_{designed}$ and $\psi_{desired}$ (unit is degree)

3.2.6. Numerical Example for five and eight precision positions

Number of precision points is increased for a better approximation. The function, scale function and range of angles in previous numerical example are used. Five and eight precision points are given in Table 3.4 and Table 3.5, respectively. The design parameters can be calculated by using least square method.

Table 3.4. Five precision points of planar seven link mechanism

i	θ (rad)	β (rad)	ψ (rad)	P_x (mm)	P_y (mm)
1	0.655821	2.36281	3.79784	6	8
2	0.788043	3.02392	4.06318	7	8.25
3	0.920265	3.68502	4.32762	8	8.75
4	0.946709	3.81725	4.38051	8.256	8.851
5	0.999598	4.08169	4.48629	9	9

Table 3.5. Eight precision points of planar seven link mechanism

i	θ (rad)	β (rad)	ψ (rad)	P_x (mm)	P_y (mm)
1	0.655821	2.36281	3.79784	6	8
2	0.682265	2.49503	3.85162	6.2085	8.0199
3	0.788043	3.02392	4.06318	7	8.25
4	0.840931	3.28836	4.16896	7.3807	8.4341
5	0.877954	3.47347	4.243	7.6546	8.5794
6	0.920265	3.68502	4.32762	8	8.75
7	0.946709	3.81725	4.38051	8.256	8.851
8	0.999598	4.08169	4.48629	9	9

The design parameters of the mechanism are calculated by using equations in Chapter 3.2.3 and then they are tabulated in Table 3.6 and Table 3.7, respectively. Note that only design parameters of the third dyad have small change. After calculating design parameters, the error graph for 5 and 8 precision points are obtained. It is clear that mean

error of 8 points is less than mean error of 5 points. Therefore, it can be concluded that number of precision points is important for approximation of function.

Table 3.6. Design parameters of planar seven link mechanism for five precision points

# of dyad	Design parameters (mm)			
1	$A_x = 0.5251$	$A_y = 10.8758$	$L_1 = 44.3314$	$L_2 = 42.1223$
2	$B_x = 5.712$	$B_y = 9.817$	$L_3 = 20.0116$	$L_4 = 21.5206$
3	$C_x = 4.94927$	$C_y = 11.4309$	$L_5 = 23.9647$	$L_6 = 22.9479$

Table 3.7. Design parameters of planar seven link mechanism for eight precision points

# of dyad	Design parameters (mm)			
1	$A_x = 0.5251$	$A_y = 10.8758$	$L_1 = 44.3314$	$L_2 = 42.1223$
2	$B_x = 5.712$	$B_y = 9.817$	$L_3 = 20.0116$	$L_4 = 21.5206$
3	$C_x = 4.93605$	$C_y = 11.4106$	$L_5 = 24.1234$	$L_6 = 23.1278$
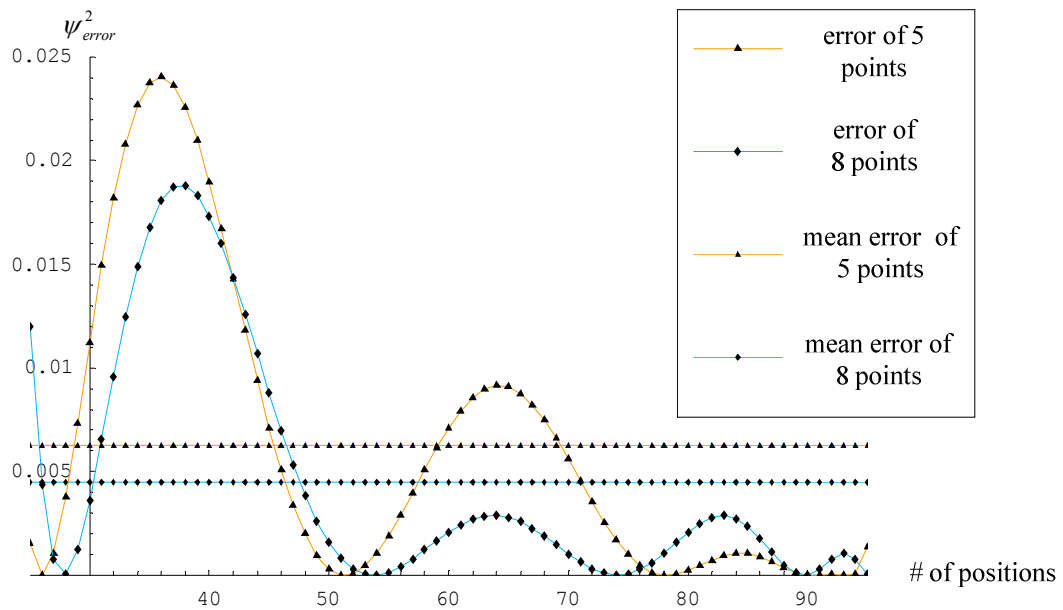
Figure 3.7. The error graph for 5 and 8 precision points

3.3. Function Generation Synthesis of Spherical Seven Link Mechanism

Spherical seven link mechanism can be divided into three spherical dyads. A spherical dyad can be introduced by four construction parameters (θ_A, ψ_A, α_1, α_2) as shown in Figure 3.8. Synthesis of this dyad is to find the construction parameters by defining the desired function and position of end of the dyad. Note that synthesis of one dyad is sufficient to understand full mechanism synthesis.
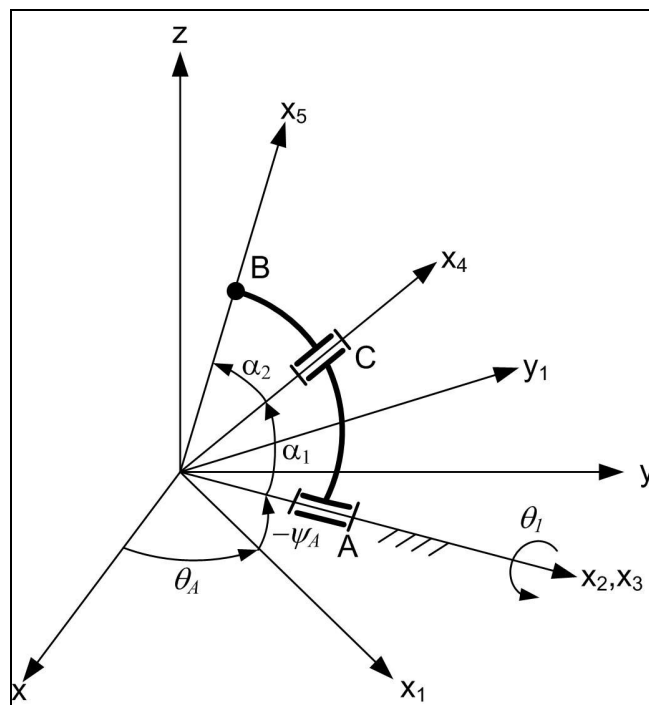
Figure 3.8. Spherical dyad with four design parameters

3.3.1 Design Equation

The direction of unit vector $\mathbf{x_4}$ can be represented in fixed frame as follows,

$$\mathbf{x}_4 = \begin{bmatrix} C_x \\ C_y \\ C_z \end{bmatrix} = R(z,\theta_A)\, R(y,\psi_A)R(x,\theta_1)R(z,\alpha_1)\begin{bmatrix} 1 \\ 0 \\ 0 \end{bmatrix} \qquad (3.31)$$

where $R(z,\theta_A)$ is three by three rotation matrix. Here, z is the axis of rotation, θ_A is angle of rotation.

Multiplying rotation matrices, the components C_x, C_y and C_z are written as,

$$\begin{pmatrix} C_x \\ C_y \\ C_z \end{pmatrix} = \begin{pmatrix} c\alpha_1\, c\theta_A\, c\psi_A + s\alpha_1\left(-c\theta_1\, s\theta_A + c\theta_A\, s\theta_1\, s\psi_A\right) \\ c\alpha_1\, s\theta_A\, c\psi_A + s\alpha_1\left(c\theta_1\, c\theta_A + s\theta_A\, s\theta_1\, s\psi_A\right) \\ s\alpha_1\, s\theta_1\, c\psi_A - c\alpha_1\, s\psi_A \end{pmatrix} \qquad (3.32)$$

The position of point B on (vector) $\mathbf{x}_5$ can be represented by using two angles θ and ψ. Therefore,

$$\mathbf{x}_5 = \begin{bmatrix} B_x \\ B_y \\ B_z \end{bmatrix} = R(z,\theta)\, R(y,\psi)\begin{bmatrix} 1 \\ 0 \\ 0 \end{bmatrix} \qquad (3.33)$$

Eq.(3.33) gives three projections of point B as,

$$B_x = c\theta\, c\psi, \quad B_y = c\psi\, s\theta, \quad B_z = -s\psi \qquad (3.34)$$

Dot product of two unit vectors equals to cosine of angle between them.

$$\mathbf{x}_4 \cdot \mathbf{x}_5 = C_x B_x + C_y B_y + C_z B_z = c\alpha_2 \qquad (3.35)$$

Substituting components in Eqs.(3.32) and (3.34) into Eq.(3.35), the design equation or objective function is found as follows;

$$
\begin{aligned}
& c\theta_A\, c\alpha_1\, c\psi_A\left(c\theta\; c\psi\right)+\; c\theta_A\, s\alpha_1\left(c\theta_1\, s\theta\, c\psi\right)-s\theta_A\, s\alpha_1\left(c\theta_1\, c\theta\, c\psi\right) \\
& +s\theta_A c\alpha_1 c\psi_A\left(s\theta\, c\psi\right)-s\alpha_1\, c\psi_A\left(s\theta_1\, s\psi\right)+c\theta_A\, s\alpha_1\, s\psi_A\left(s\theta_1\, c\theta\, c\psi\right) \\
& +s\theta_A\, s\alpha_1\, s\psi_A\left(s\theta_1\, s\theta\, c\psi\right)+c\alpha_1\, s\psi_A\left(s\psi\right)-c\alpha_2 = 0
\end{aligned}
\tag{3.36}
$$

3.3.2 Three precision positions

Let give $\psi_A = 0$ in Eq.(3.36) and reduce the number of design parameter to three. By dividing both sides of Eq.(3.36) to $s\alpha_1\, c\theta_A$, objective function will be:

$$
\begin{aligned}
& -c\alpha_2 / \left(s\alpha_1\, c\theta_A\right)+\left(c\alpha_1 / s\alpha_1\right)c\theta_i - \left(1/c\theta_A\right)s\theta_{1i}\, s\psi_i - \left(s\theta_A / c\theta_A\right)c\theta_{1i}\, c\theta_i\, c\psi_i \\
& +\left(\left(s\theta_A\, c\alpha_1\right)/\left(c\theta_A\, s\alpha_1\right)\right)c\psi_i + c\theta_{1i}\, c\psi_i\, s\theta_i = 0
\end{aligned}
\tag{3.37}
$$

where index of precision positions is $i = 1, 2, 3$. Objective function can be rewritten as,

$$
P_1\, f_{1i} + P_2\, f_{2i} + P_3\, f_{3i} + P_4\, f_{4i} + P_5\, f_{5i} - F_i = 0
\tag{3.38}
$$

where $P_1 = c\alpha_2 / \left(s\alpha_1\, c\theta_A\right)$, $f_{1i} = -1$, $\qquad P_2 = c\alpha_1 / s\alpha_1$, $\qquad f_{2i} = c\theta_i\, c\psi_i$, $\qquad P_3 = s\theta_A / c\theta_A$, $f_{3i} = -c\theta_i\, c\theta_{1i}\, c\psi_i$, $\qquad P_4 = P_2\, P_3$, $\qquad f_{4i} = s\theta_i\, c\psi_i$, $\qquad P_5 = \sqrt{1 + P_3^2}$, $\qquad f_{5i} = -s\theta_{1i}\, s\psi_i$ and $F_i = -c\theta_{1i}\, c\psi_i\, s\theta_i$

Let assume that relation of linear terms and nonlinear terms are as follows,

$$P_1 = K_1 + K_2 P_4 + K_3 P_5 \tag{3.39}$$

$$P_2 = K_4 + K_5 P_4 + K_6 P_5 \tag{3.40}$$

$$P_3 = K_7 + K_8 P_4 + K_9 P_5 \tag{3.41}$$

Substituting Eqs.(3.39-3.41) into Eq.(3.38), we obtain,

$$\left(K_1 f_{1i} + K_4 f_{2i} + K_7 f_{3i} \right) + P_4 \left(K_2 f_{1i} + K_5 f_{2i} + K_8 f_{3i} \right)$$
$$+ P_5 \left(K_3 f_{1i} + K_6 f_{2i} + K_9 f_{3i} \right) = F_i - P_4 f_{4i} - P_5 f_{5i} \tag{3.42}$$

System of linear equations (Eqs.(3.42)) is written in matrix form as follows,

$$\begin{bmatrix} [A] & & \mathbf{0} \\ & [A] & \\ \mathbf{0} & & [A] \end{bmatrix}_{9 \times 9} \cdot \mathbf{K}_{9 \times 1} = \begin{pmatrix} \mathbf{F} \\ \mathbf{f}_4 \\ \mathbf{f}_5 \end{pmatrix}_{9 \times 1} \tag{3.43}$$

where $[A] = \begin{bmatrix} f_{11} & f_{21} & f_{31} \\ f_{12} & f_{22} & f_{32} \\ f_{13} & f_{23} & f_{33} \end{bmatrix}$, $\mathbf{K} = \begin{pmatrix} K_1 & K_4 & K_7 & K_2 & K_5 & K_8 & K_3 & K_6 & K_9 \end{pmatrix}^T$,

$\mathbf{F} = \begin{pmatrix} F_1 \\ F_2 \\ F_3 \end{pmatrix}$, $\mathbf{f}_4 = \begin{pmatrix} -f_{41} \\ -f_{42} \\ -f_{43} \end{pmatrix}$ and $\mathbf{f}_5 = \begin{pmatrix} -f_{51} \\ -f_{52} \\ -f_{53} \end{pmatrix}$.

Constant coefficients in vector $\mathbf{K}$ can be computed by solving matrix Eq. (3.43). Recall the equalities $P_5 = \sqrt{1 + P_3^2}$, $P_4 = P_2 P_3$ and substitute them into Eqs.(3.39-3.41). Constant P_2 is defined with respect to P_3 by using Eqs.(3.40,3.41) as follows,

$$P_2 = \left(K_6 K_7 - K_4 K_9 - K_6 P_3\right) / \left(-K_9 + \left(-K_6 K_8 + K_5 K_9\right) P_3\right) \tag{3.44}$$

Substituting calculated P_2 into Eq.(3.41), fourth order equation is obtained as,

$$D_1 P_3^4 + D_2 P_3^3 + D_3 P_3^2 + D_4 P_3 + D_5 = 0 \tag{3.45}$$

where $D_1 = \left(K_5^2 - K_6^2 K_8^2\right) K_9^2 + 2 K_5 K_6 K_8 K_9^3 - K_5^2 K_9^4$,

$D_2 = -2 K_5 K_9^2 - 2 K_5^2 K_7 K_9^2 + 2 K_4 K_5 K_8 K_9^2 - 2 K_6 K_8 K_9^3 + 2 K_5 K_9^4$,

$D_3 = \left(1 + 4 K_5 K_7 + K_5^2 K_7^2 - 2 K_4 K_8 - 2 K_4 K_5 K_7 K_8 + K_4^2 K_8^2 - K_6^2 K_8^2\right) K_9^2 - K_9^4 - K_5^2 K_9^4$,

$D_4 = \left(-2 K_7 - 2 K_5 K_7^2 + 2 K_4 K_7 K_8\right) K_9^2 - 2 K_6 K_8 K_9^3 + 2 K_5 K_9^4$, $D_5 = K_7^2 K_9^2 - K_9^4$. This

equation can be solved analytically and we can find at most four roots.

Once P_3 is computed, P_1 and P_2 can also be determined by using Eqs.(3.39) and (3.40), respectively.

$$P_1 = K_1 + K_2 P_2 P_3 + K_3 \left(1 + P_3^2\right)^{0.5} \tag{3.46}$$

Finally, construction parameters are computed as given in Eq.(3.47).

$$\theta_A = \arctan\left(P_3\right), \quad \alpha_1 = \text{arc}\cot\left(P_2\right), \alpha_2 = \arccos\left(P_1 \, s\alpha_1 \, c\theta_A\right) \tag{3.47}$$

3.3.3 Four precision positions

Objective function can be obtained by dividing both sides of Eq.(3.36) to $c\alpha_1\, c\psi_A\, c\theta_A$. Therefore, Eq.(3.36) is reduced to

$$
\begin{aligned}
&-c\alpha_2\,/\left(c\alpha_1\, c\theta_A\, c\psi_A\right)+\left(s\alpha_1\,/\left(c\alpha_1\, c\psi_A\right)\right)c\theta_{1i}\, s\theta_i\, s\psi_i-\left(s\alpha_1\,/\left(c\alpha_1\, c\theta_A\right)\right)s\theta_{1i}\, s\psi_i \\
&-\left(s\theta_A\,/\,c\theta_A\right)\, s\theta_i\, c\psi_i-\left(\left(s\alpha_1\, s\theta_A\right)/\left(c\alpha_1\, c\theta_A\, c\psi_A\right)\right)c\theta_{1i}\, c\theta_i\, c\psi_i \\
&+\left(s\psi_A\,/\left(c\psi_A\, c\theta_A\right)\right)s\psi_i+\left(\left(s\alpha_1\, s\psi_A\right)/\left(c\alpha_1\, c\psi_A\right)\right)s\theta_{1i}\, c\theta_i\, c\psi_i \\
&+\left(\left(s\alpha_1\, s\psi_A\, s\theta_A\right)/\left(c\alpha_1\, c\psi_A\, c\theta_A\right)\right)s\theta_{1i}\, s\theta_i\, c\psi_i+c\theta_i\, c\psi_i=0
\end{aligned}
\tag{3.48}
$$

where i=1,2,3,4. Eq. (3.48) is rewritten as follows,

$$
P_1\, f_{1i}+P_2\, f_{2i}+P_3\, f_{3i}+P_4\, f_{4i}+P_5\, f_{5i}+P_6\, f_{6i}+P_7\, f_{7i}+P_8\, f_{8i}-F_i=0
\tag{3.49}
$$

where $P_1=c\alpha_2\,/\left(c\alpha_1\, c\theta_A\, c\psi_A\right)$, $f_{1i}=-1$, $P_2=s\alpha_1\,/\left(c\alpha_1\, c\psi_A\right)$, $f_{2i}=c\theta_{1i}\, s\theta_i\, s\psi_i$,

$P_3=s\theta_A\,/\,c\theta_A$, $f_{3i}=-s\theta_i\, c\psi_i$, $P_4=\left(s\alpha_1\, s\psi_A\right)/\left(c\alpha_1\, c\psi_A\right)$, $f_{4i}=s\theta_{1i}\, c\theta_i\, c\psi_i$,

$P_5=s\alpha_1\,/\left(c\alpha_1\, c\theta_A\right)=\sqrt{1+P_3^2}\,\sqrt{P_2^2-P_4^2}$, $f_{5i}=-s\theta_{1i}\, s\psi_i$, $P_6=P_2\, P_3$, $f_{6i}=-c\theta_{1i}\, c\theta_i\, c\psi_i$,

$P_7=s\psi_A\,/\left(c\psi_A\, c\theta_A\right)=\sqrt{1+P_3^2}\, P_4\,/\sqrt{P_2^2-P_4^2}$, $f_{7i}=s\psi_i$, $P_8=P_3\, P_4$, $f_{8i}=s\theta_{1i}\, s\theta_i\, c\psi_i$ and

$F_i=-c\theta_i\, c\psi_i$.

In order to convert the nonlinear system (Eq. (3.49)) to linear system, Eqs.(3.50-3.53) are utilized.

$$
P_1=N_1+N_2\, P_5+N_3\, P_6+N_4\, P_7+N_5\, P_8
\tag{3.50}
$$

$$
P_2=N_6+N_7\, P_5+N_8\, P_6+N_9\, P_7+N_{10}\, P_8
\tag{3.51}
$$

$$
P_3=N_{11}+N_{12}\, P_5+N_{13}\, P_6+N_{14}\, P_7+N_{15}\, P_8
\tag{3.52}
$$

$$
P_4=N_{16}+N_{17}\, P_5+N_{18}\, P_6+N_{19}\, P_7+N_{20}\, P_8
\tag{3.53}
$$

We substitute Eqs.(3.50-3.53) into Eq.(3.49) to find constant parameters N_j, $j = 1, 2, \ldots, 20$:

$$
\begin{aligned}
&\left(N_1 f_{1i} + N_6 f_{2i} + N_{11} f_{3i} + N_{16} f_{4i} \right) + P_5 \left(N_2 f_{1i} + N_7 f_{2i} + N_{12} f_{3i} + N_{17} f_{4i} \right) \\
&+ P_6 \left(N_3 f_{1i} + N_8 f_{2i} + N_{13} f_{3i} + N_{18} f_{4i} \right) + P_7 \left(N_4 f_{1i} + N_9 f_{2i} + N_{14} f_{3i} + N_{19} f_{4i} \right) \\
&+ P_8 \left(N_5 f_{1i} + N_{10} f_{2i} + N_{15} f_{3i} + N_{20} f_{4i} \right) = F_i - P_5 f_{5i} - P_6 f_{6i} - P_7 f_{7i} - P_8 f_{8i}
\end{aligned}
\tag{3.54}
$$

Eq.(3.54) can be written in matrix form as follows,

$$
\begin{bmatrix}
[A] & \mathbf{0} & \mathbf{0} & \mathbf{0} & \mathbf{0} \\
\mathbf{0} & [A] & \mathbf{0} & \mathbf{0} & \mathbf{0} \\
\mathbf{0} & \mathbf{0} & [A] & \mathbf{0} & \mathbf{0} \\
\mathbf{0} & \mathbf{0} & \mathbf{0} & [A] & \mathbf{0} \\
\mathbf{0} & \mathbf{0} & \mathbf{0} & \mathbf{0} & [A]
\end{bmatrix}_{20 \times 20}
. \mathbf{N}_{20 \times 1} =
\begin{pmatrix}
\mathbf{F} \\
\mathbf{f}_5 \\
\mathbf{f}_6 \\
\mathbf{f}_7 \\
\mathbf{f}_8
\end{pmatrix}_{20 \times 1}
\tag{3.55}
$$

where $[A] = \begin{bmatrix} f_{11} & f_{21} & f_{31} & f_{41} \\ f_{12} & f_{22} & f_{32} & f_{42} \\ f_{13} & f_{23} & f_{33} & f_{43} \\ f_{14} & f_{24} & f_{34} & f_{44} \end{bmatrix}$, $\quad \mathbf{F} = \begin{pmatrix} F_1 \\ F_2 \\ F_3 \\ F_4 \end{pmatrix}$, $\quad \mathbf{f}_5 = \begin{pmatrix} -f_{51} \\ -f_{52} \\ -f_{53} \\ -f_{54} \end{pmatrix}$, $\quad \mathbf{f}_6 = \begin{pmatrix} -f_{61} \\ -f_{62} \\ -f_{63} \\ -f_{64} \end{pmatrix}$, $\quad \mathbf{f}_7 = \begin{pmatrix} -f_{71} \\ -f_{72} \\ -f_{73} \\ -f_{74} \end{pmatrix}$,

$\mathbf{f}_8 = \begin{pmatrix} -f_{81} \\ -f_{82} \\ -f_{83} \\ -f_{84} \end{pmatrix}$ and $\mathbf{N} = \begin{pmatrix} N_1 & N_6 & N_{11} & N_{16} & N_2 & N_7 & N_{12} & \ldots & N_{15} & N_{20} \end{pmatrix}^T$.

Eqs.(3.50-3.53) is written in matrix form as follows,

$$
\mathbf{P}_{14} = \mathbf{U}.\mathbf{P}_{58}
\tag{3.56}
$$

where $\mathbf{P_{14}} = \begin{bmatrix} P_1 \\ P_2 \\ P_3 \\ P_4 \\ 1 \end{bmatrix}$, $\mathbf{U} = \begin{bmatrix} N_1 & N_2 & N_3 & N_4 & N_5 \\ N_6 & N_7 & N_8 & N_9 & N_{10} \\ N_{11} & N_{12} & N_{13} & N_{14} & N_{15} \\ N_{16} & N_{17} & N_{18} & N_{19} & N_{20} \\ 1 & 0 & 0 & 0 & 0 \end{bmatrix}$, $\mathbf{P_{58}} = \begin{bmatrix} 1 \\ P_5 \\ P_6 \\ P_7 \\ P_8 \end{bmatrix}$.

By taking inverse of matrix, simpler equations can be obtained as given in Eq. (3.57).

$$\mathbf{P_{58}} = \mathbf{U}^{-1}.\mathbf{P_{14}} \tag{3.57}$$

where $\mathbf{U}^{-1} = \begin{bmatrix} 0 & 0 & 0 & 0 & 1 \\ M_1 & M_2 & M_3 & M_4 & M_5 \\ M_6 & M_7 & M_8 & M_9 & M_{10} \\ M_{11} & M_{12} & M_{13} & M_{14} & M_{15} \\ M_{16} & M_{17} & M_{18} & M_{19} & M_{20} \end{bmatrix}$. ($M_1$, M_2, …, M_{20} are given in Appendix A)

We convert Eqs.(3.50-3.53) into Eqs.(3.58-3.61). Note that these equations can be solved more easily.

$$\sqrt{1+P_3^2}\sqrt{P_2^2 - P_4^2} = M_1\,P_1 + M_2\,P_2 + M_3\,P_3 + M_4\,P_4 + M_5 \tag{3.58}$$

$$P_2\,P_3 = M_6\,P_1 + M_7\,P_2 + M_8\,P_3 + M_9\,P_4 + M_{10} \tag{3.59}$$

$$\sqrt{1+P_3^2}\,P_4 / \sqrt{P_2^2 - P_4^2} = M_{11}\,P_1 + M_{12}\,P_2 + M_{13}\,P_3 + M_{14}\,P_4 + M_{15} \tag{3.60}$$

$$P_3\,P_4 = M_{16}\,P_1 + M_{17}\,P_2 + M_{18}\,P_3 + M_{19}\,P_4 + M_{20} \tag{3.61}$$

Once values of P_1, P_2, P_3 and P_4 are found, design parameters can be determined in Eq.(3.62).

$$\theta_A = \arctan(P_3), \quad \psi_A = \arctan\left(\frac{P_4}{P_2}\right), \quad \alpha_1 = \arctan(P_2\, c\psi_A),$$

$$\alpha_2 = \arccos(P_1\, c\alpha_1 c\psi_A) \tag{3.62}$$

3.3.4 Numerical Examples

Same function z=x-y is given for spherical seven link mechanism in the range of $2 \le x \le 5$, $1 \le y \le 3$. Therefore, the variable z will change from 1 to 2 ($1 \le z \le 2$). For scaling purpose, also the range of angles are selected as $\pi/8 \le \theta_1 \le \pi/2$, $\pi/9 \le \beta_1 \le \pi/3$ and $3\pi/8 \le \psi_1 \le 3\pi/4$. By using Eq.(3.30), scale function is calculated as $\psi(\theta_1, \beta_1) = 1.1781 - 3.375\beta_1 + 3\,\theta_1$. Four precision points are given in Table 3.4. Precision points are given by using functions $\theta_1 = \theta_{1\min} + k\left(\dfrac{\theta_{1\max} - \theta_{1\min}}{n}\right)$ and $\beta_1 = \beta_{1\min} + k\left(\dfrac{\beta_{1\max} - \beta_{1\min}}{n}\right)$ for $n = 99$, $k = 25$, $k = 50$, $k = 75$ and $k = 90$.

Table 3.8. Four precision points of spherical mechanism

i	θ_1 (rad)	β_1 (rad)	ψ_1 (rad)	θ (rad)	ψ (rad)
1	0.690198	0.525362	1.4756	0.19635	0.349066
2	0.987698	0.701658	1.7731	0.2618	0.31416
3	1.2852	0.877954	2.0706	0.31416	0.28559
4	1.4637	0.983731	2.24909	0.39269	0.261799

Firstly, we investigate three precision positions by using first three numerical data in Table 3.8 .The parameters are computed by Eqs.(3.39-3.41, 3.43-3.47) and they are tabulated in Table 3.9.

Table 3.9. Construction parameters of spherical seven link mechanism (three precision points)

i	κ	P_1, P_2, P_3	θ_A, α_1, α_2
1	$\begin{pmatrix} K_1 \\ K_4 \\ K_7 \\ K_2 \\ K_5 \\ K_8 \\ K_3 \\ K_6 \\ K_9 \end{pmatrix} = \begin{pmatrix} -16.3058 \\ -18.0263 \\ -0.23433 \\ -9.0804 \\ -10.4048 \\ -0.45835 \\ 12.9661 \\ 14.6205 \\ 0.40933 \end{pmatrix}$	$P_1 = \begin{pmatrix} -0.982461 \\ -7.96286 \end{pmatrix}$ $P_2 = \begin{pmatrix} -0.714151 \\ -8.70371 \end{pmatrix}$ $P_3 = \begin{pmatrix} 0.284276 \\ -0.05878 \end{pmatrix}$	$\theta_A = \begin{pmatrix} 15.8692° \\ -3.36398° \end{pmatrix}$ $\alpha_1 = \begin{pmatrix} -54.4674° \\ -6.55418° \end{pmatrix}$ $\alpha_2 = \begin{pmatrix} 39.7321° \\ 24.8602° \end{pmatrix}$
2	$\begin{pmatrix} K_1 \\ K_4 \\ K_7 \\ K_2 \\ K_5 \\ K_8 \\ K_3 \\ K_6 \\ K_9 \end{pmatrix} = \begin{pmatrix} -12.6545 \\ -14.5615 \\ -0.761614 \\ -9.56721 \\ -11.4568 \\ -1.01397 \\ 6.05179 \\ 7.19934 \\ 0.516531 \end{pmatrix}$	$P_1 = \begin{pmatrix} -2.11919 \\ -3.3929 \end{pmatrix}$ $P_2 = \begin{pmatrix} -1.99428 \\ -3.51855 \end{pmatrix}$ $P_3 = \begin{pmatrix} 0.226926 \\ 0.094551 \end{pmatrix}$	$\theta_A = \begin{pmatrix} 12.7853° \\ 5.40129° \end{pmatrix}$ $\alpha_1 = \begin{pmatrix} -26.6308° \\ -15.8656° \end{pmatrix}$ $\alpha_2 = \begin{pmatrix} 22.1266° \\ 22.5663° \end{pmatrix}$
3	$\begin{pmatrix} K_1 \\ K_4 \\ K_7 \\ K_2 \\ K_5 \\ K_8 \\ K_3 \\ K_6 \\ K_9 \end{pmatrix} = \begin{pmatrix} -8.40852 \\ -9.12854 \\ 0.145562 \\ -1.99675 \\ -2.38987 \\ -0.257047 \\ 5.2828 \\ 6.09457 \\ -0.071841 \end{pmatrix}$	$P_1 = \begin{pmatrix} -5.07339 \\ -2.37087 \end{pmatrix}$ $P_2 = \begin{pmatrix} -5.36921 \\ -2.13345 \end{pmatrix}$ $P_3 = \begin{pmatrix} -0.190533 \\ 0.161191 \end{pmatrix}$	$\theta_A = \begin{pmatrix} -10.7875° \\ 9.15681° \end{pmatrix}$ $\alpha_1 = \begin{pmatrix} -10.5503° \\ -25.1137° \end{pmatrix}$ $\alpha_2 = \begin{pmatrix} 24.1447° \\ 6.58134° \end{pmatrix}$

By using all positions in Table 3.8, synthesis of four precision positions is solved. After the computation of parameters in Eqs.(3.55-3.62), they are tabulated in Table 3.10.

Table 3.10. Construction parameters of spherical seven link mechanism (four precision points)

i	P_1, P_2, P_3, P_4	θ_A, ψ_A, α_1, α_2
1	$P_1 = \begin{pmatrix} 5.04809 \\ 0.82041 \\ 1.75752 \\ -0.92004 \\ 0.59618 \end{pmatrix}$, $P_2 = \begin{pmatrix} -28.4843 \\ 3.17962 \\ -0.09347 \\ 0.58928 \\ -0.075434 \end{pmatrix}$ $P_3 = \begin{pmatrix} 0.22504 \\ -0.80124 \\ -0.80124 \\ 0.58928 \\ -0.07543 \end{pmatrix}$, $P_4 = \begin{pmatrix} 11.0718 \\ 0.72963 \\ 0.07987 \\ -0.32375 \\ -0.10495 \end{pmatrix}$	$\theta_A = \begin{pmatrix} 12.6826° \\ 2.40836° \\ -38.7031° \\ 30.5099° \\ -4.31389° \end{pmatrix}$, $\psi_A = \begin{pmatrix} -21.241° \\ 12.9241° \\ -40.5162° \\ 44.1686° \\ -31.5697° \end{pmatrix}$ $\alpha_1 = \begin{pmatrix} 87.2527° \\ 71.4404° \\ 5.06245° \\ -18.1343° \\ 9.57976° \end{pmatrix}$, $\alpha_2 = \begin{pmatrix} 180°-96.7065°i \\ 121.761° \\ 124.841° \\ 133.043° \\ 125.597° \end{pmatrix}$
2	$P_1 = \begin{pmatrix} 4.37089 \\ 8.63987 \\ -0.0208 \\ 1.48224 \\ -0.24045 \end{pmatrix}$, $P_2 = \begin{pmatrix} 12.4503 \\ -8.0408 \\ -0.3749 \\ -0.10775 \\ 0.4552 \end{pmatrix}$ $P_3 = \begin{pmatrix} -0.23096 \\ 0.954007 \\ 0.134425 \\ -0.635845 \\ 0.275897 \end{pmatrix}$, $P_4 = \begin{pmatrix} 5.99094 \\ 6.02061 \\ -0.33982 \\ 0.082966 \\ -0.41552 \end{pmatrix}$	$\theta_A = \begin{pmatrix} -13.0052° \\ 43.6516° \\ 7.6561° \\ -32.45° \\ 15.424° \end{pmatrix}$, $\psi_A = \begin{pmatrix} 25.6964° \\ -36.8244° \\ 42.1876° \\ -37.5962° \\ -42.3902° \end{pmatrix}$ $\alpha_1 = \begin{pmatrix} 84.5722° \\ -79.0231° \\ 4.75959° \\ -6.1175° \\ -0.55455° \end{pmatrix}$, $\alpha_2 = \begin{pmatrix} 180°-111.621°i \\ 180°-130.229°i \\ 89.9875° \\ 0°-52.7285°i \\ 89.751° \end{pmatrix}$
3	$P_1 = \begin{pmatrix} 0.364795 \\ 1.03114 \\ -30.7778 \\ 0.876068 \\ 1.98703 \end{pmatrix}$, $P_2 = \begin{pmatrix} 3.01174 \\ -0.8556 \\ -13.5941 \\ -0.2522 \\ -2.1051 \end{pmatrix}$ $P_3 = \begin{pmatrix} 0.741106 \\ -0.304748 \\ 1.72414 \\ -0.252205 \\ -2.1051 \end{pmatrix}$, $P_4 = \begin{pmatrix} 1.73278 \\ 0.332431 \\ -13.5916 \\ -0.03556 \\ 0.718685 \end{pmatrix}$	$\theta_A = \begin{pmatrix} 36.5424° \\ -16.9485° \\ 59.8863° \\ -14.1551° \\ -64.5905° \end{pmatrix}$, $\psi_A = \begin{pmatrix} 29.9136° \\ -21.2328° \\ 44.9946° \\ -9.03449° \\ -42.078° \end{pmatrix}$ $\alpha_1 = \begin{pmatrix} 11.6456° \\ 31.8468° \\ -82.0963° \\ -11.6862° \\ 14.6052° \end{pmatrix}$, $\alpha_2 = \begin{pmatrix} 89.1344° \\ 132.857° \\ 180°-194.52°i \\ 121.07° \\ 72.9346° \end{pmatrix}$

3.4. Motion Generation Synthesis of a 3-DoF Spatial Platform Robot Manipulator

In this part of the chapter, motion generation synthesis problem of a 3-DoF spatial platform manipulator is solved for three, four and five precision poses. Geometric parameters and kinematic equations of the manipulator are introduced. Analytical solution for three precision poses is presented. Numerical method for four and five precision poses are investigated. Furthermore, two different manipulators are constructed and they are shown for the prescribed motion.

3.4.1. Geometry of the manipulator

Consider 3 DoF spatial parallel manipulator illustrated by computer drawing representation (Figure 3.9.a) and kinematic diagram (Figure 3.9.b) . Moving platform of the manipulator is connected to a fixed base by three legs. Each of them consists of a circular slider (C_s), an intermediate revolute joint (R) and a spherical joint (S) attached to the moving platform. Kinematic chain of a leg is called C_sRS limb. Kinematic model of one leg of the manipulator is depicted in Figure 3.10.a. In order to obtain better view, parameters of the leg are shown in radial plane (Figure 3.10.b). In Figure 3.10.a , the first coordinate system (O_F, x_F, y_F, z_F) is attached to the fixed base, the second coordinate system (O_M, x_M, y_M, z_M) is attached to the moving platform and the third coordinate system ($A_i, x_i, y_i z_i$) is attached to circular slider . Three points A_i, B_i, C_i define position of i-th leg. Due to three legs, position of the manipulator can be completely described by using coordinates of nine points (A_i, C_i, B_i, i=1,2,3).
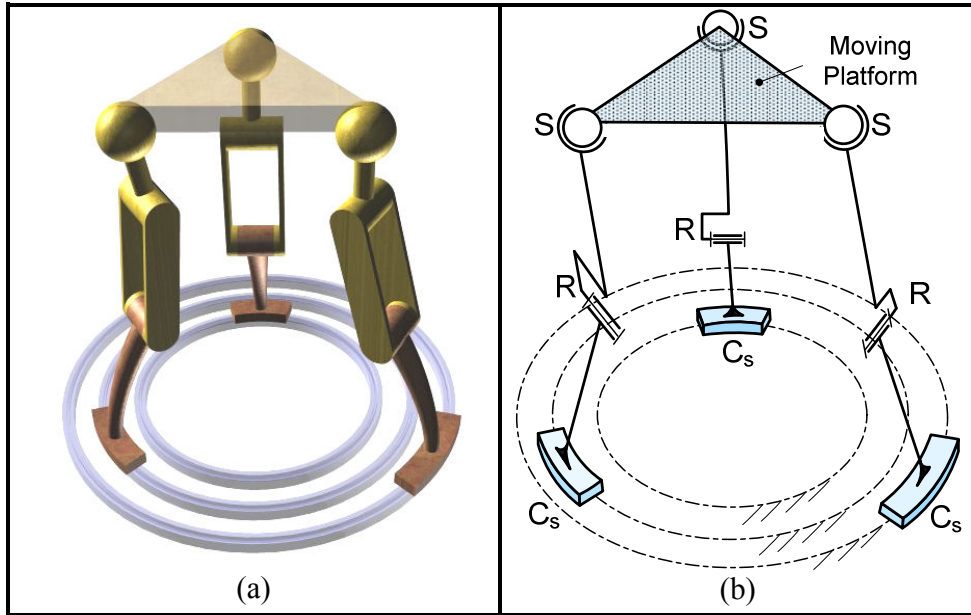
Figure 3.9. (a) Computer drawing representation (b) Kinematic diagram

Vector-loop equation of the manipulator is written as follows,

$$\overline{O_F B_i} = \overline{O_F O_M} + \overline{O_M B_i} = \overline{O_F A_i} + \overline{A_i C_i} + \overline{C_i B_i} \qquad (3.63)$$

Vector-loop equation (Eq.(3.63)) can be further arranged in matrix form

$$\mathbf{q_i} = \mathbf{p} + R\,\mathbf{b_i} = \mathbf{a_i} + \mathbf{r_{1i}} + \mathbf{r_{2i}} \qquad (3.64)$$

where $\mathbf{p}$: position vector of the origin (O_M) of the moving coordinate system with respect to the fixed coordinate system, R: rotation matrix of the moving coordinate system (x_M, y_M, z_M) measured in the fixed coordinate system (x_F, y_F, z_F) by Euler angles, $\mathbf{b_i}$: position vector of spherical pairs with respect to moving coordinate system, $\mathbf{q_i}$: position vector of spherical pairs with respect to the fixed coordinate system, $\mathbf{a_i}$: position vector of circular slider, $\mathbf{r_{1i}}$:

position vector between circular slider and revolute joint, $\mathbf{r_{2i}}$: position vector between revolute and spherical pairs. In Eq. (3.54), vectors $\mathbf{p}$ and $\mathbf{q}$ are defined in the fixed coordinate system as $\mathbf{p} = \begin{bmatrix} p_x & p_y & p_z \end{bmatrix}^T$, $\mathbf{q}_i = \begin{bmatrix} q_{xi} & q_{yi} & q_{zi} \end{bmatrix}^T$, respectively. However, vector $\mathbf{b}$ is defined in the moving coordinate system as $\mathbf{b}_i = \begin{bmatrix} b_{xi} & b_{yi} & 0 \end{bmatrix}^T$. Note that all distances are measured as *mm* for this manipulator.

Rotation matrix is defined by roll ψ, pitch ϕ and yaw θ angles that correspond to rotations about x, y and z axis, respectively as

$$R = R(z, \psi) R(y, \phi) R(x, \theta) = \begin{bmatrix} c\phi\, c\psi & c\psi\, s\theta\, s\phi - c\theta\, s\psi & c\theta\, c\psi\, s\phi + s\theta\, s\psi \\ c\phi\, s\psi & c\theta\, c\psi + s\theta\, s\phi\, s\psi & -c\psi\, s\theta + c\theta\, s\phi\, s\psi \\ -s\phi & c\phi\, s\theta & c\phi\, c\theta \end{bmatrix} \qquad (3.65)$$
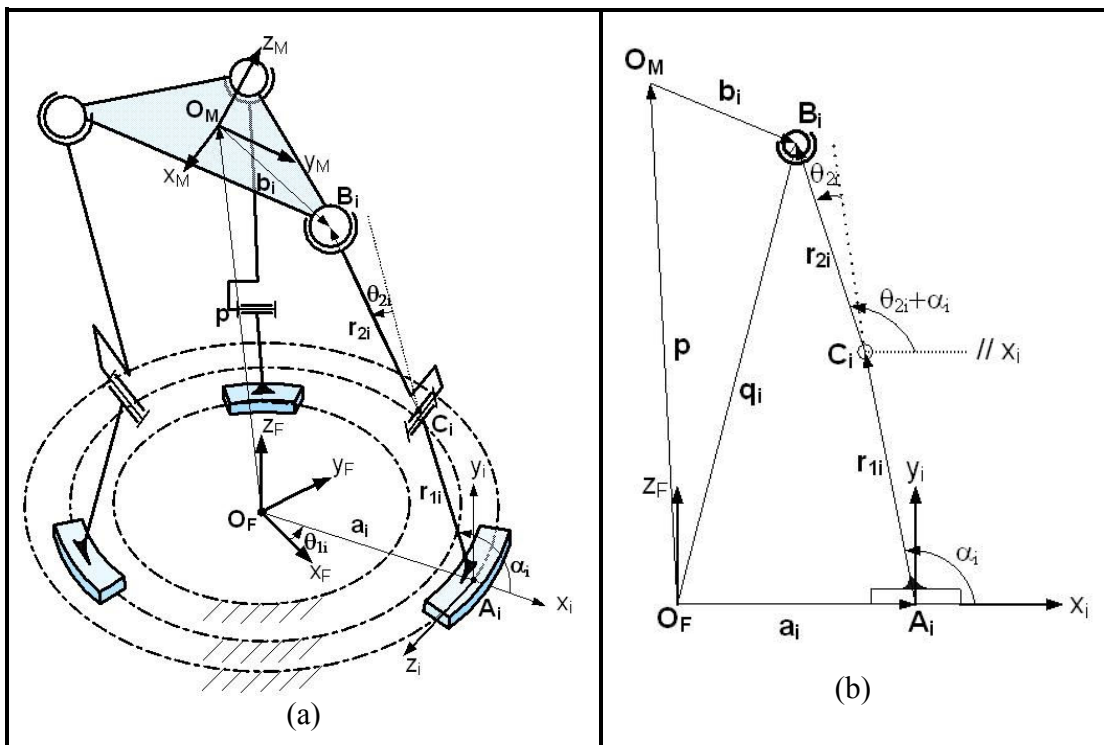
Figure 3.10. (a) Kinematic model (b) Kinematic model in radial plane

Note that the terms $c\phi$ and $s\phi$ in Eq. (3.65) refer to $\cos\phi$ and $\sin\phi$, respectively.

The vectors in radial plane $\mathbf{r_{1i}}$, $\mathbf{r_{2i}}$ and $\mathbf{a_i}$ are described in (x_i, y_i, z_i) coordinate system as

$$
{}^{i}\mathbf{r_{1i}} = \begin{bmatrix} r_{1i}\,c\,\alpha_i \\ r_{1i}\,s\,\alpha_i \\ 0 \end{bmatrix}, \quad
{}^{i}\mathbf{r_{2i}} = \begin{bmatrix} r_{2i}\,c\left(\alpha_i+\theta_{2i}\right) \\ r_{2i}\,s\left(\alpha_i+\theta_{2i}\right) \\ 0 \end{bmatrix}, \quad
{}^{i}\mathbf{a_i} = \begin{bmatrix} a_i \\ 0 \\ 0 \end{bmatrix}
\tag{3.66}
$$

Rotation matrix between the fixed coordinate system (O_F, x_F, y_F, z_F) and the moving coordinate system (A_i, x_i, y_i, z_i) is represented by rotation about $z_F(\theta_{1i})$ and rotation about $x_i(\dfrac{\pi}{2})$ respectively:

$$
{}^{F}R_i = R\left(z_F,\theta_{1i}\right).R\left(x_i,\pi/2\right) = \begin{bmatrix} c\theta_{1i} & 0 & s\theta_{1i} \\ s\theta_{1i} & 0 & -c\theta_{1i} \\ 0 & 1 & 0 \end{bmatrix}
\tag{3.67}
$$

By multiplying rotation matrix ${}^{F}R_i$ (Eq. (3.67)) and the vectors ${}^{i}\mathbf{r_{1i}}$, ${}^{i}\mathbf{r_{2i}}$ and ${}^{i}\mathbf{a_i}$ (Eq. (3.66)), we can describe the vectors in the fixed coordinate system as follows,

$$
\mathbf{r_{1i}} = {}^{F}R_i\,{}^{i}\mathbf{r_{1i}} = r_{1i}\begin{bmatrix} c\theta_{1i}\,c\,\alpha_i \\ s\theta_{1i}\,c\,\alpha_i \\ s\,\alpha_i \end{bmatrix}, \quad
\mathbf{r_{2i}} = {}^{F}R_i\,{}^{i}\mathbf{r_{2i}} = r_{2i}\begin{bmatrix} c\theta_{1i}\,c\left(\alpha_i+\theta_{2i}\right) \\ s\theta_{1i}\,c\left(\alpha_i+\theta_{2i}\right) \\ s\left(\alpha_i+\theta_{2i}\right) \end{bmatrix},
$$

$$
\mathbf{a_i} = {}^{F}R_i\,{}^{i}\mathbf{a_i} = a_i\begin{bmatrix} c\theta_{1i} \\ s\theta_{1i} \\ 0 \end{bmatrix}
\tag{3.68}
$$

Using Eqs. (3.64) and (3.68), the components of spherical pair's coordinate B_i are found in the fixed coordinate system (O_F, x_F, y_F, z_F) as:

$$q_{xi} = p_x + b_{xi}\, c\phi\, c\psi + b_{yi}\left(c\psi\, s\theta\, s\phi - c\theta\, s\psi\right) = c\theta_{1i}\left(a_i + r_{1i}\, c\alpha_i + r_{2i}\, c\left(\alpha_i + \theta_{2i}\right)\right) \qquad (3.69a)$$

$$q_{yi} = p_y + b_{xi}\, c\phi\, s\psi + b_{yi}\left(s\psi\, s\theta\, s\phi + c\theta\, c\psi\right) = s\theta_{1i}\left(a_i + r_{1i}\, c\alpha_i + r_{2i}\, c\left(\alpha_i + \theta_{2i}\right)\right) \qquad (3.69b)$$

$$q_{zi} = p_z - b_{xi}\, s\phi + b_{yi}\, c\phi\, s\theta = r_{1i}\, s\alpha_i + r_{2i}\, s\left(\alpha_i + \theta_{2i}\right) \qquad (3.69c)$$

3.4.2. Design Equation

Design equation or objective function can be introduced as one polynomial equation which does not contain joint variables such as θ_{1i} and θ_{2i} for our case. Therefore, they must be eliminated from Eqs. (3.69a-c). Variable parameter θ_{2i} is eliminated after some mathematical manipulations and two equations are obtained as follows;

$$r_{2i}^2 = \left(q_{xi}\, c\theta_{1i} + q_{yi}\, s\theta_{1i} - a_i - r_{1i}\, c\alpha_{1i}\right)^2 + \left(q_{zi} - r_{1i}\, s\alpha_{1i}\right)^2 \qquad (3.70)$$

$$q_{yi} = q_{xi}\, \tan\theta_{1i} \qquad (3.71)$$

Eq. (3.71) refers a right triangle which has a hypotenuse $\sqrt{q_{xi}^2 + q_{yi}^2}$. Therefore, the variable θ_{1i} can be eliminated from Eq. (3.70) and the design equation or objective function can be introduced as:

$$\left(\sqrt{q_{xi}^2 + q_{yi}^2} - a_i - r_{1i}\, c\alpha_i\right)^2 + \left(q_{zi} - r_{1i}\, s\alpha_i\right)^2 - r_{2i}^2 = 0 \qquad (3.72)$$

3.4.3. Analytical Solution for Three Precision Poses

In this problem, design parameters $\left(a_i, r_{1i}, r_{2i}\right)$ are calculated for given angles α_i and three poses. Objective function of legs for three precision poses can be obtained from Eq. (3.72) in the following form:

$$P_{1i}\,f_{1ij} + P_{2i}\,f_{2ij} + P_{3i}\,f_{3ij} - F_{ij} = 0 \qquad\qquad (3.73)$$

where $P_{1i} = a_i^2 + r_{1i}^2 - r_{2i}^2 + 2\,a_i\,r_{1i}\,c\alpha_i$, $P_{2i} = r_{1i}\,s\alpha_i$, $P_{3i} = a_i + r_{1i}\,c\alpha_i$, $f_{1ij} = 1$, $f_{2ij} = -2\,q_{zij}$,

$f_{3ij} = -2\sqrt{q_{xij}^2 + q_{yij}^2}$, $F_{ij} = -\left(q_{xij}^2 + q_{yij}^2 + q_{zij}^2\right)$ and number of precision poses is $j = 1, 2, 3$.
The synthesis problem is to find P_{1i}, P_{2i} and P_{3i} for a given set of $f_{1ij}, f_{2ij}, f_{3ij}$ and F_{ij}.
Firstly, using three given motion $(p_x,\ p_y,\ p_z,\ \psi,\ \phi,\ \theta)_j$ and the constant shape
parameters $(b_{xi},\ b_{yi})$ of the platform, the variable coordinates of spherical pairs B$_i$ $(q_{xij}$,
q_{yij}, $q_{zij})$ can be calculated from Eqs. (3.69a-c). Secondly, variable parameters
$(f_{1ij}, f_{2ij}, f_{3ij}$ and $F_{ij})$ of polynomial equation (Eq. (3.73)) can be specified. Then, constant
parameters P_{1i}, P_{2i} and P_{3i} of polynomial equation can be found from three linear
equations for each leg ($i = 1, 2, 3$). Finally, nine linear equations for three legs are obtained
in matrix form as:

$$S_i\,\mathbf{P}_i = \mathbf{F}_i \ (i = 1, 2, 3) \qquad\qquad (3.74)$$

where $S_i = \begin{bmatrix} f_{1i1} & f_{2i1} & f_{3i1} \\ f_{1i2} & f_{2i2} & f_{3i2} \\ f_{1i3} & f_{2i3} & f_{3i3} \end{bmatrix}$, $\mathbf{P}_i = \begin{bmatrix} P_{1i} \\ P_{2i} \\ P_{3i} \end{bmatrix}$ and $\mathbf{F}_i = \begin{bmatrix} F_{i1} \\ F_{i2} \\ F_{i3} \end{bmatrix}$.

Values of P_{1i}, P_{2i} and P_{3i} are found by multiplying both sides of Eq. (3.74) by the
inverse of matrix, as:

$$\mathbf{P}_i = S_i^{-1}\,\mathbf{F}_i \qquad\qquad (3.75)$$

Parameters of each leg is designed after finding values of P_{1i}, P_{2i} and P_{3i}. After selection of the angle α_i by designer, other design parameters are determined as follows;

$$r_{1i} = \frac{P_{2i}}{s\alpha_i}, \quad a_i = P_{3i} - r_{1i}\,c\alpha_i, \quad r_{2i} = \sqrt{a_i^2 + r_{1i}^2 + 2a_i r_{1i} c\alpha_i - P_{1i}} \qquad (3.76)$$

3.4.4. Numerical Example of Three Precision Poses

A 3 DoF spatial platform manipulator is to be synthesized for three precision poses (Figure 3.10). The prescribed motion is given in Table 3.11. The shape of platform is given by constant parameters $b_{x1} = 40.878$, $b_{y1} = 0$, $b_{x2} = -20.193$, $b_{y2} = 39.632$, $b_{x3} = -20.741$ and $b_{y3} = -39.009$. Incline angles are selected as $\alpha_1 = \alpha_2 = \alpha_3 = 110°$.

Table 3.11. Prescribed three poses for the platform of the manipulator

# of precision poses(j)	$\left(p_x,\ p_y,\ p_z,\ \theta,\ \phi,\ \psi\right)$
1	$\left(-2.23,\ -0.247,\ 133.7513,\ 0.9761°,\ -0.1906°,\ 0.3462°\right)$
2	$\left(-2.2022,\ 6.8252,\ 133.1189,\ 1.8598°,\ -0.8738°,\ 4.9079°\right)$
3	$\left(-2.143,\ 14.834,\ 131.7907,\ 3.111°,\ -1.8629°,\ 10.084°\right)$

Firstly, the coordinates of spherical pairs are obtained by using Eqs. (3.69a-c), and then, necessary matrices and columns in Eqs. (3.74), and (3.75) are calculated. After finding values of constant parameters, design parameters are determined by using Eq. (3.76). The design parameters of the platform manipulator (Figure 3.10) are shown in Table 3.12.

Table 3.12. Design parameters for the manipulator

I	r_{1i}	a_i	r_{2i}
1	$r_{11} = \dfrac{P_{21}}{s\alpha_1} = 58.5298$	$a_1 = P_{31} - r_{11}c\alpha_1 = 50.0184$	$r_{21} = \sqrt{a_1^2 + r_{11}^2 + 2a_1 r_{11} c\alpha_1 - P_{11}} = 79.36$
2	$r_{12} = \dfrac{P_{22}}{s\alpha_2} = 58.5298$	$a_2 = P_{32} - r_{12}c\alpha_2 = 65.0184$	$r_{22} = \sqrt{a_2^2 + r_{12}^2 + 2a_2 r_{12} c\alpha_2 - P_{12}} = 79.36$
3	$r_{13} = \dfrac{P_{23}}{s\alpha_3} = 58.5298$	$a_3 = P_{33} - r_{13}c\alpha_3 = 80.0184$	$r_{23} = \sqrt{a_3^2 + r_{13}^2 + 2a_3 r_{13} c\alpha_3 - P_{13}} = 79.36$

3.4.5. Numerical Solution for Four and Five Precision Poses

The four and the five poses of the manipulator's platform gives four and five nonlinear equations, respectively. The equations are determined by substituting relations between positions of spherical pairs B_i and poses of the platform in Eqs. (3.69a-c) into Eq. (3.72). The nonlinear equations are given as follows;

$$
\left(\left(\left(\left(p_{xj} + b_{xi}\, c\phi_j\ c\psi_j + b_{yi}\left(c\psi_j\, s\theta_j\, s\phi_j - c\theta_j\, s\psi_j \right) \right)^2 \right. \right. \right.
$$
$$
\left. \left. + \left(p_{yj} + b_{xi}\, c\phi_j\ s\psi_j + b_{yi}\left(s\psi_j\, s\theta_j\, s\phi_j + c\theta_j\, c\psi_j \right) \right)^2 \right)^{0.5} - K_i \right)^2 \tag{3.77}
$$
$$
\left. + \left(p_{zj} - b_{xi}\, s\phi_j + b_{yi}\, c\phi_j\, s\theta_j - r_{1yi} \right)^2 - r_{2i}^2 = 0 \right.
$$

where $K_i = a_i + r_{1xi}$, $r_{1xi} = r_{1i}c\alpha_i$, $r_{1yi} = r_{1i}s\alpha_i$. Note that a_i and r_{1xi} cannot be found separately. Hence, they will be calculated together. For five poses, number of precision poses is $j = 1, 2, 3, 4, 5$ and design parameters are $\left(b_{xi},\, b_{yi}, K_i, r_{1yi}, r_{2i}\right)$. On the other hand, design parameter r_{2i} can be selected freely for four poses. Therefore, design parameters are $\left(b_{xi},\, b_{yi}, K_i, r_{1yi}\right)$ and number of precision poses is $j = 1, 2, 3, 4$.

Analytical solution of two problems is very hard due to coupled terms such as multiplication of two design parameters and also square root. Therefore, a very well known numerical method, Newton-Raphson, is applied to the problems. Newton-Raphson method for nonlinear system of equations (Press et al. 1993, Chapter 9.6), is adapted to our problems. Furthermore, a Mathematica notebook is developed by using the presented method.

3.4.6. Numerical Example for Four Precision Poses

Design a 3 DoF spatial platform manipulator consisting of 3 C_sRS limb for four precision poses (Figure 3.10). The prescribed poses and initial guesses are given in Table 3.13 and Table 3.14 respectively. Select allowable error for design parameters as 10^{-4}. Let give one design parameter as $r_2 = 80$.

Table 3.13. Prescribed four poses for the platform of the manipulator

# of precision poses*(j)*	$\left(p_x,\ p_y,\ p_z,\ \theta,\ \phi,\ \psi \right)$
1	$(-2.23,\ -0.247,\ 133.7513,\ 0.9761°,\ -0.1906°,\ 0.3462°)$
2	$(-2.2022,\ 6.8252,\ 133.1189,\ 1.8598°,\ -0.8738°,\ 4.9079°)$
3	$(-1.9843,\ 25.2204,\ 128.850,\ 5.5674°,\ -3.1892°,\ 16.8815°)$
4	$(-1.1137,\ 41.1894,\ 120.2653,\ 14.351°,\ -4.8637°,\ 28.0428°)$

Four nonlinear equations are obtained by substituting prescribed poses into Eq.(3.77).

$$f_1\left(\mathbf{x} \right) = \left(\left(\left(-2.23 + 0.9999\,b_{xi} - 0.0061\,b_{yi} \right)^2 + \left(-0.247 + 0.0060\,b_{xi} + 0.9998\,b_{yi} \right)^2 \right)^{0.5} - K_i \right)^2$$

$$+ \left(133.751 + 0.0033\,b_{xi} + 0.0170\,b_{yi} - r_{1yi} \right)^2 - 6400 = 0$$

$$f_2(\mathbf{x}) = \left(\left(\left(-2.2022 + 0.9962\, b_{xi} - 0.086\, b_{yi} \right)^2 + \left(6.8251 + 0.0855\, b_{xi} + 0.9957\, b_{yi} \right)^2 \right)^{0.5} - K_i \right)^2$$

$$+ \left(133.119 + 0.0152\, b_{xi} + 0.0324\, b_{yi} - r_{1yi} \right)^2 - 6400 = 0$$

$$f_3(\mathbf{x}) = \left(\left(\left(-1.9843 + 0.9554\, b_{xi} - 0.2942\, b_{yi} \right)^2 + \left(25.2205 + 0.2899\, b_{xi} + 0.9508\, b_{yi} \right)^2 \right)^{0.5} - K_i \right)^2$$

$$+ \left(128.85 + 0.0556\, b_{xi} + 0.09686\, b_{yi} - r_{1yi} \right)^2 - 6400 = 0$$

$$f_4(\mathbf{x}) = \left(\left(\left(-1.1137 + 0.8794\, b_{xi} - 0.474\, b_{yi} \right)^2 + \left(41.1894 + 0.4684\, b_{xi} + 0.8452\, b_{yi} \right)^2 \right)^{0.5} - K_i \right)^2$$

$$+ \left(120.265 + 0.0847\, b_{xi} + 0.2469\, b_{yi} - r_{1yi} \right)^2 - 6400 = 0$$

where $\mathbf{x} = \left(b_{xi}, b_{yi}, K_i, r_{1yi} \right)^T$. Jacobian matrix is computed by using formulation in the study of (Press et. al., 1993). Then, design parameters are determined by using computer software (Mathematica) with initial guesses given in Table 3.14. Results for design parameters corresponding to initial guesses are given in Table 3.14.

Table 3.14 Initial guesses and results for four poses

#	Initial guess ($\mathbf{x}_0$) $\left(b_{x_{in}}, b_{y_{in}}, K_{in}, r_{1y_{in}} \right)$	Result $\left(b_{xi}, b_{yi}, K_i, r_{1yi} \right)$
1	$(-20.193,\ 39.692,\ 45,\ 55)$	$(-20.1935,\ 39.632,\ 45,\ 55)$
2	$(40.878,\ 0,\ 30, 55)$	$(40.88,\ 0,\ 30,\ 55)$
3	$(-20.741,\ -39.009,\ 60,\ 55)$	$(-20.7413,\ -39.0086,\ 60,\ 55)$
4	$(-20,\ -35,\ 16,\ 16)$	$(-42.4678,\ -97.7686, 133.054,\ 56.0685)$

3.4.7. Numerical Example for Five Precision Poses

A 3 DoF spatial platform manipulator is to be synthesized for five precision poses (Figure 3.10). The prescribed motion is given in Table 3.15. Use initial guesses given in Table 3.16. Note that allowable error for design parameters is selected as 10^{-6}.

Table 3.15. Prescribed five poses for the platform of the manipulator

# of precision poses(j)	$\left(p_x,\ p_y,\ p_z,\ \theta,\ \phi,\ \psi\right)$
1	$\left(-2.23,\ -0.247,\ 133.7513,\ 0.9761°,\ -0.1906°,\ 0.3462°\right)$
2	$\left(-2.2022,\ 6.8252,\ 133.1189,\ 1.8598°,\ -0.8738°,\ 4.9079°\right)$
3	$\left(-2.143,\ 14.834,\ 131.7907,\ 3.111°,\ -1.8629°,\ 10.084°\right)$
4	$\left(-1.9843,\ 25.2204,\ 128.850,\ 5.5674°,\ -3.1892°,\ 16.8815°\right)$
5	$\left(-1.1137,\ 41.1894,\ 120.2653,\ 14.351°,\ -4.8637°,\ 28.0428°\right)$

By substituting precision poses into Eq. (3.77), five nonlinear equations are found as follows,

$$f_1(\mathbf{x}) = \left(\left(\left(-2.23+0.9999\,b_{xi}-0.0061\,b_{yi}\right)^2+\left(-0.247+0.0060\,b_{xi}+0.9998\,b_{yi}\right)^2\right)^{0.5}-K_i\right)^2$$
$$+\left(133.751+0.0033\,b_{xi}+0.0170\,b_{yi}-r_{1yi}\right)^2-r_{2i}^2=0$$

$$f_2(\mathbf{x}) = \left(\left(\left(-2.2022+0.9962\,b_{xi}-0.086\,b_{yi}\right)^2+\left(6.8251+0.0855\,b_{xi}+0.9957\,b_{yi}\right)^2\right)^{0.5}-K_i\right)^2$$
$$+\left(133.119+0.0152\,b_{xi}+0.0324\,b_{yi}-r_{1yi}\right)^2-r_{2i}^2=0$$

$$f_3(\mathbf{x}) = \left(\left(\left(-2.143+0.984\,b_{xi}-0.1765\,b_{yi}\right)^2+\left(14.834+0.1749\,b_{xi}+0.9827\,b_{yi}\right)^2\right)^{0.5}-K_i\right)^2$$
$$+\left(131.791+0.0325\,b_{xi}+0.0542\,b_{yi}-r_{1yi}\right)^2-r_{2i}^2=0$$

$$f_4(\mathbf{x}) = \left(\left(\left(-1.9843 + 0.9554b_{xi} - 0.2942b_{yi}\right)^2 + \left(25.2205 + 0.2899b_{xi} + 0.9508b_{yi}\right)^2\right)^{0.5} - K_i\right)^2$$

$$+ \left(128.85 + 0.0556b_{xi} + 0.09686b_{yi} - r_{1yi}\right)^2 - r_{2i}^2 = 0$$

$$f_5(\mathbf{x}) = \left(\left(\left(-1.1137 + 0.8794b_{xi} - 0.474b_{yi}\right)^2 + \left(41.1894 + 0.4684b_{xi} + 0.8452b_{yi}\right)^2\right)^{0.5} - K_i\right)^2$$

$$+ \left(120.265 + 0.0847b_{xi} + 0.2469b_{yi} - r_{1yi}\right)^2 - r_{2i}^2 = 0$$

where $\mathbf{x} = \left(b_{xi}, b_{yi}, K_i, r_{1yi}, r_{2i}\right)^T$. Procedure of five poses synthesis is very similar to four poses. But one difference is that the size of jacobian matrix and other vectors are more. Jacobian matrix is computed before the calculation of the design parameters with initial guesses given in Table 3.16. Results for design parameters corresponding to initial guesses are given in Table 3.16.

Table 3.16. Initial guesses and results for five poses

#	Initial guess $(\mathbf{x}_0)$ $\left(b_{x_{in}}, b_{y_{in}}, K_{in}, r_{1y_{in}}, r_{2_{in}}\right)$	Result $\left(b_{xi}, b_{yi}, K_i, r_{1yi}, r_{2i}\right)$
1	$(-20.193,\ 39.632,\ 45,\ 55,\ 79.36)$	$(-20.1935,\ 39.632,\ 45,\ 55,\ 79.36)$
2	$(-20.741,\ -39.009,\ 60,\ 55,\ 79.36)$	$(-20.7413,\ -39.0086,\ 60,\ 55,\ 79.36)$
3	$(40.878,\ 0,\ 30,\ 55,\ 79.36)$	$(40.88,\ 0,\ 30,\ 55,\ 79.36)$
4	$(20,\ 20,\ 30,\ 15,\ 10)$	$(28.5167,\ 29.7369,\ 46.1567,\ 2.62538,\ 131.895)$

Four different manipulators, which satisfy precision poses in Table 3.11, can be constructed by combining the four results in Table 3.16. Let select $r_{1xi} = -20$ and then other parameter (a) is calculated by using $a_i = K_i - r_{1xi}$ which is mentioned in Eq. (3.67). Figure 3.11 and Figure 3.12 depict the manipulators constructed by using the first three results (1,2,3) and the last three results (2,3,4) as the C_sRS chains, respectively.
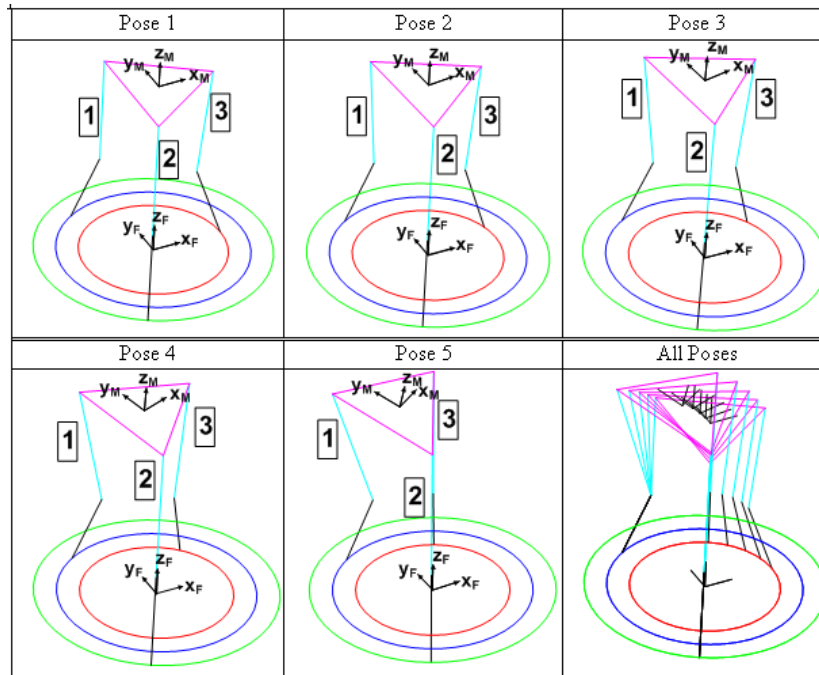
Figure 3.11. Five poses of a manipulator constructed by using the first three results (1,2,3)
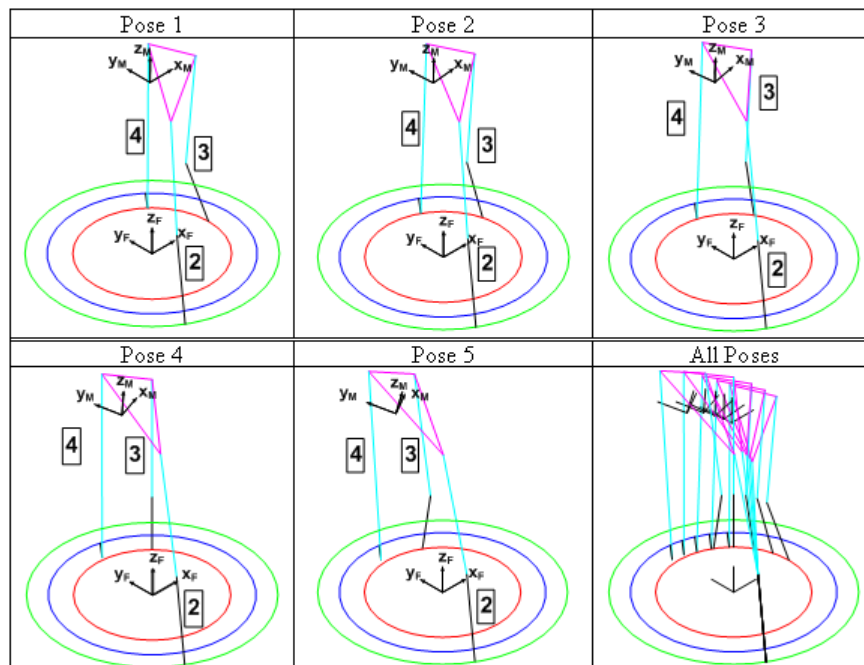
Figure 3.12. Five poses of a manipulator constructed by using the last three results (2,3,4)

74

CHAPTER 4
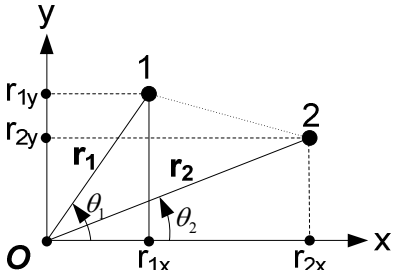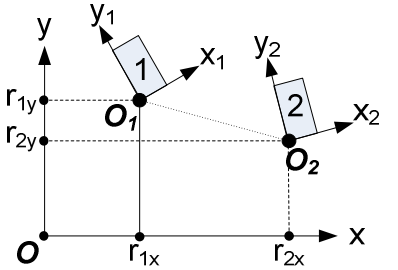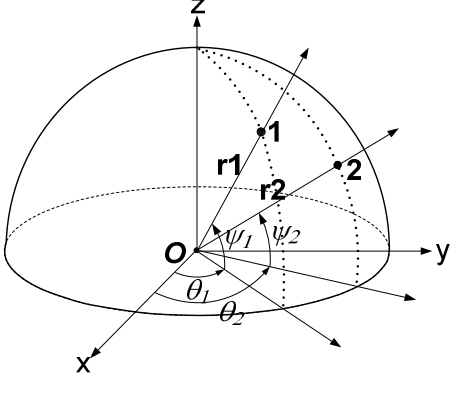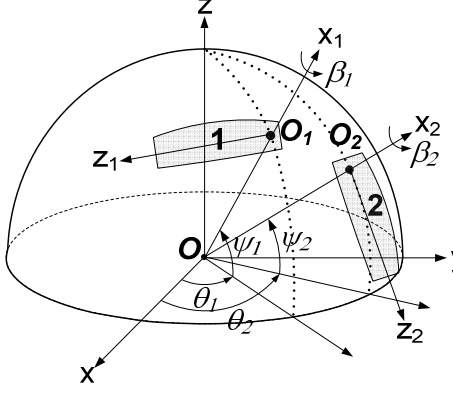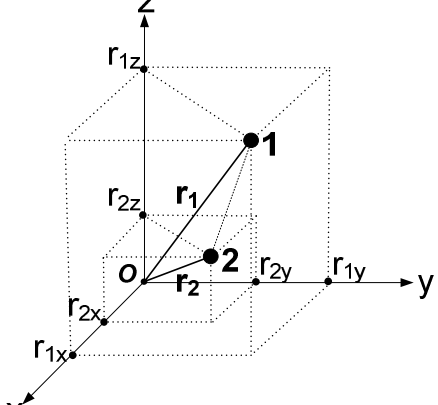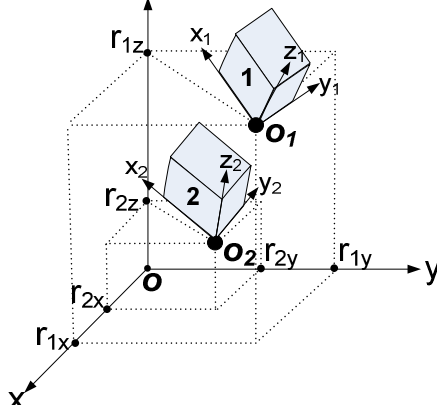
KINEMATIC ANALYSIS OF PARALLEL ROBOT MANIPULATORS

4.1. Introduction to Kinematic Analysis of Manipulators

Kinematic analysis is to investigate displacement of manipulators (and mechanisms) and also variation of displacement in a specified time. It must be noted that displacement of a rigid body is different from displacement of a point. In Table 4.1.a, displacement of a point on plane can be described by x and y projections (r_{1x}, r_{1y}) where as displacement of a rigid body on plane needs three independent variables that are x and y projections (r_{1x}, r_{1y}) and direction of one moving axis (x_1 or y_1). Origin O and axes x, y construct fixed coordinate system. There is no change in this system when time is changing. On the other hand, origin O_1 and axes x_1, y_1 defines moving coordinate system. Position of origin (r_{1x}, r_{1y}) and direction of axes (x_1, y_1) may vary when time is running. For instance, the rigid body is moved from first pose (r_{1x}, r_{1y}, $O_1x_1y_1$) to second pose (r_{2x}, r_{2y}, $O_2x_2y_2$). Displacement on sphere is very similar to displacement on plane. Three parameters (θ_1, ψ_1, β_1) are enough to describe displacement of a rigid body on sphere while two parameters (θ_1, ψ_1) are required to describe displacement of a point. The parameters are different for displacement on space. Three position parameters (r_{1x}, r_{1y}, r_{1z}) define displacement of a point on space. However, six parameters are necessary to describe displacement of a rigid body. Three of them are position parameters (r_{1x}, r_{1y}, r_{1z}) and remaining three are direction cosine or orientation parameters of $O_1x_1y_1z_1$ coordinate system. It is clear that $O_1x_1y_1z_1$ coordinate system has nine elements however axes are orthogonal and also they are unit vectors. Using these conditions, six of these nine elements can be written in terms of other three independent elements. Cartesian system is commonly used in kinematics. But, it is also possible to use polar and spherical coordinate systems

when it is necessary. When displacement of a point on plane is defined in polar coordinate system, the parameters ($\|\mathbf{r_1}\|$, θ_1) will be used instead of the parameters (r_{1x}, r_{1y}).

Table 4.1. Displacements of a point and a rigid body on (a) plane (b) sphere (c) space

	geometry	Displacement of a point	Displacement of a rigid body
(a)	Plane		
(b)	Sphere		
(c)	Space		

Two mathematical models are possible to investigate relations between actuated joint variables and location of end-effector for a specified geometry of parallel manipulator. The first one, inverse kinematics is to find actuated joint variables for a specified location of end-effector. The second one, direct kinematics is to determine the location of end-effector for specified actuated joint variables. Inverse kinematics is generally easier than direct kinematics for closed-loop mechanical system such as a parallel manipulator. Velocity analysis is variation of position in a specified time. That is, time derivative of position gives velocity of a mechanism or parallel manipulator.

4.2. Methods for kinematic analysis

There are several methods to investigate displacement and variation of displacement of a manipulator or mechanism. Graphical approach is an easy way with computer but it is not usable when full motion of manipulator is considered. Therefore, analytical approach is convenient to describe full motion of manipulator. Some analytical methods are vector algebra method, complex algebra method (for planar manipulators and mechanisms), rotation matrix method, homogeneous transformation matrix method, quaternion, screw algebra, recurrent screw equations. In this section, some of the methods are presented to explain next sections.

4.2.1. Vector Algebra Method

In this method, unit vector $\mathbf{i}, \mathbf{j}, \mathbf{k}$ are used to describe vectors parallel to x, y and z axes, respectively. For instance, in Table 4.1.a, planar vector $\mathbf{r_1}$ can be written as, $\mathbf{r_1} = r_{1x}\,\mathbf{i} + r_{1y}\,\mathbf{j}$. Similarly, spherical vector $\mathbf{r_1}$ in Table 4.1.b is expressed as $\mathbf{r_1} = r\,c\theta_1\,c\psi_1\,\mathbf{i} + r\,s\theta_1\,c\psi_1\,\mathbf{j} + r\,s\psi_1\,\mathbf{k}$. It is easy to see that spatial vector $\mathbf{r_1}$ in Table 4.1.c is equal to $r_{1x}\,\mathbf{i} + r_{1y}\,\mathbf{j} + r_{1z}\,\mathbf{k}$. Relative displacement on space between two positions can be calculated by subtracting two vectors: $\Delta\mathbf{r} = \mathbf{r_2} - \mathbf{r_1} = \left(r_{2x} - r_{1x}\right)\mathbf{i} + \left(r_{2y} - r_{1y}\right)\mathbf{j} + \left(r_{2z} - r_{1z}\right)\mathbf{k}$.

This method can be used both planar and spatial manipulators, mechanisms. But it is worthy to note that rotations of a body cannot be easily expressed by this method. Therefore, rotation matrix and quaternion approaches are developed to overcome this problem.

4.2.2. Complex Algebra Method

This method is convenient for only planar mechanisms - manipulators. Using complex algebra method, vector is represented in two parts such as real and imaginary. Axis x refers to real part while axis y defines imaginary part. If planar vector $\mathbf{r_1}$ in Table 4.1.(a) is used as an example, vector is represented in complex form as $\mathbf{r_1} = r_{1x} + j\,r_{1y}$ where j is unit imaginary number ($j = \sqrt{-1}$). In polar form, vector will be $\mathbf{r_1} = \|\mathbf{r_1}\|\cos(\theta_1) + j\|\mathbf{r_1}\|\sin(\theta_1)$. Recall that well known Euler equation, $e^{\pm j\theta} = \cos\theta \pm j\sin\theta$. Therefore, vector is represented in complex polar form as $\mathbf{r_1} = \|\mathbf{r_1}\|e^{j\theta}$. The magnitude and direction of the vector is clearly distinguished. Fortunately, differentiation of vectors in this form is simpler than same vectors in other form.

4.2.3. Rotation Matrix Method

Spherical mechanisms and manipulators have only rotational degrees of freedom. Therefore, displacement of these kind manipulators can be completely defined by rotation matrices. Rotation matrix can be derived from rotation of a vector about an axis. Rodrigues formula represents correlation between the vector and rotated vector. Elementary rotation matrices can be derived from Rodriques formula.

Euler angle sequences are developed to define any orientation in space. For example, in aerospace engineering, yaw-pitch-roll sequence is frequently used to describe orientation of airplane with respect to earth. The sequences are also identified with the order of selected axes.

Table 4.2. Elementary rotation matrices
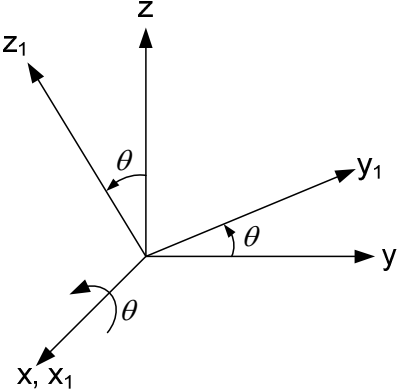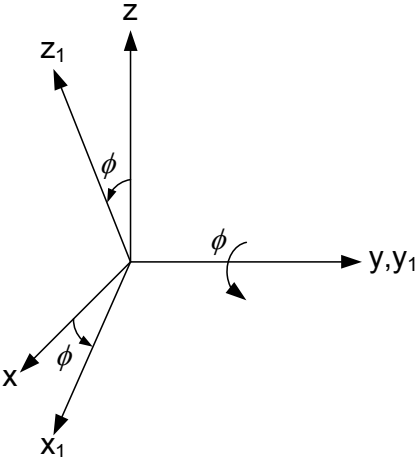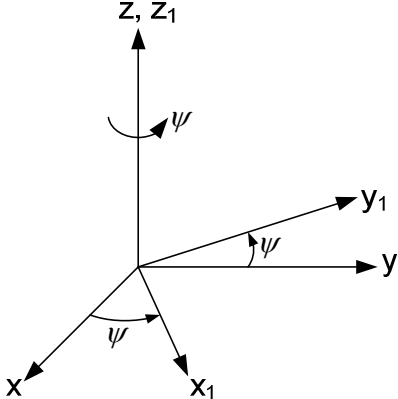
Axis of rotation	Illustration	Rotation Matrix
x		$R(x,\theta) = \begin{bmatrix} 1 & 0 & 0 \\ 0 & c\theta & -s\theta \\ 0 & s\theta & c\theta \end{bmatrix}$
y		$R(y,\phi) = \begin{bmatrix} c\phi & 0 & s\phi \\ 0 & 1 & 0 \\ -s\phi & 0 & c\phi \end{bmatrix}$
z		$R(z,\psi) = \begin{bmatrix} c\psi & -s\psi & 0 \\ s\psi & c\psi & 0 \\ 0 & 0 & 1 \end{bmatrix}$

Table 4.3. Euler angle sequences

Axes of sequence	Matrices
z-y-x	$R = R(z,\psi)R(y,\phi)R(x,\theta) = \begin{bmatrix} c\phi\,c\psi & c\psi\,s\theta\,s\phi - c\theta\,s\psi & c\theta\,c\psi\,s\phi + s\theta\,s\psi \\ c\phi\,s\psi & c\theta\,c\psi + s\theta\,s\phi\,s\psi & -c\psi\,s\theta + c\theta\,s\phi\,s\psi \\ -s\phi & c\phi\,s\theta & c\phi\,c\theta \end{bmatrix}$
z-y-z	$R = R(z,\psi)R(y,\phi)R(z,\theta) = \begin{bmatrix} c\theta\,c\phi\,c\psi - s\theta\,s\psi & -c\phi\,c\psi\,s\theta - c\theta\,s\psi & s\phi\,c\psi \\ c\theta\,c\phi\,s\psi + s\theta\,c\psi & c\theta\,c\psi - c\phi\,s\theta\,s\psi & s\phi\,s\psi \\ -s\phi\,c\theta & s\phi\,s\theta & c\phi \end{bmatrix}$

4.2.4. Homogenous Transformation Matrix Method

Any displacement of a rigid body on space can be completely defined by homogenous transformation matrix. Homogenous transformation matrices have one more row and column then rotation matrices. Therefore, these matrices are 4 by 4 elements. Transformation matrix includes both orientation and position of a rigid body. The first three columns and three rows define orientation of the rigid body where as the last column of matrix identifies translation.

$$\mathbf{T} = \begin{bmatrix} \mathbf{R}_{3\times3} & \mathbf{P}_{3\times1} \\ \mathbf{0}_{1\times3} & 1 \end{bmatrix} \tag{4.1}$$

where $\mathbf{R}$ is rotation matrix, $\mathbf{P}$ is translation vector, and $\mathbf{0}_{1\times3}$ is a row having only zeros. $\left(\mathbf{0}_{1\times3} = \begin{pmatrix} 0 & 0 & 0 \end{pmatrix} \right)$
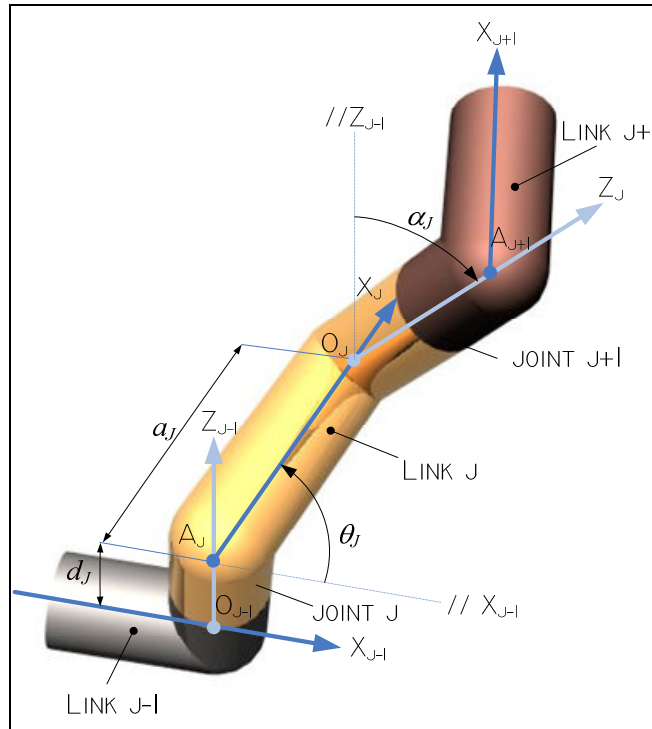
Figure 4.1. Denavit –Hartenberg parameters

Denavit and Hartenberg developed a notation to analyze single-loop lower-pair linkages by labeling the links systematically. After labeling, homogenous transformation matrices are written with Denavit-Hartenberg (D-H) parameters. As an advantage of the method, once homogenous transformation matrix is constructed for every single link of linkage, loop-closure matrix equation can be easily obtained by multiplying matrices successively. The D-H parameters on serial open chain are shown in Figure 4.1. However, geometric definition of closed chains can be also possible by using cyclic numbers for J. The placement of joint and link axes is important and recursive. The Z_{J-1} joint axis and Z_J-joint axis are placed on direction of joint motion. The X_J-axis is common normal and it is always perpendicular to both Z_{J-1} and Z_J joint axes. The right-hand rule can be used for the y_J-axis. But, note that the y_J-axis is not necessary in most cases.

There are four D-H parameters such that two joint parameters (d_J, θ_J) and two link parameters (a_J, α_J). The following parameters are defined for the construction of the links.

d_J : translational distance measured from the axis X_{J-1} to the axis X_J along direction of the axis Z_{J-1}. (*Joint offset*)

θ_J: joint angle measured from the axis X_{J-1} to the axis X_J around the direction of the axis Z_{J-1}. (*Angle of rotation*)

a_J: distance between the joint axes Z_{J-1} and Z_J along the axis X_J. (*Link length*)

α_J: angle between the joint axes Z_{J-1} and Z_J around the axis X_J. (*Twist Angle*)

Revolute, prismatic and cylindrical joints can be easily identified with the D-H parameters. Table 4.4 depicts variable and constant parameters for these joint types. The parameters of other joints such as spherical, spherical in torus, hooke, planar joints can be achieved by combining kinematic exchangeability and parameters of revolute and prismatic joints.

Table 4.4. Variable and constant parameters for j th joint

J th joint type	Variable parameters	Constant parameters
revolute joint	θ_J	d_J, a_J, α_J
prismatic joint	d_J	θ_J, a_J, α_J
cylindrical joint	d_J, θ_J	a_J, α_J

Once coordinate systems and the parameters are defined, the homogenous transformation matrix can be constructed between link $J-1$ and J. The following rotations and translations define D-H transformation.

1.   The $O_{J-1}X_{J-1}Z_{J-1}$ coordinate system is translated by joint offset d_J along the axis Z_{J-1}. After this translation, the origin O_{J-1} coincidence with A_J. The transformation matrix contains only translation and rotation matrix is equal to identity matrix. Therefore,

$$T\left(z_{J-1}, d_J\right) = \begin{bmatrix} 1 & 0 & 0 & 0 \\ 0 & 1 & 0 & 0 \\ 0 & 0 & 1 & d_J \\ 0 & 0 & 0 & 1 \end{bmatrix}$$

2. The translated coordinate system is now rotated by angle of rotation θ_J along the axis z_{J-1}. Then, the transformation matrix is

$$T\left(z_{J-1}, \theta_J\right) = \begin{bmatrix} c\theta_J & -s\theta_J & 0 & 0 \\ s\theta_J & c\theta_J & 0 & 0 \\ 0 & 0 & 1 & 0 \\ 0 & 0 & 0 & 1 \end{bmatrix}$$

3. The new coordinate system is translated again by link length a_J along the axis x_J. Hence,

$$T\left(x_J, a_J\right) = \begin{bmatrix} 1 & 0 & 0 & a_J \\ 0 & 1 & 0 & 0 \\ 0 & 0 & 1 & 0 \\ 0 & 0 & 0 & 1 \end{bmatrix}$$

4. Finally, the last coordinate system is rotated by twist angle α_J about the axis x_J. The transformation matrix is

$$T\left(x_J, \alpha_J\right) = \begin{bmatrix} 1 & 0 & 0 & 0 \\ 0 & c\alpha_J & -s\alpha_J & 0 \\ 0 & s\alpha_J & c\alpha_J & 0 \\ 0 & 0 & 0 & 1 \end{bmatrix}$$

The destination coordinate system $O_J X_J Z_J$ is reached after all these transformations. Overall transformation can be calculated by multiplying all matrices successively. Then, the overall transformation matrix is written in the following form.

$$\mathbf{T}_{J-1,J} = \begin{bmatrix} c\theta_J & -c\alpha_J s\theta_J & s\alpha_J s\theta_J & a_J c\theta_J \\ s\theta_J & c\alpha_J c\theta_J & -s\alpha_J c\theta_J & a_J s\theta_J \\ 0 & s\alpha_J & c\alpha_J & d_J \\ 0 & 0 & 0 & 1 \end{bmatrix} \qquad (4.2)$$

4.3. Inverse Analysis of a Three DoF Planar Parallel Manipulator

A three DoF planar robot manipulator is depicted in Figure 4.2. This manipulator constructed by three RR dyads. Manipulator is actuated by angle of rotations θ_1, θ_2 and θ_3. Link lengths and other geometric parameters are defined as $|O_1A_1| = L_1$, $|A_1B_1| = L_2$, $|O_2A_2| = L_3$, $|A_2B_2| = L_4$, $|O_3A_3| = L_5$, $|A_3B_3| = L_6$, $|O_MB_1| = |O_MB_2| = |O_MB_3| = b$, $|O_1O_2| = d_1$, $|O_1O_3| = d_2$, $\angle xO_1O_2 = \alpha_1$, $\angle xO_1O_3 = \alpha_2$.
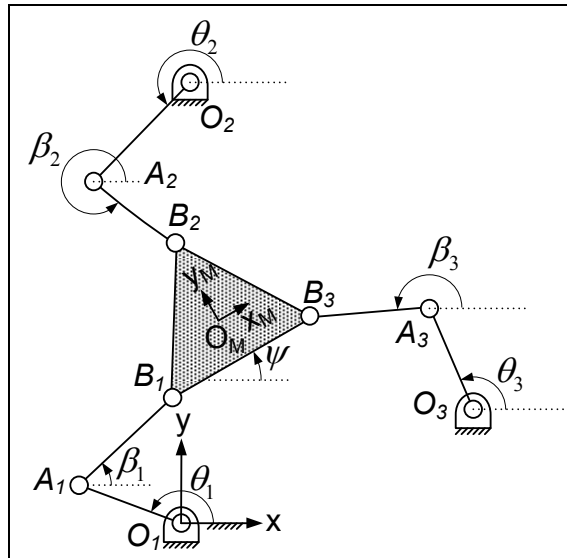
Figure 4.2. A three DoF planar robot manipulator

In order to solve position problem, necessary displacement equations must be obtained. Corner points of triangle and vector loop-closure equations for each dyad are written as follows,

$$\overline{O_1B_i} = \overline{O_1O_M} + \overline{O_MB_i}, \quad \overline{O_1O_i} + \overline{O_iA_i} + \overline{A_iB_i} = \overline{O_1B_i}, \quad i = 1,2,3 \tag{4.3}$$

All vectors in Eq(4.2) can be described by using unit vectors mentioned in vector algebra method. Therefore, the vectors become,

For $\quad i = 1, \quad \overline{O_1A_1} = L_1 c\theta_1 \mathbf{i} + L_1 s\theta_1 \mathbf{j}, \quad \overline{A_1B_1} = L_2 c\beta_1 \mathbf{i} + L_2 s\beta_1 \mathbf{j}, \quad \overline{O_1O_1} = 0\mathbf{i} + 0\mathbf{j},$

$$\overline{O_MB_1} = b c\left(\psi + \frac{7\pi}{6}\right)\mathbf{i} + b s\left(\psi + \frac{7\pi}{6}\right)\mathbf{j}.$$

For $\quad i = 2, \quad \overline{O_2A_2} = L_3 c\theta_2 \mathbf{i} + L_3 s\theta_2 \mathbf{j}, \quad \overline{A_2B_2} = L_4 c\beta_2 \mathbf{i} + L_4 s\beta_2 \mathbf{j}, \quad \overline{O_1O_2} = d_1 c\alpha_1 \mathbf{i} + d_1 s\alpha_1 \mathbf{j},$

$$\overline{O_MB_2} = b c\left(\psi + \frac{\pi}{2}\right)\mathbf{i} + b s\left(\psi + \frac{\pi}{2}\right)\mathbf{j}.$$

For $\quad i = 3, \quad \overline{O_3A_3} = L_5 c\theta_3 \mathbf{i} + L_5 s\theta_3 \mathbf{j}, \quad \overline{A_2B_2} = L_6 c\beta_3 \mathbf{i} + L_6 s\beta_3 \mathbf{j}, \quad \overline{O_1O_3} = d_2 c\alpha_2 \mathbf{i} + d_2 s\alpha_2 \mathbf{j},$

$$\overline{O_MB_3} = b c\left(\psi - \frac{\pi}{6}\right)\mathbf{i} + b s\left(\psi - \frac{\pi}{6}\right)\mathbf{j}.$$

If the calculated vectors are substituted into Eq.(4.3), we get the following vector equations, respectively

$$\overline{O_1B_1} = \overline{O_1O_M} + \overline{O_MB_1} = \left(R_x + b\left(-\frac{\sqrt{3}}{2}c\psi + \frac{1}{2}s\psi\right)\right)\mathbf{i} + \left(R_y + b\left(-\frac{1}{2}c\psi - \frac{\sqrt{3}}{2}s\psi\right)\right)\mathbf{j} \tag{4.4}$$

$$\overline{O_1B_2} = \overline{O_1O_M} + \overline{O_MB_2} = \left(R_x - b s\psi\right)\mathbf{i} + \left(R_y + b c\psi\right)\mathbf{j} \tag{4.5}$$

$$\overline{O_1B_3} = \overline{O_1O_M} + \overline{O_MB_3} = \left(R_x + b\left(\frac{\sqrt{3}}{2}c\psi + \frac{1}{2}s\psi\right)\right)\mathbf{i} + \left(R_y + b\left(-\frac{1}{2}c\psi + \frac{\sqrt{3}}{2}s\psi\right)\right)\mathbf{j} \tag{4.6}$$

$$\overline{O_1O_1} + \overline{O_1A_1} + \overline{A_1B_1} = \left(L_1\,c\theta_1 + L_2\,c\beta_1\right)\mathbf{i} + \left(L_1\,s\theta_1 + L_2\,s\beta_1\right)\mathbf{j}$$

$$= \left(R_x + b\left(-\frac{\sqrt{3}}{2}c\psi + \frac{1}{2}s\psi\right)\right)\mathbf{i} + \left(R_y + b\left(-\frac{1}{2}c\psi - \frac{\sqrt{3}}{2}s\psi\right)\right)\mathbf{j} \tag{4.7}$$

$$\overline{O_1O_2} + \overline{O_2A_2} + \overline{A_2B_2} = \left(d_1c\alpha_1 + L_3\,c\theta_2 + L_4\,c\beta_2\right)\mathbf{i} + \left(d_1\,s\alpha_1 + L_3\,s\theta_2 + L_4\,s\beta_2\right)\mathbf{j}$$

$$= \left(R_x - b\,s\psi\right)\mathbf{i} + \left(R_y + b\,c\psi\right)\mathbf{j} \tag{4.8}$$

$$\overline{O_1O_3} + \overline{O_3A_3} + \overline{A_3B_3} = \left(d_2c\alpha_2 + L_5\,c\theta_3 + L_6\,c\beta_3\right)\mathbf{i} + \left(d_2\,s\alpha_2 + L_5\,s\theta_3 + L_6\,s\beta_3\right)\mathbf{j}$$

$$= \left(R_x + b\left(\frac{\sqrt{3}}{2}c\psi + \frac{1}{2}s\psi\right)\right)\mathbf{i} + \left(R_y + b\left(-\frac{1}{2}c\psi + \frac{\sqrt{3}}{2}s\psi\right)\right)\mathbf{j} \tag{4.9}$$

Eq.(4.4), Eq.(4.5) and Eq.(4.6) are equal to Eq.(4.7), Eq.(4.8) and Eq.(4.9), respectively. After equating Eq.(4.4) and Eq.(4.7), the following two scalar equations are calculated by separating coefficients of i and j unit vectors.

$$L_2\,c\beta_1 = R_x + b\left(-\frac{\sqrt{3}}{2}c\psi + \frac{1}{2}s\psi\right) - L_1\,c\theta_1 \tag{4.10}$$

$$L_2\,s\beta_1 = R_y + b\left(-\frac{1}{2}c\psi - \frac{\sqrt{3}}{2}s\psi\right) - L_1\,s\theta_1 \tag{4.11}$$

Now, we will deal with only the first dyad. Calculations for other dyads are similar to the first one. The joint angle β_1 is eliminated by squaring Eqs.(4.10) and (4.11). The result is,

$$b^2 + L_1^2 + R_x^2 + R_y^2 - L_2^2 - 2L_1\,R_x\,c\theta_1 - 2L_1\,R_y\,s\theta_1 - b\,c\psi\left(\sqrt{3}\,R_x + R_y\right)$$

$$+ b\,s\psi\left(-\sqrt{3}\,R_y + R_x\right) + \sqrt{3}\,b\,L_1\left(c\theta_1\,c\psi + s\theta_1\,s\psi\right) + b\,L_1\left(s\theta_1\,c\psi - c\theta_1\,s\psi\right) = 0 \tag{4.12}$$

If similar process is applied to the second and third dyad, equations become,

$$b^2 + d_1^2 + L_3^2 + R_x^2 + R_y^2 - L_4^2 - 2d_1\left(R_x c\alpha_1 + R_y s\alpha_1\right) - 2L_3\left(R_x c\theta_2 + R_y s\theta_2\right) + 2b\left(R_y c\psi - R_x s\psi\right)$$
$$+ 2d_1 L_3\left(c\alpha_1 c\theta_2 + s\alpha_1 s\theta_2\right) + 2bd_1\left(-c\psi s\alpha_1 + c\alpha_1 s\psi\right) + 2bL_3\left(-c\psi s\theta_2 + c\theta_2 s\psi\right) = 0$$

$$b^2 + d_2^2 + L_5^2 + R_x^2 + R_y^2 - L_6^2 - 2d_2\left(R_x c\alpha_2 + R_y s\alpha_2\right) - 2L_5\left(R_x c\theta_3 + R_y s\theta_3\right) + b\left(-R_y c\psi + R_x s\psi\right)$$
$$+ \sqrt{3}\,b\left(R_x c\psi + R_y s\psi\right) + 2d_2 L_5\left(c\alpha_2 c\theta_3 + s\alpha_2 s\theta_3\right) + bd_2\left(c\psi s\alpha_2 - c\alpha_2 s\psi\right)$$
$$- \sqrt{3}\,bd_2\left(c\psi c\alpha_2 + s\alpha_2 s\psi\right) + bL_5\left(c\psi s\theta_3 - c\theta_3 s\psi\right) - \sqrt{3}\,bL_5\left(c\psi c\theta_3 + s\theta_3 s\psi\right) = 0$$

Eq.(4.12) is rearranged as,

$$A_1 c\theta_1 + B_1 s\theta_1 + C_1 = 0 \tag{4.13}$$

where $A_1 = -2L_1 R_x + \sqrt{3}\,bL_1 c\psi - bL_1 s\psi$, $\qquad\qquad B_1 = -2L_1 R_y + bL_1 c\psi + \sqrt{3}\,bL_1 s\psi$,

$C_1 = b^2 + L_1^2 + R_x^2 + R_y^2 - L_2^2 - bc\psi\left(\sqrt{3}\,R_x + R_y\right) + bs\psi\left(-\sqrt{3}\,R_y + R_x\right)$. $\qquad$ By $\qquad$ using

trigonometric identities $\quad \cos(\theta_1) = \dfrac{1-t^2}{1+t^2}$, $\sin(\theta_1) = \dfrac{2t}{1+t^2}$ where $\tan(\theta_1/2) = t$, two

unknowns ($c\theta_1, s\theta_1$) are reduced to one unknown (t),

$$\left(C_1 - A_1\right)t^2 + 2B_1 t + \left(C_1 + A_1\right) = 0 \tag{4.14}$$

Solution of second order Eq.(4.12) is well known and for the first rotation angle ,

$$\theta_1 = 2\arctan\left(\frac{-B_1 \mp \sqrt{B_1^2 + A_1^2 - C_1^2}}{C_1 - A_1}\right) \tag{4.15}$$

Eq.(4.15) can be generalized for all angles,

$$\theta_i = 2\arctan\left(\frac{-B_i \mp \sqrt{B_i^2 + A_i^2 - C_i^2}}{C_i - A_i}\right) \tag{4.16}$$

where $i = 1, 2, 3$, $A_2 = -2 L_3 R_x + 2 d_1 L_3 c\alpha_1 + 2 b L_3 s\psi$, $B_2 = -2 L_3 R_y - 2 b L_3 c\psi + 2 d_1 L_3 s\alpha_1$,

$C_2 = b^2 + d_1^2 + L_3^2 + R_x^2 + R_y^2 - L_4^2 - 2 d_1 \left(R_x c\alpha_1 + R_y s\alpha_1 \right) + 2 b \left(R_y c\psi - R_x s\psi \right) + 2 b d_1 \left(-c\psi s\alpha_1 + c\alpha_1 s\psi \right)$

, $A_3 = -2 L_5 R_x + 2 d_2 L_5 c\alpha_2 - \sqrt{3} b L_5 c\psi - b L_5 s\psi$, $B_3 = -2 L_5 R_y + b L_5 c\psi + 2 d_2 L_5 s\alpha_2 - \sqrt{3} b L_5 s\psi$,

$C_3 = b^2 + d_1^2 + L_5^2 + R_x^2 + R_y^2 - L_6^2 - 2 d_2 \left(R_x c\alpha_2 + R_y s\alpha_2 \right) + b \left(-R_y c\psi + R_x s\psi \right) + \sqrt{3} b \left(R_x c\psi + R_y s\psi \right)$

$+ b d_2 \left(c\psi s\alpha_2 - c\alpha_2 s\psi \right) + \sqrt{3} b d_2 \left(-c\psi c\alpha_2 - s\alpha_2 s\psi \right)$

Let illustrate the analysis on an numerical example. Geometric parameters of manipulator are selected as $L_1 = L_2 = L_3 = L_5 = 100$, $L_4 = 200$, $L_6 = 150$, $b = 50$, $d_1 = 200$, $d_3 = 300$, $\alpha_1 = 90°$, $\alpha_2 = 30°$. Pose of platform is also given: $R_x = 150$, $R_y = 150$, $\psi = 30°$. If these numerical data is substituted into Eq.(4.16), two results for each rotation of angle are calculated. These results cause eight possible manipulator cases as tabulated in Table 4.5.

Table 4.5. Eight possible manipulator cases

Table 4.5.(cont.) Eight possible manipulator cases

4.4. Inverse and Direct Position Analyses of a Three DoF Parallel Manipulator

In this part, direct and inverse position analyses of a three DoF parallel manipulator are introduced. It is shown that generally inverse position analysis problem of a parallel manipulator is easier than direct position analysis. Therefore, a numerical example of direct position analysis is presented. The twelve real results of nonlinear equations are given and the corresponding assembly configurations are illustrated in a table.

4.4.1. Inverse Position Analysis

Inverse kinematics problem is to find sliding angles (θ_{11}, θ_{12} and θ_{13}) for given the location of moving platform ($p_x, p_y, p_z, \psi, \phi$ and θ) as shown in Figure 3.10.

By dividing both sides of Eqs. (3.69a) and (3.69b), the sliding angles are determined in Eq. (4.17).

$$\theta_{1i} = \text{Atan}_2 \begin{pmatrix} p_y + b_{xi}\, c\phi\, s\psi + b_{yi}\left(s\psi\, s\theta\, s\phi + c\theta\, c\psi\right), \\ p_x + b_{xi}\, c\phi\, c\psi + b_{yi}\left(c\psi\, s\theta\, s\phi - c\theta\, s\psi\right) \end{pmatrix} \tag{4.17}$$

where Atan_2 is a two-argument arctangent function that result one unique solution for the angle.

4.4.2. Direct Position Analysis

Direct kinematics problem is to determine the location of moving platform ($p_x, p_y, p_z, \psi, \phi$ and θ) for given inputs (θ_{11}, θ_{12} and θ_{13}). The angle of rotation θ_{2i} is variable and it must be eliminated from Eqs. (3.69 a-c). Recall that this angle is eliminated in Eqs. (3.70) and (3.71).

Platform shape of manipulator is a triangle so that distance between points B_1, B_2 and B_3 is constant. Therefore,

$$\left(q_{xj} - q_{xi}\right)^2 + \left(q_{yj} - q_{yi}\right)^2 + \left(q_{zj} - q_{zi}\right)^2 = \left(b_{xj} - b_{xi}\right)^2 + \left(b_{yj} - b_{yi}\right)^2 \tag{4.18}$$

where $j = \text{mod}\left(i+1,3\right)$ and $i = 1$, 2, 3.

Nine nonlinear equations can be obtained in terms of nine variables for $i = 1$, 2, 3 by using Eqs. (3.70), (3.71) and (4.18). Analytical solution of these equations is very hard and complex. Therefore equations can be solved by using numerical methods when constant parameters of manipulator are given. Furthermore, "*NSolve*" in Mathematica program which is a numerical equation solver command that can be utilized to solve these equations. When position vectors of spherical pairs with respect to fix coordinate system

are determined, the location of platform can be found by solving system of linear equations as follows,

$$q_{xi} = p_x + b_{xi}\, u_x + b_{yi}\, v_x \tag{4.19a}$$

$$q_{yi} = p_y + b_{xi}\, u_y + b_{yi}\, v_y \tag{4.19b}$$

$$q_{zi} = p_z + b_{xi}\, u_z + b_{yi}\, v_z \tag{4.19c}$$

where $u_x = c\phi\, c\psi$, $u_y = c\phi\, s\psi$, $u_z = -s\phi$, $v_x = c\psi\, s\theta\, s\phi - c\theta\, s\psi$, $v_y = s\psi\, s\theta\, s\phi + c\theta\, c\psi$, $v_z = c\phi\, s\theta$ .Eqs. (4.19a), (4.19b) and (4.19c) can be combined in a matrix as follows,

$$
\begin{bmatrix}
q_{x1} \\
q_{y1} \\
q_{z1} \\
q_{x2} \\
q_{y2} \\
q_{z2} \\
q_{x3} \\
q_{y3} \\
q_{z3}
\end{bmatrix}
=
\begin{bmatrix}
1 & 0 & 0 & b_{x1} & 0 & 0 & b_{y1} & 0 & 0 \\
0 & 1 & 0 & 0 & b_{x1} & 0 & 0 & b_{y1} & 0 \\
0 & 0 & 1 & 0 & 0 & b_{x1} & 0 & 0 & b_{y1} \\
1 & 0 & 0 & b_{x2} & 0 & 0 & b_{y2} & 0 & 0 \\
0 & 1 & 0 & 0 & b_{x2} & 0 & 0 & b_{y2} & 0 \\
0 & 0 & 1 & 0 & 0 & b_{x2} & 0 & 0 & b_{y2} \\
1 & 0 & 0 & b_{x3} & 0 & 0 & b_{y3} & 0 & 0 \\
0 & 1 & 0 & 0 & b_{x3} & 0 & 0 & b_{y3} & 0 \\
0 & 0 & 1 & 0 & 0 & b_{x3} & 0 & 0 & b_{y3}
\end{bmatrix}
\begin{bmatrix}
p_x \\
p_y \\
p_z \\
u_x \\
u_y \\
u_z \\
v_x \\
v_y \\
v_z
\end{bmatrix}
\tag{4.20}
$$

By using inverse of square matrix in Eq. (4.20), the location of platform of manipulator is computed as follows,

$$
p_x = \frac{\sum_{i=1}^{3} q_{xi}\left(b_{yj}b_{xk} - b_{yk}b_{xj}\right)}{\sum_{i=1}^{3} b_{yi}\left(b_{xj} - b_{xk}\right)}, \quad
p_y = \frac{\sum_{i=1}^{3} q_{yi}\left(b_{yj}b_{xk} - b_{yk}b_{xj}\right)}{\sum_{i=1}^{3} b_{yi}\left(b_{xj} - b_{xk}\right)}, \quad
p_z = \frac{\sum_{i=1}^{3} q_{zi}\left(b_{yj}b_{xk} - b_{yk}b_{xj}\right)}{\sum_{i=1}^{3} b_{yi}\left(b_{xj} - b_{xk}\right)} \tag{4.21a}
$$

$$
u_x = \frac{\sum_{i=1}^{3} q_{xi}\left(b_{yj} - b_{yk}\right)}{\sum_{i=1}^{3} b_{yi}\left(b_{xk} - b_{xj}\right)}, \quad
u_y = \frac{\sum_{i=1}^{3} q_{yi}\left(b_{yj} - b_{yk}\right)}{\sum_{i=1}^{3} b_{yi}\left(b_{xk} - b_{xj}\right)}, \quad
u_z = \frac{\sum_{i=1}^{3} q_{zi}\left(b_{yj} - b_{yk}\right)}{\sum_{i=1}^{3} b_{yi}\left(b_{xk} - b_{xj}\right)} \tag{4.21b}
$$

$$v_x = \frac{\sum\limits_{i=1}^{3} q_{xi}\left(b_{xj} - b_{xk}\right)}{\sum\limits_{i=1}^{3} b_{yi}\left(b_{xj} - b_{xk}\right)}, \quad v_y = \frac{\sum\limits_{i=1}^{3} q_{yi}\left(b_{xj} - b_{xk}\right)}{\sum\limits_{i=1}^{3} b_{yi}\left(b_{xj} - b_{xk}\right)}, \quad v_z = \frac{\sum\limits_{i=1}^{3} q_{zi}\left(b_{xj} - b_{xk}\right)}{\sum\limits_{i=1}^{3} b_{yi}\left(b_{xj} - b_{xk}\right)} \tag{4.21c}$$

where $j = \mod(i+1,3)$, $k = \mod(i+2,3)$. Euler angles can be easily found as follows,

$$\phi = -\arcsin\left(u_z\right) \tag{4.22a}$$

$$\psi = \text{Atan}_2\left(u_x / \cos(\phi), u_y / \cos(\phi)\right) \tag{4.22b}$$

$$\theta = \text{Atan}_2\left(v_y \cos(\psi) - v_x \sin(\psi), v_z / \cos(\phi)\right) \tag{4.22c}$$

Numerical Example. In this example, we solve the direct position analysis for geometry of manipulator given in Table 4.6. And the input angles are given as $\theta_{11} = 1°$, $\theta_{12} = 120°$ and $\theta_{13} = 240°$.

Table 4.6. Geometric constant parameters of manipulator

	First leg, $i=1$	Second leg, $i=2$	Third leg $i=3$
α_i	110°	110°	110°
r_{1i}	58.52	58.52	58.52
r_{2i}	79.36	79.36	79.36
b_{xi}	40.88	-20.19	-20.74
b_{yi}	0	39.63	-39.00
a_i	50	65	80

Substituting constant parameters into Eqs. (3.70), (3.71) and (4.18) for $i = 1, 2, 3$, nine nonlinear equations are found as follows,

$$q_{z1}^2 - 110 q_{z1} - 60 \cos(\theta_{11}) q_{x1} - (\cos(\theta_{11}))^2 q_{x1}^2 - 60 \sin(\theta_{11}) q_{y1}$$
$$+ \cos(\theta_{11}) \sin(\theta_{11}) q_{x1} q_{y1} - 2373.01 = 0$$

$$q_{z2}^2 - 110 q_{z2} - 90 \cos(\theta_{12}) q_{x2} - (\cos(\theta_{12}))^2 q_{x2}^2 - 90 \sin(\theta_{12}) q_{y2}$$
$$+ \cos(\theta_{12}) \sin(\theta_{12}) q_{x2} q_{y2} - 1248.01 = 0$$

$$q_{z3}^2 - 110 q_{z3} - 120 \cos(\theta_{13}) q_{x3} - (\cos(\theta_{13}))^2 q_{x3}^2 - 120 \sin(\theta_{13}) q_{y3}$$
$$+ \cos(\theta_{13}) \sin(\theta_{13}) q_{x3} q_{y3} + 326.99 = 0$$

$$q_{y1} - q_{x1} \tan(\theta_{11}) = 0, \quad q_{y2} - q_{x2} \tan(\theta_{12}) = 0, \quad q_{y3} - q_{x3} \tan(\theta_{13}) = 0$$

$$(q_{x2} - q_{x1})^2 + (q_{y2} - q_{y1})^2 + (q_{z2} - q_{z1})^2 - 5300.67 = 0$$

$$(q_{x3} - q_{x2})^2 + (q_{y3} - q_{y2})^2 + (q_{z3} - q_{z2})^2 - 6184.64 = 0$$

$$(q_{x1} - q_{x3})^2 + (q_{y1} - q_{y3})^2 + (q_{z1} - q_{z3})^2 - 5318.85 = 0$$

At most, sixteen results of nonlinear equations can be found for each of input values. The number of imaginary results is four. The real results of the equations are listed in Table 4.7 for given input values.

Table 4.7. The real results of the numerical example

No.	$\mathbf{q}_1^{\mathrm{T}} = (q_{x1}, q_{y1}, q_{z1})$	$\mathbf{q}_2^{\mathrm{T}} = (q_{x2}, q_{y2}, q_{z2})$	$\mathbf{q}_3^{\mathrm{T}} = (q_{x3}, q_{y3}, q_{z3})$
1	$(35.8021, \ 0.6249, \ 134.147)$	$(-24.1828, \ 41.8858, \ 134.289)$	$(9.1448, \ 15.8393, \ 67.9901)$
2	$(-49.3339, \ -0.8611, \ 56.7161)$	$(15.9109, \ -27.5586, 74.9099)$	$(-0.0345, \ -0.0597, \ 2.978)$
3	$(-48.4877, \ -0.8463, \ 43.3152)$	$(17.1785, \ -29.7541, \ 55.6828)$	$(-12.8906, \ -22.3272, \ -16.6037)$
4	$(-46.1729, \ -0.8059, \ 77.2403)$	$(-21.3262, \ 36.9381, \ 134.325)$	$(-24.0481, \ -41.6526, \ 133.462)$
5	$(38.6483, \ 0.6746, \ 133.887)$	$(-22.8693, \ 39.6108, \ 134.357)$	$(-22.5272, \ -39.0182, \ 132.94)$
6	$(35.8021, \ 0.6249, \ -24.1472)$	$(-24.1828, \ 41.8858, -24.2886)$	$(9.1448, \ 15.8393, \ 42.0099)$
7	$(-46.1729, -0.8059, 32.7597)$	$(-21.3262, \ 36.9381, -24.325)$	$(-24.0481, -41.6526, \ -23.4622)$
8	$(38.6483, \ 0.6746, -23.8867)$	$(-22.8693, \ 39.6108, -24.3566)$	$(-22.5272, -39.0182, -22.94)$
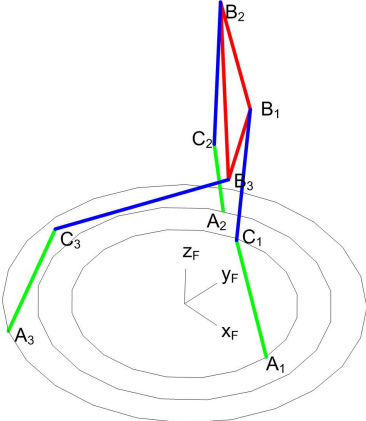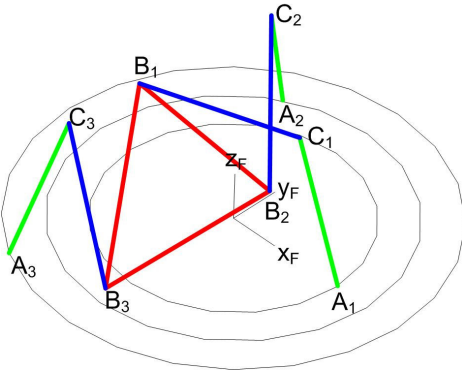
Table 4.7.(cont.) The real results of the numerical example

9	$(31.7758,\ 0.5546,\ -24.34)$	$(16.5212,\ -28.6156,\ 40.5989)$	$(-25.641,\ -44.4115,\ -23.8797)$
10	$(-49.3339,\ -0.8611,\ 53.2839)$	$(15.9109,\ -27.5586,\ 35.0901)$	$(-0.0345,\ -0.0597,\ 107.022)$
11	$(-48.4877,\ -0.8463,\ 66.6848)$	$(17.1785,\ -29.7541,\ 54.3172)$	$(-12.8906,\ -22.3272,\ 126.604)$
12	$(31.7758,\ 0.5546,\ 134.34)$	$(16.5212,\ -28.6156,\ 69.4011)$	$(-25.641,\ -44.4115,\ 133.88)$

The twelve assembly configurations of the manipulator, which correspond to the results in Table 4.7, are shown in Table 4.8. Note that the first assembly configuration is drawn by using the first result in Table 4.8. For assembly configurations, the location of moving coordinate system can be determined by Eqs.(4.21 a-c) and Euler angles can be found by utilizing Eqs.(4.22 a-c).

Table 4.8. Assembly modes of the manipulator

No.	Assembly Configuration	No.	Assembly Configuration
1		7	

Table 4.8 (cont.) Assembly modes of the manipulator

Table 4.8 (cont.) Assembly modes of the manipulator
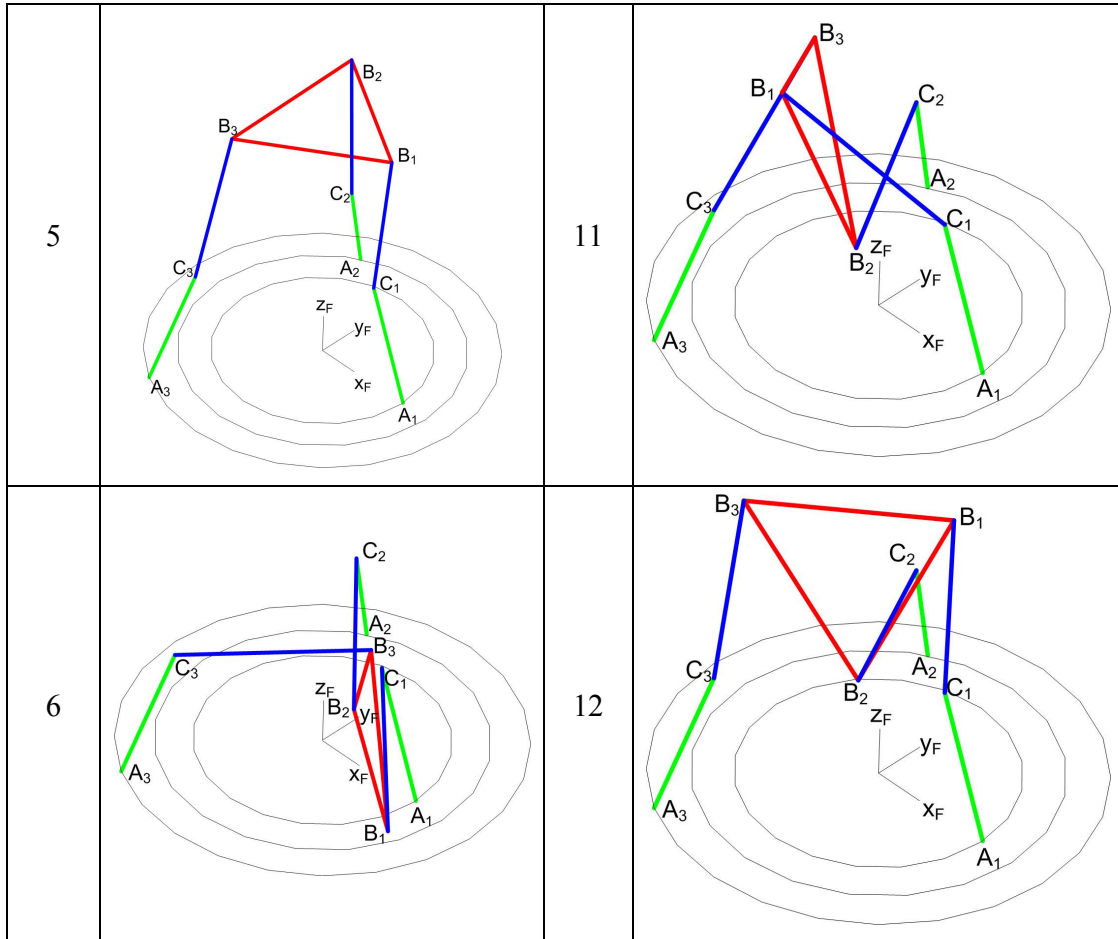
4.4.3. Workspace Analysis

If the kinematic model manipulator shown in Figure 3.10.a is reconsidered, it is easy to see that the platform of the manipulator moves on three surfaces created by point B_i of i th leg. Therefore, firstly, the surfaces created by legs must be investigated. The design equation given in Eq.(3.72) defines the reachable surface for each leg of the manipulator. Three surfaces can be plotted in Mathematica by using constant geometric parameters in Table 4.6. Three plots corresponding to the first, the second and the third legs of the manipulator are shown in Figure 4.3.a-c, respectively. Three surfaces are depicted together in Figure 4.3.d. However, the surfaces are not enough to imagine reachable workspace of

the manipulator. Therefore, translation workspace of manipulator can be reached by keeping orientation of the platform constant in Eq.(3.77). For each leg (i=1,2,3) , the workspace of the moving platform is plotted by selecting orientation of the platform as $\theta = 0°, \psi = 0°, \beta = 0°$ (Figure 4.4.a-c). Three workspaces are shown together in Figure 4.4.d. In Mathematica, there is no way to find the intersection of these surfaces. Hence, a CAD program is used to describe the intersection. Firstly, the workspaces are transported to CAD program (Figure 4.4.e). Then, the intersection of the leg workspaces are found by using CAD tools (Figure 4.4.f).
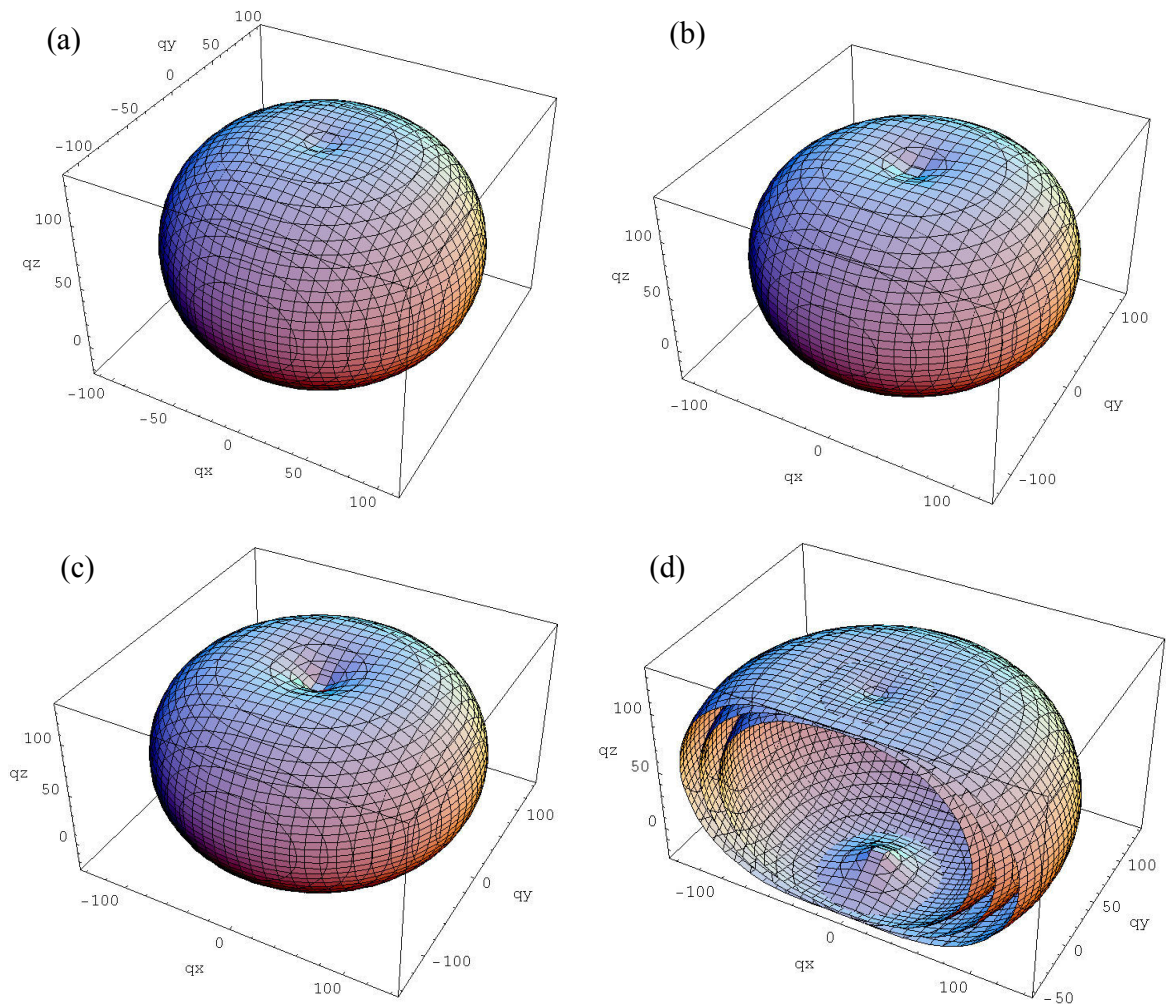
Figure 4.3. Work surfaces of the legs (a) surface for the first leg (b) surface for the second leg (c) surface for the third leg (d) three surfaces together

Another method of describing workspace is to make the direct position analysis for 1000 points. The constant parameters in Table 4.6 are utilized for analysis and the inputs are changed in some range ($0 \le \theta_{11} \le 135°$ step 15°, $120° \le \theta_{12} \le 210°$ step 10° , $240° \le \theta_{13} \le 267°$ step 3°). The position workspace of the manipulator's end-effector is shown in Figure 4.5. The upper half of the workspace is symmetric to the lower half.

(a) Workspace of the platform from the first leg

(b) Workspace of the platform from the second leg

(c) Workspace of the platform from the third leg

(d) Three workspaces together
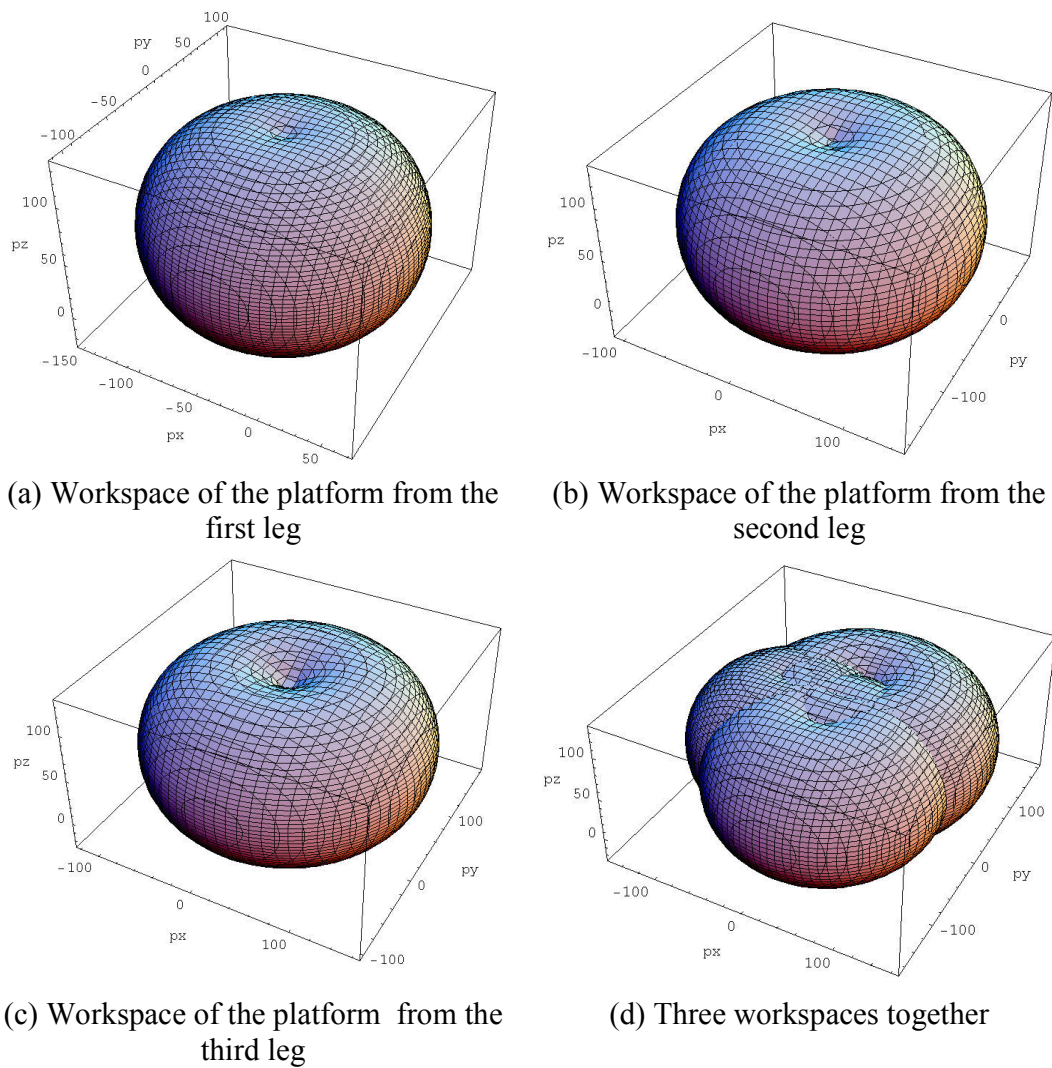
Figure 4.4. Constant orientation workspace of the manipulator
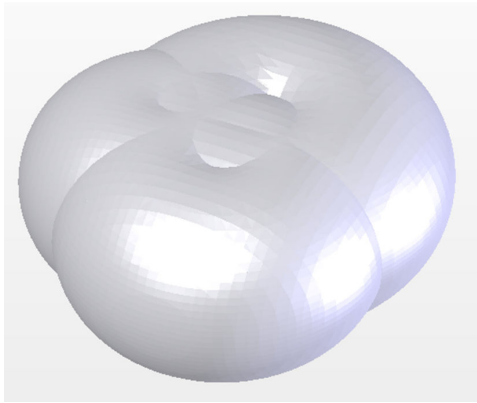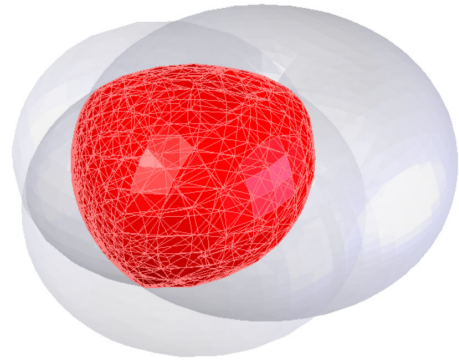
(e) CAD of workspace   (f) Intersection of three workspaces.

Figure 4.4.(cont.) Constant orientation workspace of the manipulator
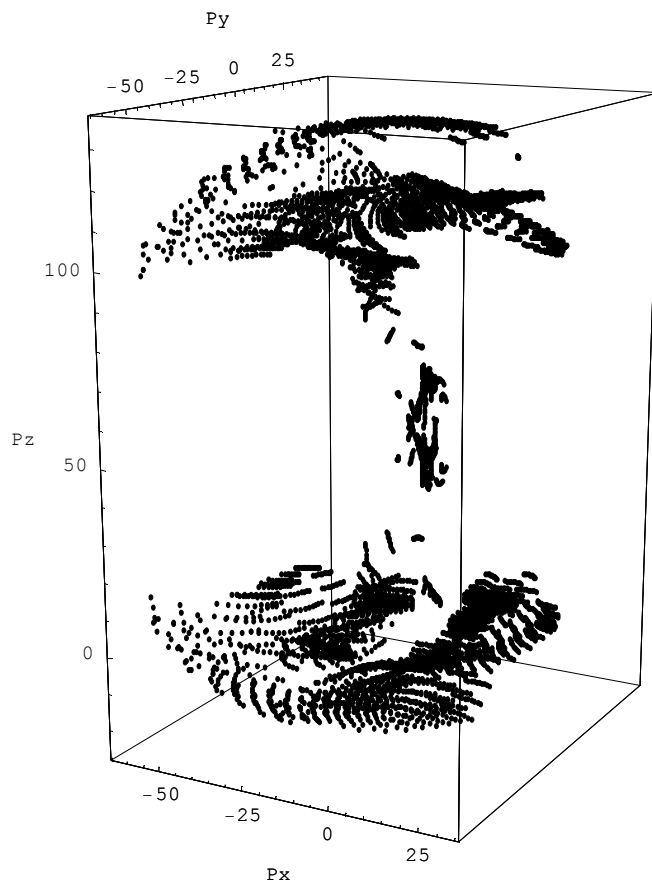
Figure 4.5. Workspace of the end-effector's position of the manipulator.

4.5. Position Analysis of a Three DoF EPRM

Consider a three DoF EPRM shown in Figure 4.6. Three identical legs are placed on three different Euclidean planes. Geometry of these planes is identified by an angle α_i. Other geometric parameters are very similar to the previous example (3 C_sRS manipulator) but only the joint variable is switched. In Figure 4.6 , the first coordinate system (O_F, x_F, y_F, z_F) is fixed to the base, the second coordinate system (O_M, x_M, y_M, z_M) is attached to the moving platform and the third coordinate system (A_i, x_i, y_i z_i) is aligned to Euclidean plane.
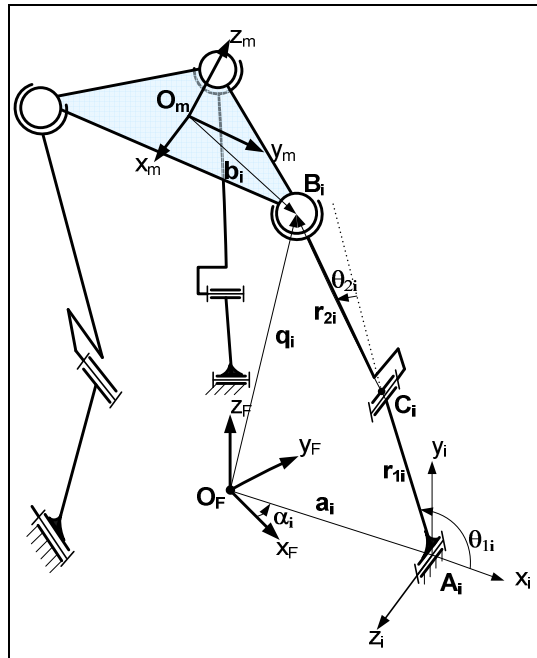
Figure 4.6. A three DoF EPRM

Transformation of moving platform is described as follows,

$$\mathbf{T}_{F,M} = \begin{bmatrix} U_x & V_x & W_x & P_x \\ U_y & V_y & W_y & P_y \\ U_z & V_z & W_z & P_z \\ 0 & 0 & 0 & 1 \end{bmatrix} \tag{4.21}$$

Coordinates of point B$_i$ are calculated by using transformation matrix in Eq.(4.21),

$$\begin{pmatrix} q_{xi} \\ q_{yi} \\ q_{zi} \\ 1 \end{pmatrix} = \mathbf{T}_{F,M} \begin{pmatrix} b_{xi} \\ b_{yi} \\ 0 \\ 1 \end{pmatrix} \tag{4.22}$$

Another transformation matrix can be represented as follows,

$$\mathbf{T}_{F,B_i} = \mathbf{T}_{F,A_i} \, \mathbf{T}_{A_i,C_i} \, \mathbf{T}_{C_i,B_i} \tag{4.23}$$

where $\mathbf{T}_{F,A_i} = T(z_F, \alpha_i) \cdot T(x_i, a_i) . T\left(x_i, \dfrac{\pi}{2}\right) = \begin{bmatrix} c\alpha_i & 0 & s\alpha_i & a_i \, c\alpha_i \\ s\alpha_i & 0 & -c\alpha_i & a_i \, s\alpha_i \\ 0 & 1 & 0 & 0 \\ 0 & 0 & 0 & 1 \end{bmatrix}$,

$$\mathbf{T}_{A_i,C_i} = \begin{bmatrix} c\theta_{1i} & -s\theta_{1i} & 0 & r_{1i} \, c\theta_{1i} \\ s\theta_{1i} & c\theta_{1i} & 0 & r_{1i} \, s\theta_{1i} \\ 0 & 0 & 1 & 0 \\ 0 & 0 & 0 & 1 \end{bmatrix} \text{ and } \mathbf{T}_{C_i,B_i} = \begin{bmatrix} c\theta_{2i} & -s\theta_{2i} & 0 & r_{2i} \, c\theta_{2i} \\ s\theta_{2i} & c\theta_{2i} & 0 & r_{2i} \, s\theta_{2i} \\ 0 & 0 & 1 & 0 \\ 0 & 0 & 0 & 1 \end{bmatrix}.$$

Coordinates of point B$_i$ can also be calculated by using other transformation matrix in Eq.(4.23) as follows,

$$\begin{pmatrix} q_{xi} \\ q_{yi} \\ q_{zi} \\ 1 \end{pmatrix} = \mathbf{T}_{F,B_i} \begin{pmatrix} 0 \\ 0 \\ 0 \\ 1 \end{pmatrix} \tag{4.24}$$

It is clear that Eqs.(4.22) and (4.24) are equal. Then we can write three equations,

$$q_{xi} = P_x + U_x\, b_{xi} + V_x\, b_{yi} = c\alpha_i \left(a_i + r_{1i}\, c\theta_{1i} + r_{2i}\, c\theta_{1i}\, c\theta_{2i} - r_{2i}\, s\theta_{1i}\, s\theta_{2i} \right) \tag{4.25a}$$

$$q_{yi} = P_y + U_y\, b_{xi} + V_y\, b_{yi} = s\alpha_i \left(a_i + r_{1i}\, c\theta_{1i} + r_{2i}\, c\theta_{1i}\, c\theta_{2i} - r_{2i}\, s\theta_{1i}\, s\theta_{2i} \right) \tag{4.25b}$$

$$q_{zi} = P_z + U_z\, b_{xi} + V_z\, b_{yi} = r_{1i}\, s\theta_{1i} + r_{2i}\, s\theta_{1i}\, c\theta_{2i} + r_{2i}\, c\theta_{1i}\, s\theta_{2i} \tag{4.25c}$$

Multiplying Eq. (4.25 a) with $s\alpha_i$ and Eq. (4.25 b) with $-c\alpha_i$, the conditions for the EPRMs are obtained as follows,

$$q_{xi}\, s\alpha_i - q_{yi}\, c\alpha_i = 0 \tag{4.26}$$

Eq. (4.26) implies that point B$_i$ must move always on ith Euclidean plane.

Inverse position analysis of this manipulator is to find angle θ_{1i} for given position and orientation of the platform (P_x, P_y, P_z, U_x, U_y, V_z).

Applying mathematical operation as Eq. (4.25 a)$\times c\alpha_i$ + Eq. (4.25 b)$\times s\alpha_i$, we get Eq. (4.27).

$$q_{xi}\, c\alpha_i + q_{yi}\, s\alpha_i = a_i + r_{1i}\, c\theta_{1i} + r_{2i}\, c\theta_{1i}\, c\theta_{2i} - r_{2i}\, s\theta_{2i}\, s\theta_{1i} \tag{4.27}$$

The second revolute joint angle θ_{2i} is eliminated by using some mathematical manipulation $\left(\text{Eq. (4.25 c)} \right)^2 + \left(\text{Eq. (4.27)} \right)^2$.

$$q_{xi}^2\, c\alpha_i^2 + 2 q_{xi}\, q_{yi}\, c\alpha_i\, s\alpha_i - 2 q_{xi}\, a_i\, c\alpha_i - 2 q_{xi}\, r_{1i}\, c\alpha_i\, c\theta_{1i} + q_{yi}^2\, s\alpha_i^2 - 2 q_{yi}\, a_i\, s\alpha_i$$
$$-2 q_{yi}\, r_{1i}\, s\theta_{1i}\, c\theta_{1i} + a_i^2 + 2 a_i\, r_{1i}\, c\theta_{1i} + r_{1i}^2 + q_{zi}^2 - 2 q_{zi}\, r_{1i}\, s\theta_{1i} - r_{2i}^2 = 0 \tag{4.28}$$

Eq.(4.28) can be rewritten as follows,

$$A_i\, c\theta_{1i} + B_i\, s\theta_{1i} + C_i = 0 \tag{4.29}$$

where
$$A_i = -2\,q_{xi}\,c\alpha_i\,r_{1i} - 2\,q_{yi}\,s\alpha_i\,r_{1i} + 2\,a_i\,r_{1i}, \qquad\qquad B_i = -2q_{zi}r_{1i} \qquad\qquad \text{and}$$
$$C_i = q_{xi}^2\,c\alpha_i^2 + 2\,q_{xi}\,q_{yi}\,c\alpha_i\,s\alpha_i - 2\,q_{xi}\,a_i\,c\alpha_i + q_{yi}^2\,s\alpha_i^2 - 2\,q_{yi}\,a_i\,s\alpha_i + a_i^2 + r_{1i}^2 + q_{zi}^2 - r_{2i}^2.$$

By substituting trigonometric identities $\cos\left(\theta_{1i}\right) = \dfrac{1 - t_{1i}^{\;2}}{1 + t_{1i}^{\;2}}$, $\sin\left(\theta_{1i}\right) = \dfrac{2\,t_{1i}}{1 + t_{1i}^{\;2}}$ where

$\tan\left(\theta_{1i}/2\right) = t_{1i}$ into Eq.(4.29), two unknowns ($c\theta_{1i}, s\theta_{1i}$) are reduced to one unknown (t_{1i}),

$$\left(C_i - A_i\right)t_{1i}^2 + 2\,B_i\,t_{1i} + \left(C_i + A_i\right) = 0 \qquad\qquad (4.30)$$

The second degree equation can be solved analytically. Therefore, angle θ_{1i} can be calculated by using Eq.(4.30) .

$$\theta_{1i} = 2\arctan\left(\frac{-B_i \mp \sqrt{B_i^2 + A_i^2 - C_i^2}}{C_i - A_i}\right) \qquad\qquad (4.31)$$

It is worthy to note that Eq.(4.16) is very close to Eq.(4.31). In inverse position analysis of 3 DoF planar parallel manipulator, eight possible cases were presented. Therefore, we can conclude that at most eight solutions can be obtained for spatial EPRM.

4.6. Position Analysis of a Six DoF Parallel Robot Manipulator

The manipulator shown in Figure 4.7 has six DoF and three identical legs. Each of legs consists of a spherical slider (S_S), an intermediate cylindrical joint (C) and a hooke or cardan joint (U) attached to the moving platform. Kinematic chain of a leg is called S_S CU limb.
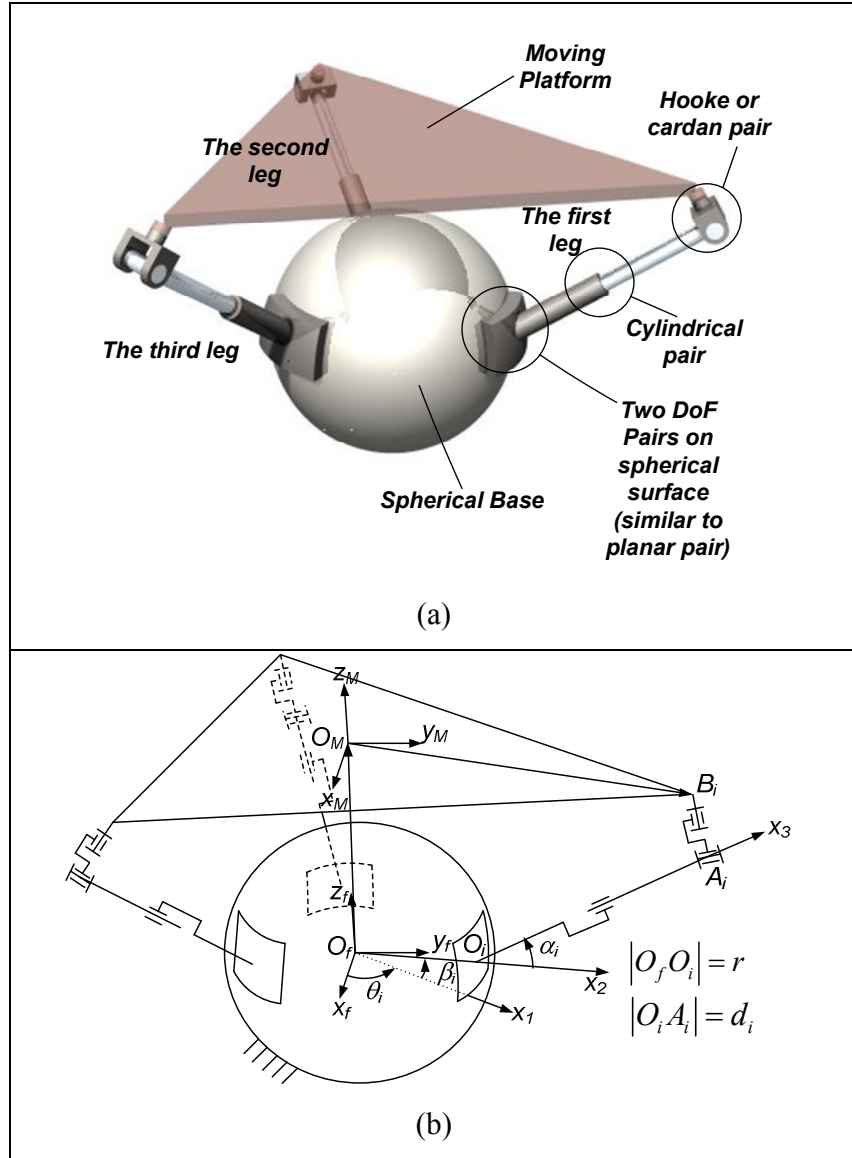
Figure 4.7. Novel 6 DoF parallel robot manipulator (a) CAD representation (b) kinematic model

Note that the distance between points A_i and B_i is very small with respect to other dimensions. Therefore, it can be neglected from kinematic equations. Therefore, $\overrightarrow{O_i B_i} = \overrightarrow{O_i A_i} + \overrightarrow{A_i B_i} = \overrightarrow{O_i A_i}$. Then, the vector loop equations for ith leg can be represented as follows,

$$\overrightarrow{O_f O_i} + \overrightarrow{O_i B_i} = \overrightarrow{O_f O_M} + \overrightarrow{O_M B_i} \qquad (4.32)$$

Equating coefficients of unit vectors **i**, **j**, **k** ends up with three scalar equations,

$$r\, c\theta_i\, c\beta_i + d_i\, c\theta_i\, c(\beta_i + \alpha_i) = q_{xi} \qquad (4.33)$$
$$r\, s\theta_i\, c\beta_i + d_i\, s\theta_i\, c(\beta_i + \alpha_i) = q_{yi} \qquad (4.34)$$
$$r\, s\beta_i + d_i\, s(\beta_i + \alpha_i) = q_{zi} \qquad (4.35)$$

where $q_{xi} = P_x + U_x\, b_{xi} + V_x\, b_{yi}$, $q_{yi} = P_y + U_y\, b_{xi} + V_y\, b_{yi}$ and $q_{zi} = P_z + U_z\, b_{xi} + V_z\, b_{yi}$. Three parameters (P_x, P_y, P_z) define the position of the platform whereas other three ones (U_x, U_y, V_z) specify the orientation of the platform. Parameters b_{xi} and b_{yi} defines geometric shape of the platform. Using Eqs.(4.33) and (4.34), the following equation can be derived.

$$q_{xi}\, s\theta_i = q_{yi}\, c\theta_i \qquad (4.36)$$

The first actuation parameter of slider can be calculated as follows,

$$\theta_i = \mathrm{Atan}_2\left(q_{xi}, q_{yi}\right) \qquad (4.37)$$

Mathematical operation $\mathrm{Eq.}(4.33)^2 + \mathrm{Eq.}(4.34)^2 + \mathrm{Eq.}(4.35)^2$ eliminates all variable angles,

$$r^2 + 2r\, d_i\, c\alpha_i + d_i^{\,2} = q_{xi}^2 + q_{yi}^2 + q_{zi}^2 \qquad (4.38)$$

Linear motion (d_i) of cylindrical pair can be calculated from Eq.(4.38). Eqs.(4.33) and (4.35) can be combined in matrix form as follows,

$$\begin{bmatrix} r\, c\theta_i + d_i\, c\theta_i\, c\alpha_i & -d_i\, c\theta_i\, s\alpha_i \\ d_i\, s\alpha_i & r\, c\alpha_i \end{bmatrix} \begin{bmatrix} c\beta_i \\ s\beta_i \end{bmatrix} = \begin{bmatrix} q_{xi} \\ q_{zi} \end{bmatrix} \qquad (4.39)$$

Solution of matrix Eq.(4.39) yields,

$$c\beta_i = \frac{q_{xi}\, r\, c\alpha_i\, /\, c\theta_{1i} + d_i\, q_{zi}\, s\alpha_i}{r^2 c\alpha_i + d_i\, r\left(c\alpha_i\right)^2 + \left(d_i\, s\alpha_i\right)^2}\ ,\ \ s\beta_i = \frac{q_{zi}\, r + d_i\, q_{zi}\, c\alpha_i - d_i\, q_{xi}\, s\alpha_i\, /\, c\theta_1}{r^2 c\alpha_i + d_i\, r\left(c\alpha_i\right)^2 + \left(d_i\, s\alpha_i\right)^2} \tag{4.40}$$

The second actuation parameters can be calculated as follows,

$$\beta_i = \text{Atan}_2\left(c\beta_i,\ s\beta_i\right) \tag{4.41}$$

Calculations of angles in Eqs.(4.37) and (4.41) defines the position point O_i on sphere.

CHAPTER 5

MECHANIC ANALYSIS OF PARALLEL ROBOT MANIPULATORS

This chapter presents mechanic analysis that includes static force analyses. The force analysis is important and considered at design stage due to the fact that the sizing of link and other mechanical elements can be selected by these analyses. Static force analysis is considered when the movement acceleration and speed of manipulator's links and platform are slow. On the other hand, if the speed is high, dynamic analysis is under the consideration. Difference between static and dynamic analysis comes from especially inertial force effects of mechanical elements. Inertial forces are related to angular and linear accelerations. Other forces are external forces, reaction forces and actuator forces.

5.1. Static Force Analysis

The recursive method of serial manipulators and single-loop spatial mechanism cannot be applied to parallel manipulators due to several closed loops. Generally, the force and moment equations must be derived for each link and the simultaneous linear equations must be solved. The principle of virtual work is an alternative way to obtain the actuator drive forces-torques. But note that the reaction forces are not calculated by this method.

5.1.1 Static Force Analysis of a three DoF Euclidean Parallel Robot Manipulator

A three DoF manipulator with three step motors is shown in Figure 5.1. In static force analysis of the manipulator, our aim is to find driving torque of step motors. This torque is also called holding torque that is need to hold the system in static equilibrium.

External force F_z and moments M_x and M_y are applied on at the center of the platform. For simplicity, the rotation matrix of the platform is taken to be identity matrix or in other words the platform is parallel to the ground ($O_m x_m y_m z_m$ // $O_F x_F y_F z_F$).
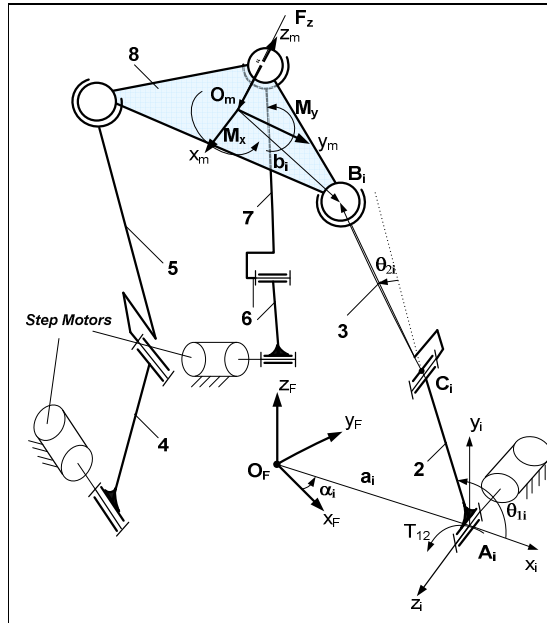
Figure 5.1. A three DoF parallel robot manipulator
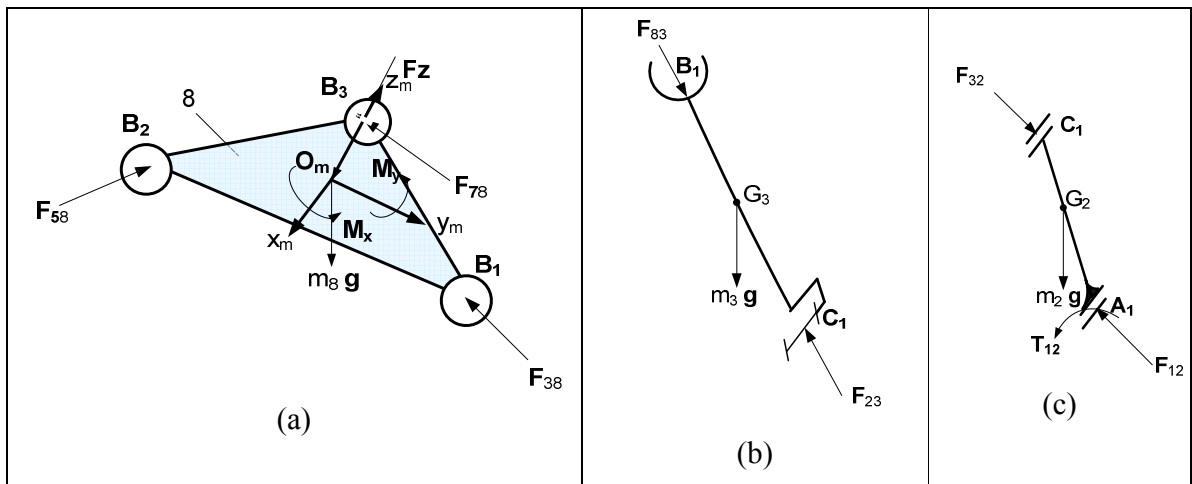
Figure 5.2. Free body diagrams of (a) platform, (b) link 3 and (c) link 2

Firstly, free body diagrams of platform, link3 and link2 are drawn to show reaction forces. Spherical joints cannot have any reaction moments because of its three independent rotational motions. Therefore, Figure 5.2.a depicts reaction forces of the spherical pairs which are labeled as $\mathbf{F_{38}}$, $\mathbf{F_{58}}$, $\mathbf{F_{78}}$. Force and moment equilibrium is written as,

$$\sum \mathbf{F} = 0, \quad \mathbf{F}' + \mathbf{F_{38}} + \mathbf{F_{58}} + \mathbf{F_{78}} = 0 \tag{5.1}$$

$$\sum \mathbf{M_{B2}} = 0, \quad \overrightarrow{B_2 O_m} \times \mathbf{F}' + \overrightarrow{B_2 B_1} \times \mathbf{F_{38}} + \overrightarrow{B_2 B_3} \times \mathbf{F_{78}} + \mathbf{M} = 0 \tag{5.2}$$

where $\mathbf{F}' = \mathbf{F} + m_p\, \mathbf{g}$, $\mathbf{g} = -g\, \mathbf{k}$, $\overrightarrow{B_2 O_m} = b_{2x}\, \mathbf{i} + b_{2y}\, \mathbf{j}$, $\overrightarrow{B_3 O_m} = b_{3x}\, \mathbf{i} + b_{3y}\, \mathbf{j}$, $\overrightarrow{B_2 B_3} = k_{2x}\, \mathbf{i} + k_{2y}\, \mathbf{j}$ and $\overrightarrow{B_2 B_1} = k_{1x}\, \mathbf{i} + k_{1y}\, \mathbf{j}$.

The following scalar equations can be obtained by separating coefficients of $\mathbf{i}$, $\mathbf{j}$ and $\mathbf{k}$ unit vectors of Eq. (5.1). Scalar components of forces and moments are as follows;

$$F_{38x} + F_{58x} + F_{78x} = -F_x$$
$$F_{38y} + F_{58y} + F_{78y} = -F_y \tag{5.3}$$
$$F_{38z} + F_{58z} + F_{78z} = -F_z + m_p\, g$$

Equating coefficients of $\mathbf{i}$, $\mathbf{j}$ and $\mathbf{k}$ unit vectors of Eq. (5.2), the additional scalar equations can be written as follows,

$$F_{78z}\,k_{2y} + F_{38z}\,k_{1y} = -\left(F_z - m_p\,g\right) b_{2y} - M_x$$

$$-F_{78z}\,k_{2x} - F_{38z}\,k_{1x} = \left(F_z - m_p\,g\right) b_{2x} - M_y \qquad (5.4)$$

$$F_{38y}k_{1x} - F_{38x}\,k_{1y} + F_{78y}\,k_{2x} - F_{78x}\,k_{2y} = -b_{2x}\,F_y + b_{2y}\,F_x - M_z$$

If the last line of Eq.(5.3) and the first two line of Eq.(5.4) are composed, the system of linear equations is reached,

$$
\begin{bmatrix}
1 & 1 & 1 \\
k_{1y} & 0 & k_{2y} \\
-k_{1x} & 0 & -k_{2x}
\end{bmatrix}
\begin{bmatrix}
F_{38z} \\
F_{58z} \\
F_{78z}
\end{bmatrix}
=
\begin{bmatrix}
-F_z + m_p\,g \\
-F_z\,b_{2y} + b_{2y}\,m_p\,g - M_x \\
F_z\,b_{2x} - b_{2x}\,m_p\,g - M_y
\end{bmatrix}
\qquad (5.5)
$$

Three unknowns (F_{38z}, F_{58z}, F_{78z}) in Eq.(5.5) are calculated by using inverse of square matrix. The reaction forces will be as follows,

$$\mathbf{F}_{38} = \begin{pmatrix} 0 & 0 & F_{38z} \end{pmatrix}^T, \ \mathbf{F}_{58} = \begin{pmatrix} 0 & 0 & F_{58z} \end{pmatrix}^T, \ \mathbf{F}_{78} = \begin{pmatrix} 0 & 0 & F_{78z} \end{pmatrix}^T \qquad (5.5)$$

Once the reaction forces applied on platform are calculated, the reactions forces acting on the legs can be found. For the link 3, only one force equation is sufficient to find unknown reaction force $\mathbf{F}_{23}$ which is shown in Figure 5.2.b:

$$\sum \mathbf{F} = 0, \quad \mathbf{F}_{23} = -\mathbf{F}_{83} - m_3\,\mathbf{g} \qquad (5.6)$$

Finally, holding torque of the first step motor in Figure 5.2.c is determined by taking moment with respect to point $\mathbf{A_1}$. Other actuator torques are found in a similar way.

$$\sum \mathbf{M}_{A_1} = 0, \qquad \mathbf{T_{12}} = -\overrightarrow{A_1C_1} \times \mathbf{F}_{32} - m_2\,\overrightarrow{A_1G_2} \times \mathbf{g} \qquad (5.7)$$

Numerical Example: Consider external a force $F_z = 1500\ N$ and no external moment applied to the platform of the manipulator. Geometry of the manipulator is given in Table 5.1. Note that joints angles are set to be $\theta_{11} = \theta_{12} = \theta_{13} = 60°$.

Table 5.1. Geometry of the manipulator

$\overrightarrow{B_2O_m} = 3\sqrt{3}\,\mathbf{i} + 0.3\,\mathbf{j}\ m$		$\overrightarrow{B_2B_1} = 6\sqrt{3}\,\mathbf{i} + 0\,\mathbf{j}\ m$		$\overrightarrow{B_2B_3} = 3\sqrt{3}\,\mathbf{i} + 0.9\,\mathbf{j}\ m$
$\alpha_1 = -60°$		$\alpha_2 = 60°$		$\alpha_3 = 180°$
$\overrightarrow{A_1C_1} = 0.1875\mathbf{i} - 0.3248\mathbf{j} - 0.64952\mathbf{k}\ m$		$\overrightarrow{A_1G_2} = 0.0625\mathbf{i} - 0.1083\mathbf{j} - 0.2165\mathbf{k}\ m$	
$\overrightarrow{A_2C_2} = 0.1875\mathbf{i} + 0.3248\mathbf{j} - 0.64952\mathbf{k}\ m$		$\overrightarrow{A_2G_4} = 0.0625\mathbf{i} + 0.1083\mathbf{j} - 0.2165\mathbf{k}\ m$	
$\overrightarrow{A_3C_3} = -0.375\mathbf{i} + 0\mathbf{j} - 0.64952\mathbf{k}\ m$		$\overrightarrow{A_2G_6} = -0.125\mathbf{i} + 0\,\mathbf{j} - 0.2165\mathbf{k}\ m$	

Weights of the platform and all links: $m_p = 30\,kg$, $m_3 = m_5 = m_7 = 15\,kg$, $m_2 = m_4 = m_6 = 20\,kg$. Gravitational acceleration: $g = 9.81\ m/s^2$. If the constant parameters are substituted into Eqs.(5.5) and (5.6), the components of the reaction forces acting on the platform will be $\left(F_{38z}\quad F_{58z}\quad F_{78z} \right) = \left(598.1\quad 598.1\quad 598.1 \right) N$. Actuator torques in fix frame are calculated as follows,

$\mathbf{T_{12}} = -\overrightarrow{A_1C_1} \times \mathbf{F}_{32} - m_2\,\overrightarrow{A_1G_2} \times \mathbf{g} = 220.809\,\mathbf{i} + 127.472\,\mathbf{j} + 0\mathbf{k}\ \ N\,m$
$\mathbf{T_{14}} = -\overrightarrow{A_2C_2} \times \mathbf{F}_{45} - m_4\,\overrightarrow{A_2G_2} \times \mathbf{g} = -220.809\,\mathbf{i} + 127.472\,\mathbf{j} + 0\mathbf{k}\ \ N\,m$
$\mathbf{T_{16}} = -\overrightarrow{A_3C_3} \times \mathbf{F}_{67} - m_6\,\overrightarrow{A_3G_3} \times \mathbf{g} = 0\mathbf{i} - 254.994\,\mathbf{j} + 0\mathbf{k}\ \ N\,m$

The torques can be described in Euclidean planes.

$\mathbf{T_{12}^1} = \left(R(z,\alpha_1)R(x,90°) \right)^T \mathbf{T}_{12} = 0.01\mathbf{i}_1 + 0\mathbf{j}_1 - 254.962\,\mathbf{k}_1\ \ N\,m$
$\mathbf{T_{14}^2} = \left(R(z,\alpha_2)R(x,90°) \right)^T \mathbf{T}_{14} = -0.01\mathbf{i}_2 + 0\mathbf{j}_2 - 254.962\,\mathbf{k}_2\ \ N\,m$
$\mathbf{T_{16}^3} = \left(R(z,\alpha_3)R(x,90°) \right)^T \mathbf{T}_{16} = 0\mathbf{i}_3 + 0\mathbf{j}_3 - 254.944\,\mathbf{k}_3\ \ N\,m$

Step motor's holding torque must be equal or greater than 260 *Nm* to hold the system in static equilibrium. If the motor does not satisfy the torque, alternatively, gearboxes can be used to increase the torque.

CHAPTER 6

CONSTRUCTION ELEMENTS AND CONTROL OF PARALLEL ROBOT MANIPULATORS

In this study, our aim is to solve an industrial pick and place problem. In the company, bricks are carried by workers. Weight of bricks changes from 10 kg to 100 kg in production line. When the weight of bricks increases, workers are easily tired and efficiency of the production decreases. In order to solve this problem, a novel hybrid manipulator is developed. This manipulator has two layers such that the first layer is a parallel structure and the second layer is an open serial chain. Parallel structure is a three DoF EPRM while open serial chain is a two DoF XY table. This chapter presents how the manipulator is constructed and how control algorithm is developed.

The body of parallel robot manipulators is constructed with some mechanical parts such as bearings, gears, pneumatic cylinders, belt systems, grippers and e.t.c. These parts must be selected from company catalogs according to their physical and mechanical capabilities. After mechanical construction of the manipulator, the actuators and sensors are assembled into necessary place.

6.1. Mechanical Elements

6.1.1. Bearings
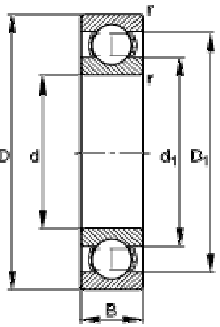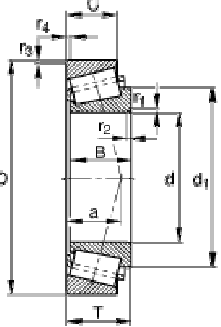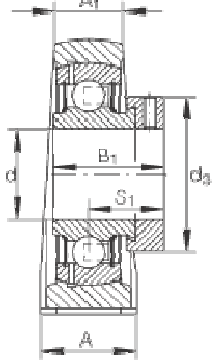
The kinematic structure of parallel manipulators generally needs some revolute pairs (pivots). From dynamic analysis, these pairs must resist some reaction forces. Bearings are convenient for both the generation of necessary motion and the resistance of reaction forces.

When any machine is designed, some properties of the bearings must be considered to fulfill necessary conditions. Firstly, designer determines dimensions of bearings such as inner and outer diameter with respect to the diameter of shaft and the diameter of housing.

Then, designer checks whether the load capacity of the bearing is appropriate or not. Finally, designer calculates service life of the bearing under the specified conditions.

We select the bearings as follows, FAG 16008 radial ball bearing (Table 6.1.a), FAG 30205-Tapered roller bearing (Table 6.1.b), UBC Plummer block housing unit(Table 6.1.c).

Table 6.1. Technical characteristic of bearings (a) radial ball bearing (b) tapered ball bearing (c) Plummer block housing unit

Technical Drawings	(a)	(b)	(c)
Dimensions	d=40 mm, D=68 mm, B=9mm	d=25 mm, D=52 mm, T=16.25 mm	d=30 mm, d_3=44 mm, A=40 mm, A1=25 mm, B1=35.7 mm
Forces	The bearing can support the radial forces and only small axial forces.	The bearing can support both the radial forces and the axial forces.	The bearing can support both the radial forces and the axial forces.
Load capacity	Basic dynamic load rating, radial (C_r) 13200 N Basic static load rating, radial (C_{0r}) 10200 N	Basic dynamic load rating, radial (C_r) 32500 N. Basic static load rating, radial (C_{0r}) 35500 N	Basic dynamic load rating, radial (C_r) 19500 N Basic static load rating, radial (C_{0r}) 11300 N

6.1.2. Grippers

Grippers are mechanical devices to pick an object and hold it during transportation. Generally, they are controlled by pneumatic pressure or hydraulic pressure. But, some new small grippers have been developed with servo motors to obtain high precision and more position interval. Pneumatic and hydraulic grippers are convenient for heavy loads. Pneumatic gripper PGN 200-2 is selected for transportation of bricks in our project. Technical capabilities of the gripper are given in Table 6.2.

Figure 6.1. Pneumatic gripper PGN 200-2

Table 6.2. Technical capabilities of PGN 200-2

Technical capability	Value
Stroke per finger	14 mm
Gripping force at 6 bars	3300 N
Recommended workpiece weight	16.5 kg
Air consumption per double stroke	306 cm^3
Opening time	0.3 s
Closing time	0.3 s
Mass	5.1 kg
Mass moment of inertia	230 kg cm^2
Repeatability	0.02 mm

6.1.3. Gearboxes

Gears are used to transmit rotary motion between parallel or non-parallel shafts. Four principal types of gears are spur, helical, bevel and worm. Gearboxes are constructed by assembling two or more gear types. Transmission ratio and out torque are important technical properties for gearboxes. In our applications, three gearboxes whose transmission ratio is 1/149 are used to obtain smooth motion and high torque (~200 Nm). (Figure 6.2)
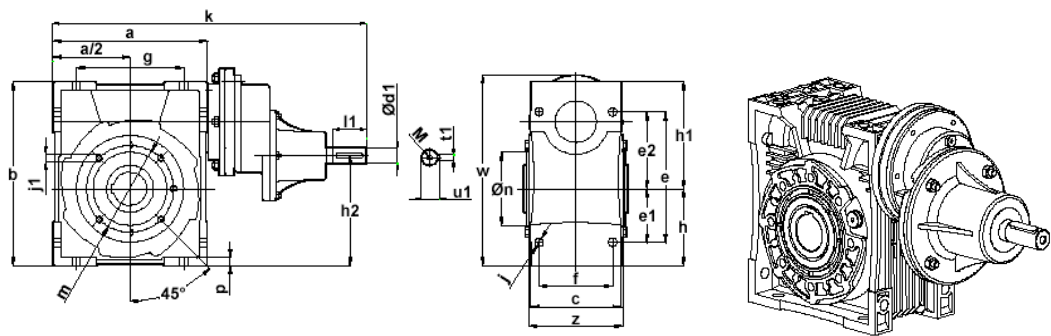
Figure 6.2. Gearbox

6.1.4. Timing Belts

Belts transmit power in case of the considerable long distance the shaft of actuators and the shaft of machine. Fortunately, they protect the actuators from bad effects of vibration and shock loads due to their elastic property. Four main belt types are defined by shapes of their cross-sections: flat, round, V and timing. Timing belts are produced from rubberized fabric consisting of steel wire to absorb tension load. The main advantage of timings belts is to transmit power without slip. Therefore, the power transmission at a constant angular-velocity ratio is possible for timing belts. There are five standard pitches which can be identified with their letter designations: Extra light (XL), light (L), heavy (H),

extra heavy (XH), Double extra heavy (XXH). In the manipulator project, heavy type is used for power transmission between motor and gearbox.

6.2. Actuators

6.2.1. Stepper Motors

Basic structure of stepper motors are depicted in Figure 6.3. The motor shaft is rotated by means of two parts, the stator and rotor. The stator is fixed to housing of the motor while the rotor is fixed to the shaft. The rotor consists of three components: rotor1, rotor2 and the permanent magnet. Two bearings are used to place the shaft on housing of the motor. The stator and rotors have several small teeth. When the motor is excited, there is a main flux through these teeth. The stepping motors can be 2 or 5 phases. 2-phase step motor is shown in Figure 6.3.b. When phase A-A´ is firstly excited and then phase B-B´ is excited, the shaft rotates clockwise direction. The shaft rotates counterclockwise direction for reverse excitement.
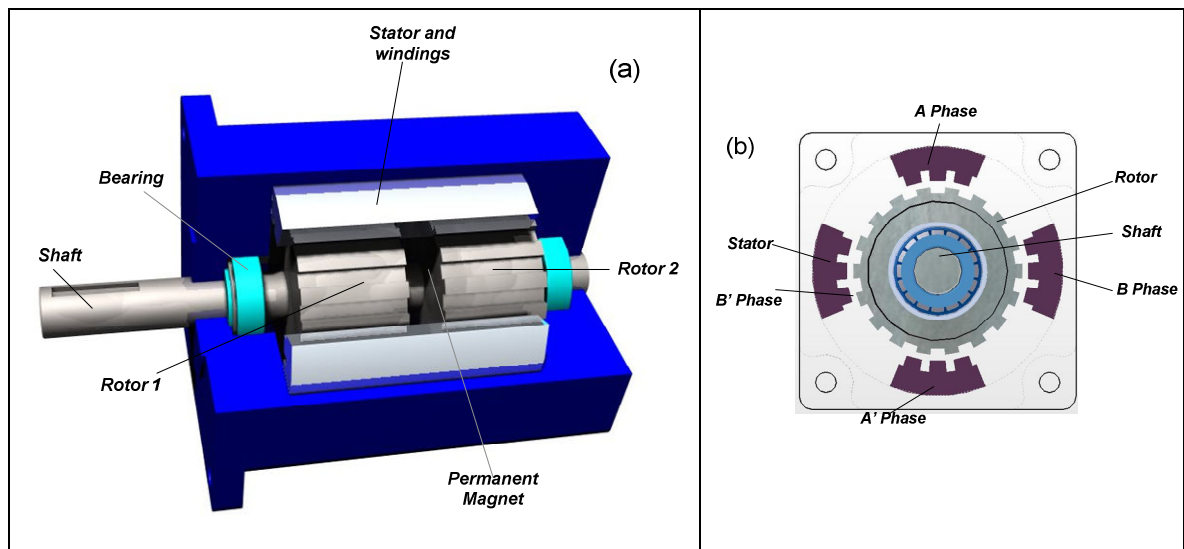
Figure 6.3. Basic structure of step motor (a) Half section parallel to shaft (b) Full section perpendicular to the shaft

A Stepper motor has a constant rotation angle for each step. Generally, these angles can be 15°, 7.5° or 1.8°. Step numbers through a full cycle of the motor shaft depend on these step angles. For instance, 24, 48 and 200 step numbers are calculated for 15°, 7.5° and 1.8° step angles, respectively. One can generalize the formulation as follows

$$N_s = \frac{360°}{\beta}$$ (6.1)

where N_s is number of step in a full cycle, β is step angle. Note that step number N_s is also named as resolution of the motor. However, the formulation should be changed, if and only if half, quarter and micro stepping techniques are used. These techniques depend on electronic construction of motor driver and its properties. Formulations for half, quarter and micro stepping techniques are given in Table 6.3.

Table 6.3. Formulations for stepping techniques

Stepping Techniques	Resolutions	Resolution Values for a 1.8° step angle motor
Normal	$N_s = \frac{360°}{\beta}$	200
Half	$N_s = 2 \cdot \frac{360°}{\beta}$	400
Quarter	$N_s = 4 \cdot \frac{360°}{\beta}$	800
Micro Stepping (250 Microstep)	$N_s = 250 \cdot \frac{360°}{\beta}$	50000

Step motors are selected for actuating due to the following features:

1. Easy rotation and velocity control: The shaft of stepping motors rotates in steps of the constant step angle. The position and velocity of the motor shaft are digitally controlled using *on* and *off* signals or in other word pulses. These signals can be obtained by a

computer or other micro processor electronics. Note that *on* signals is always +5 volt where as *off* is 0 volt.
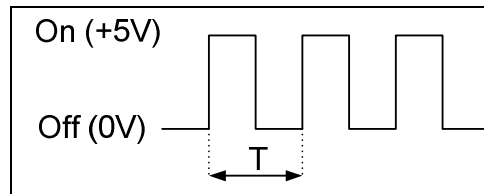
Figure 6.4. *On* and *off* signals or pulses

Figure 6.4 shows that pulses are generated by a computer or some electronics over a time. Here, T is the period of signals and it is described in seconds. Frequency of signals can be calculated as

$$f = \frac{1}{T} \qquad (6.2)$$

The rotation angle of the motor shaft is controlled by increasing or decreasing number of pulses. In Table 6.4, the angle of rotation corresponding to number of pulses is shown to illustrate control of motor.

If resolution and frequency of signals are known, angular velocity of the shaft can be calculated as

$$\omega = \frac{f}{N_s} \qquad (6.3)$$

The higher frequency of signals causes higher angular velocity of the shaft. (Table 6.5)

Table 6.4. Controlling rotation of the shaft by changing number of pulses
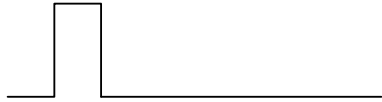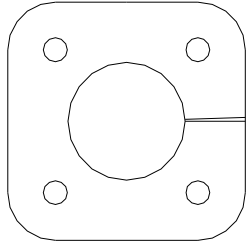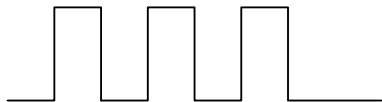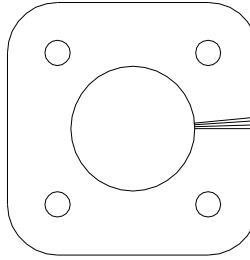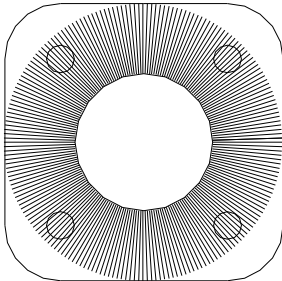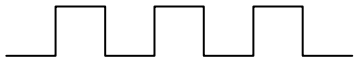
# of pulse	signals	angle of rotation	illustration of rotation of the motor shaft
1 pulse		1.8°	
3 pulses		5.4°	
200 pulses		360°	

Table 6.5.Controlling velocity of the shaft by changing frequency of pulses

f frequency	signals	angular velocity of the motor shaft
200 Hz		1 rev/s 60 rev/min
400 Hz		2 rev/s 120 rev/min
2000 Hz		10 rev/s 600 rev/min

2. <u>High Torque:</u> Stepping motors generate high torque. Therefore, the variable movement in high speed can be achieved.

3. <u>High Positioning Precision:</u> The very smooth movement is possible using micro stepping. Some companies present motor drivers enable million step resolution in a full cycle. However, the speed decreases when resolution is increased.

4. <u>Holding Torque</u>: Stepping motors hold high torque even if it is stopped. The position of the motor shaft can be preserved without a mechanical brake.

- **Characteristics of Step Motors**

Before using a stepper motor, the motor characteristics must be considered in the design stage. Two main characteristics are static and dynamic characteristics. Static characteristics relates to angular deviation when stepper motor is stopped but it is still powered on. On the other hand, dynamic characteristics relates to angular velocity and torque when the shaft of stepping motor moves.

1. **Static Characteristics**

Static Holding Torque: When motor stops but power is still supplied, motor shaft can only be loaded as much as static holding torque. This characteristic is usually given in motor catalogs. If the load on motor shaft exceeds static holding torque, this system will continue its motion towards to gravity direction. However, even if the load is smaller then static holding torque, always an angular deviation from the desired equilibrium position will be observed, no matter how small the load torque and no matter how large the motor restoring torque. Angle-Torque characteristic of a step motor is similar to curve shown in Figure 6.5. A load torque T is applied to shaft for an angle of rotation angle θ. An approximation to the static restoring and holding torque is given by the sine wave. The static positioning error is calculated as follows,

$$\theta_{error} = \frac{1}{n_t} \sin^{-1}\left(\frac{T}{T_H}\right) \tag{6.4}$$

where n_t is number of rotor teeth.
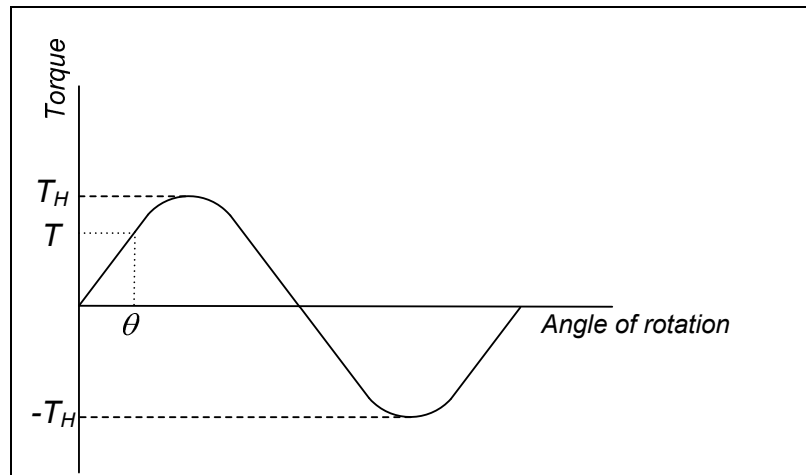
Figure 6.5. Angle-Torque characteristic

Step Angle Accuracy: Generally, the stepping motor's shaft can precisely be rotated by step angle accuracy within ± 0.05° when no-load is applied to the shaft. This very small error is a result of the mechanical precision between the stator and rotor teeth and also the electrical precision of DC resistance of the stator coil. Stopping accuracy is difference between theoretical stopping position and actual stopping position of the rotor.

2. **Dynamic Characteristics**

Speed-Torque Characteristics: The stepping motor performance is commonly measured by this characteristic. In manuals, it is also called performance curve. On the performance curve (Figure 6.6), the horizontal axis defines the variation of angular velocity as expressed in Eq. (6.3) while the vertical axis expresses torque. Noting that angular velocity changes with frequency of pulses, three numbers 1, 2 and 3 on the graph are defined as follows,

1. **Holding Torque (T_H):** The holding torque is the maximum load which can be applied to shaft when the shaft is not rotating but power is being supplied.

2. **Pullout Torque:** Pullout torque is the maximum torque that can be generated at a given angular velocity. The required torque must fall within this curve while selecting a motor.

3. **Maximum Starting Frequency:** This frequency is related to the maximum pulse speed at which the motor shaft can rotate or stop instantly when there is no external or internal load. Gradual acceleration or deceleration is necessary to drive the motor bigger than this pulse speed. The frequency decreases when there is an internal load on the motor.
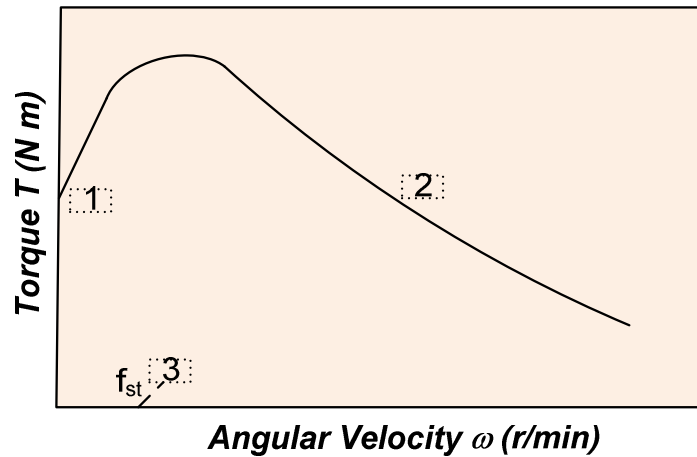
Figure 6.6. Angular Velocity- Torque Characteristics (Performance Curve)

In application part of this thesis, Powerpac Nema 42 (2 phase) step motor is selected for actuation of robot manipulator. Holding torque and performance curve of this motor are given in Figure 6.7 and Figure 6.8, respectively. Motor Code of the selected motor is N42HRFM-LNK-NS-01 and supply voltage is 75 V.
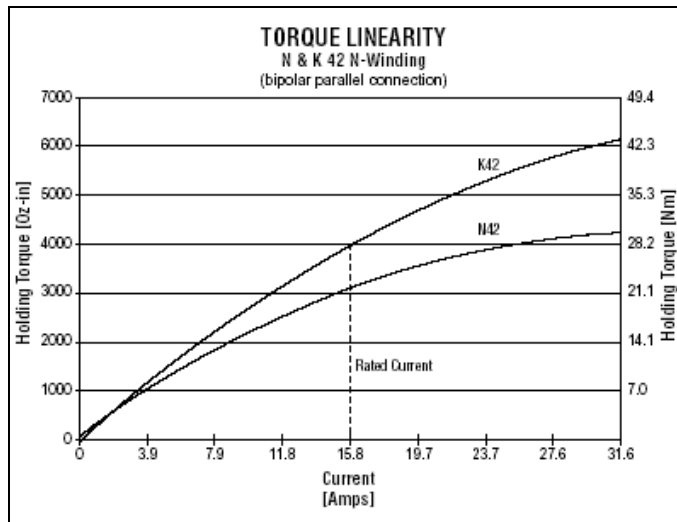
Figure 6.7. Torque Linearity- Holding Torque
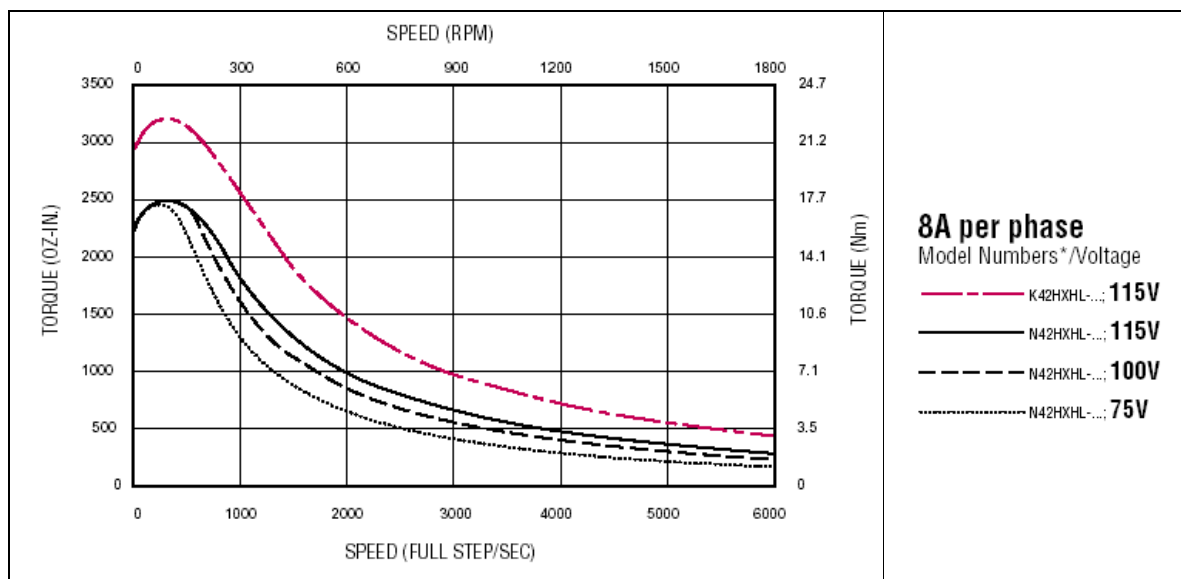
Figure 6.8. Performance curve of Powerpac Nema 42 step motor

6.2.2. Motor Driver

Considering supply voltage and current, convenient motor driver is selected from catalog. The selected motor driver is Pacific Scientific MA 6410. This driver receives step

and direction input from a controller or computer and it send necessary energy to motor winding currents. Main features include microstepping and mid-band instability compensation for high resolution and smooth operation through both the low speed and mid-band resonance regions. The output current of the driver is dip switch selectable from 5 A rms (7.1 A peak in microstep mode) to 0.625 A rms (0.88 A peak in microstep mode). The drive supplies regulated phase currents for supply voltages between 24 and 75 Vdc. It is designed for use with Pacific Scientific hybrid stepping motors.

Drive features:

- Bipolar chopper drive (reduced heat dissipation, low electric noise and improved current control during motor breaking)
- Microstepping (switch selectable: full, 1/2 , 1/4, 1/8, 1/10, 1/50, 1/12, and 1/250 step capability)
- Digital Electronic Damping
- Short circuit protection circuitry
- MOSFET power devices
- Optically isolated signal interface connection
- UL Recognized- 508C (Type R)

Typical Applications for this driver: X-Y tables and slides, packaging machinery, robotics, specialty machinery, index feed of material and labeling machines.

Numeric Controller

GOYA (Numeric Controller) can control 1, 2 or 3 axes of the types stepper, dc. or brushless, both for point to point positioning and linear and circular interpolation. It can handle machine I/O (16in/8out) either in sequential mode or as a PLC program. The I/O can be expanded up to 128 in + 128 out using Can-Bus.

Main features:

- 1, 2 or 3 axes stepper, d.c. or brushless (the third axis is for stepper motor only)
- PID control algorithm with programmable feedforward action

- Point to point positioning, linear interpolation, circular interpolation

- Programmable velocity profiles

- Encoder feedback even for stepper motors

- 16 discrete inputs and 8 discrete outputs can be handled in sequential mode or PLC logic. It is expandable to 128+ 128 via industrial Can-Bus.

- Programming language: ISO (extended) for the axes' control section, AWL on PC or the PLC section.

- Fast input for the reading of the axes' coordinates (sensor)

- Auxiliary analogue inputs (6 max.)

- Handling of "Variables" from program

- 2 incremental encoders with encoder feedback (F_{MAX}: 37 kHz on the encoder signal), possible also for stepper motors

- Control of parallel process

Overall electronic circuits and connections to PC and CNC are illustrated in Figure 6.9.
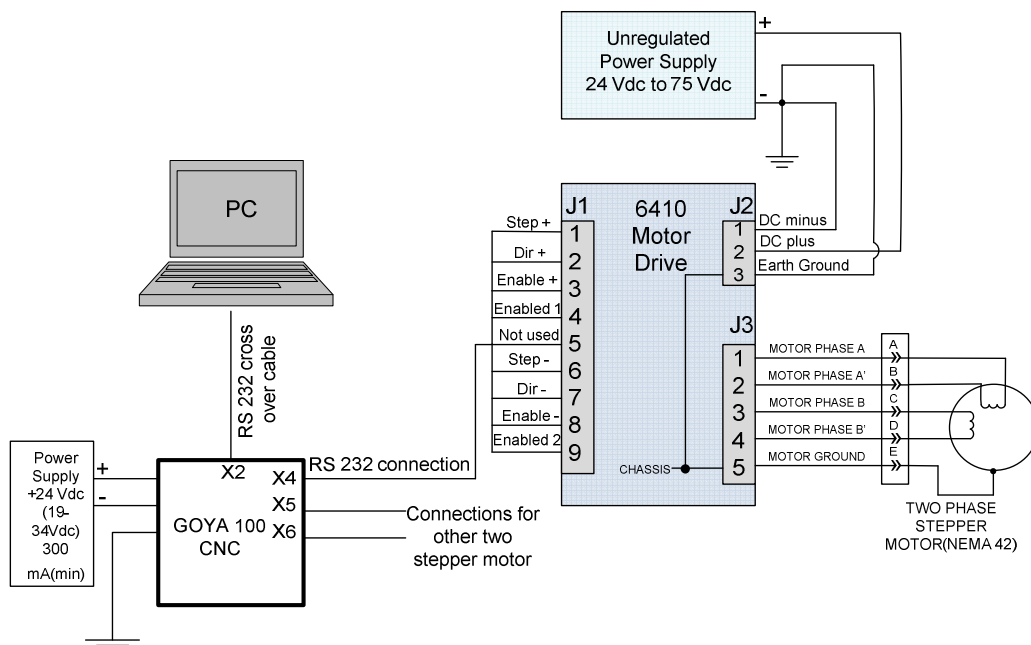
Figure 6.9. PC or CNC Control of Stepper Motor

6.3. Assembly of the parallel manipulator

A three DoF EPRM is assembled by using manufactured parts and mechanical elements. Firstly, the fixed base of the manipulator is mounted to ground by using some bolts. (Figure 6.10).   The fixed base consists of two different manufactured parts. Dimensions of these parts are shown in Figure 6.11.
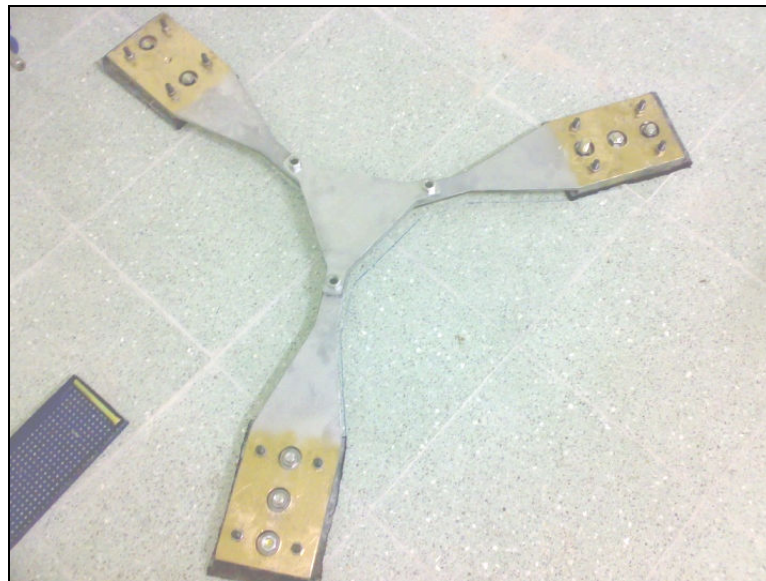
Figure 6.10. The fixed base of the manipulator
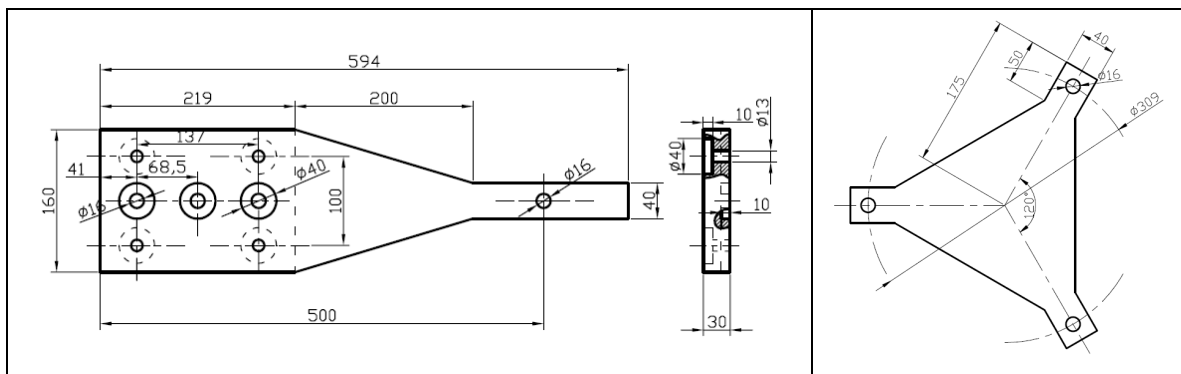
Figure 6.11. Two manufactured parts for the fixed base

127

There gearboxes are used to transmit power from step motors to parallel manipulator. Three gearboxes are prepared as shown in Figure 6.12.
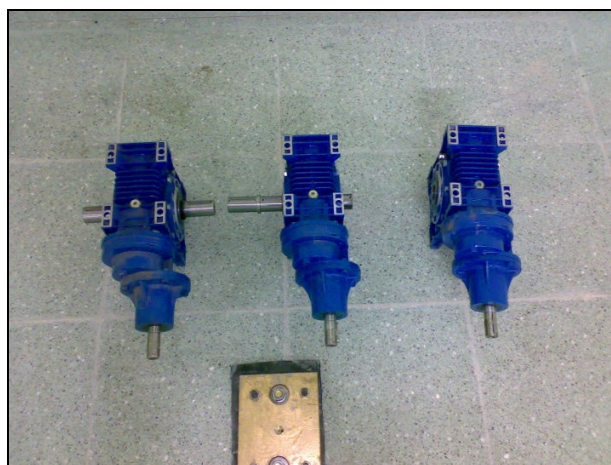
Figure 6.12. Preparation of gearboxes

Three gears boxes are mounted on the fixed base (Figure 6.13)
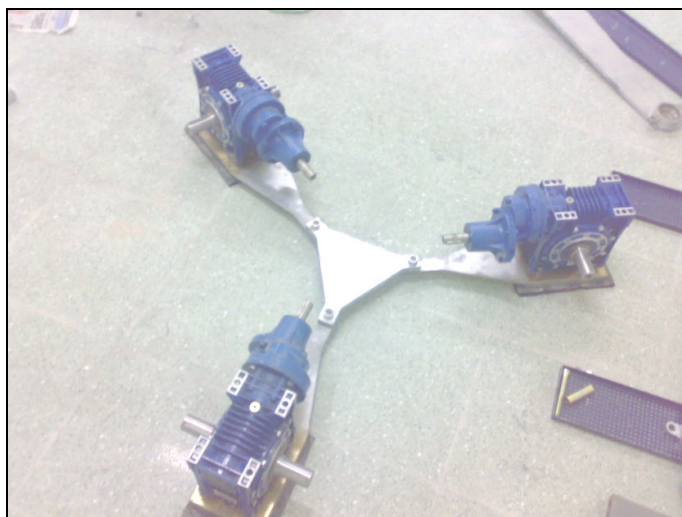
Figure 6.13. Assembly of gearboxes

Assembly of three DoF EPRM is completed by placing bearings and other manufactured links. Instead of spherical pairs, three intersected revolute joints are used. Therefore, workspace of the manipulator is increased. Kinematic analysis of this parallel manipulator is studied in Chapter 4.5. Furthermore, static force analysis of the manipulator is explained in Chapter 5.
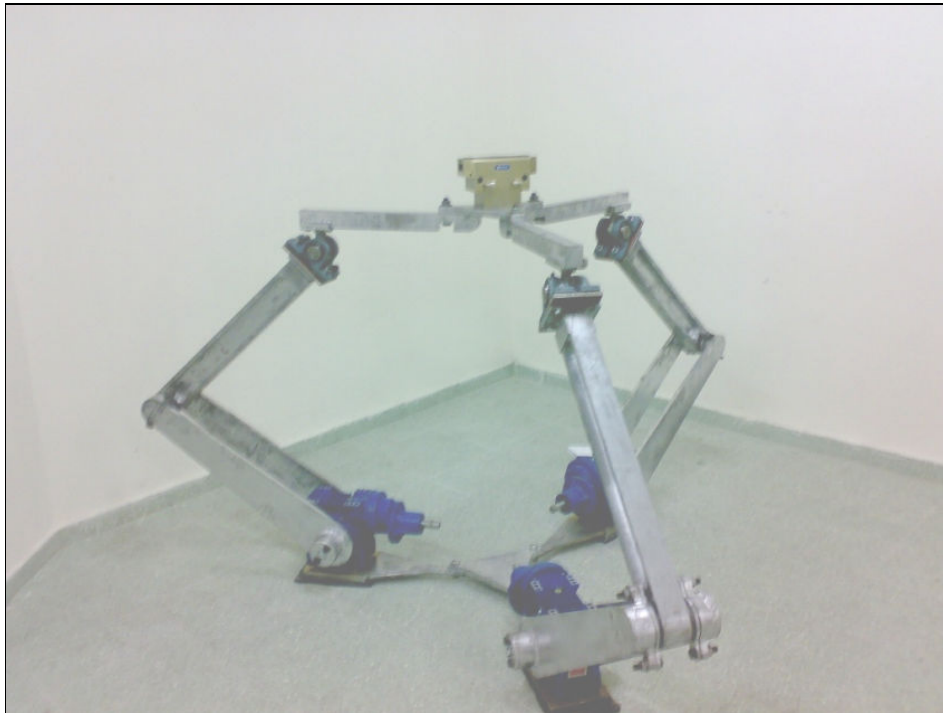
Figure 6.14. Three DoF EPRM

CHAPTER 7

CONCLUSION

This thesis includes both theoretical and practical design steps of parallel manipulators. When the parallel manipulators are designed, structural synthesis is the first problem. Therefore, new structural formulations are presented to design various new parallel Euclidean robot manipulators with variable general constraints. With respect to the new formulations new serial, parallel, and serial-parallel Euclidean platform manipulators are created and explained along with examples. Also their illustrations are presented in the tables including structural parameters, structural bondings and kinematic structures. The second problem of the design is dimensional synthesis. Dimensional synthesis of planar and spherical seven link mechanism is achieved with a new method. Furthermore, motion generation synthesis problem of a three DoF spatial parallel manipulator is solved for three, four and five poses. After the design problems, kinematic analysis of some manipulators is investigated. Moreover, constant orientation workspace of a three DoF parallel manipulator is shown. Mechanic analysis is studied to determine the actuator torque of the manipulator. Finally, construction elements, control of actuators and assembly of a parallel manipulator are explained. Future works can be ordered as:

- Further development of structural synthesis formulation for new type manipulators.
- Kinematic synthesis and analysis of serial and serial-parallel Euclidean platform robot manipulators.
- Construction of new medical and industrial robotic systems.

REFERENCES

Affi, Z., Romdhane, L. and Maalej, A., 2004. Dimensional synthesis of a 3-translational-DOF in-parallel manipulator for a desired workspace. *European Journal of Mechanics A/Solids* 23:311-324.

Alizade, R. and Bayram, Ç., 2004. Structural synthesis of parallel manipulators. *Mechanism and Machine Theory* 39:857-870.

Alizade, R., Bayram, Ç. and Gezgin, E., 2007. Structural synthesis of serial platform manipulators. *Mechanism and Machine Theory* 42:580-599.

Alizade, R., Can, F. C. and Gezgin E., 2008. Structural synthesis of Euclidean platform robot manipulators with variable general constraints. *Mechanism and Machine Theory* 43:1431-1449.

Alizade, R. I., Can, F. C., Gezgin, E. and Selvi, O., 2007. Structural Synthesis of New Parallel and Serial Platform Manipulators. 12th IFToMM World Congress, Besancon, France, June 18-21. A853.

Alizade, R. I. and Kilit, Ö., 2005. Analytical synthesis of function generating spherical four-bar mechanism for the five precision points. *Mechanism and Machine Theory* 40:863-878.

Alizade R. I., Tagiyev N. R. and Temirov A. M., 08.02.1987, Manipulator Patent N 1315290, USSR.

Alizade R. I., Tagiyev N. R. and Duffy J., 1994. A forward and reverse displacement analysis of a 6 DoF in-parallel manipulator. *Mechanism and Machine Theory* 29(1): 115-124.

Altuzarra, O., Salgado, O., Petuya, V. and Hernandez, A., 2006. Point-based Jacobian formulation for computational kinematics of manipulators. *Mechanism and Machine Theory* 41:1407-1423.

Balli, S. S. and Chand, S., 2002. Five-bar motion and path generators with variable topology for motion between extreme positions. *Mechanism and Machine Theory* 37: 1435-1445.

Balli, S. S. and Chand, S., 2003. Synthesis of a planar seven-link mechanism with variable topology for motion between two dead-center positions. *Mechanism and Machine Theory* 38:1271-1287.

Ben-Horin, R., Shoham, M. and Djerassi, S., 1998. Kinematics, dynamics and construction of a planarly actuated parallel robot. *Mechanism and Machine Theory,* 14:163-172.

Ceccarelli, M. and Vinciguerra, A., 2000. Approximate four-bar circle tracing mechanisms: classical and new synthesis. *Mechanism and Machine Theory*, 35:1579-1599.

Ceccarelli M., Fino P. M. D., Jimenez J. M., 2002. Dynamic performance of CaPaMan by numerical simulations. *Mechanism and Machine Theory* 37:241-266.

Crocesi, S. and Pennestrı`, E., 2005. Kinematic synthesis of a curve-scribing mechanism for prescribed finite motion. *Mechanism and Machine Theory* 40: 91-98.

Crossley F. R. E., 1964. A contribution to Grubler's theory in the number synthesis of plane mechanisms. *J. Eng. Ind-T ASME*, 86(01):1-8.

Cui H., Zhu Z., Gan Z. and Brogardh T., 2005. Kinematic analysis and error modeling of TAU parallel robot. *Robotics and Computer- Integrated Manufacturing* 21:497-505.

Denavit, J. and Hartenberg, R. S., 1955. A kinematic notation for lower pair mechanisms based on matrices. *Journal of Appl. Mech.* 22:215-221.

Diab, N. and Smaili, A., 2008. Optimum exact/approximate point synthesis of planar mechanisms. *Mechanism and Machine Theory* 43:1610-1624.

Fang, Y. and Huang , Z., 1996. Kinematics Of A Three-Degree-Of-Freedom In-Parallel Actuated Manipulator Mechanism. *Mechanism and Machine Theory*. 32:789–796.

Fang, Y. and Tsai, L.-W., 2002. Structure Synthesis of a Class of 4-DoF and 5-DoF Parallel Manipulators with Identical Limb Structures, *The International Journal of Robotics Research* 21:799-810.

Gatti, G., Mundo, D., 2007. Optimal synthesis of six-bar cammed-linkages for exact rigid-body guidance, *Mechanism and Machine Theory* 42:1069-1081.

Goehler, C.M., Stanisic, M.M. and Perez, V.M., 2004. A generalized parameterization of T1 motion and its application to the synthesis of planar mechanisms. *Mechanism and Machine Theory* 39:1223-1244.

Gogu, G., 2005. Mobility of mechanisms: a critical review. *Mechanism and Machine Theory* 40:1068-1097.

Gray, A., 1993. *Modern Differential Geometry of Curves and Surfaces*. CRC Press, Florida USA.

Gregorio, R. D., 2006. Analytic form solution of the forward position analysis of three-legged parallel mechanisms generating SR–PS–RS structures. *Mechanism and Machine Theory* 41:1062-1071.

Herve, J. M., 1999. The Lie group of rigid body displacements, a fundamental tool for mechanism design. *Mechanism and Machine Theory* 34:719-730.

Huang, T., M. Li, X. M. Zhao, J. P. Mei, D. G. Chetwynd, and S. J. Hu, JUNE 2005, Conceptual Design and Dimensional Synthesis for a 3-DOF Module of the TriVariant—A Novel 5-DOF Reconfigurable Hybrid Robot. *IEEE Transactions On Robotics* 21(3):449-456.

Huang Z. and Li Q. C., 2002. General Methodology for Type Synthesis of Symmetrical Lower-Mobility Parallel Manipulators and Several Novel Manipulators. *The International Journal of Robotics Research* 21:131-145.

Huang, Z., Li, S., H., Zuo, R., G., 2004. Feasible instantaneous motions and kinematic characteristics of a special 3-DOF 3-UPU parallel manipulator. *Mechanism and Machine Theory* 39: 957-970.

Husty, M. L., Pfurner, M. and Schröcker, H.-P., 2007. A new and efficient algorithm for the inverse kinematics of a general serial 6R manipulator, *Mechanism and Machine Theory*, 42:66-81.

Hwang, W. M., Hwang, Y. W., 1992. Computer-aided structural synthesis of planar kinematic chains with simple joints. *Mechanism and Machine Theory* 27(2):189-199.

Jiminéz, J. M., Alvarez, G., Cardenal, J. and Cuadrado, J., 1997. A Simple and General Method for Kinematic Synthesis of Spatial Mechanisms. *Mechanism and Machine Theory* 32:323-341.

Khalil, W. and Kleifinger, J., 1985. Nouvelles notations pour decrire la structure géometrique des robots. *Note interne* No 05/85, LAN Nantes.

Kim, H. S. and Tsai, L.-W., 2003. Kinematic Synthesis of a Spatial 3-RPS Parallel Manipulator, *Journal of Mechanical Design*, 125:92-97.

Laribi, M. A., Romdhane, L. and Zegnloul, S., 2006, Analysis and dimensional synthesis of the DELTA robot for a prescribed workspace. *Mechanism and Machine Theory* 42: 859-870.

Liu, X.-J., Wang, J. and Pritschow, G., 2005, A new family of spatial 3-DoF fully-parallel manipulators with high rotational capability. *Mechanism and Machine Theory* 40:475–494.

Liu X.-J. and Wang, J., 2003. Some New Parallel Mechanisms Containing the Planar Four-Bar Parallelogram. *The International Journal of Robotics Research* 22:717-732.

Liu, X.-J., Jinsong, W. and Pritschow, G., 2006. Kinematics, singularity and workspace of planar 5R symmetrical parallel mechanisms, *Mechanism and Machine Theory,* 41:145-169.

Manolescu, N., 1979. A unified method for the formulation of all planar joined kinematic chains and Baranov trusses. *Enviroment and Planning* B6:447-454.

Manolescu, N., 1987. Sur la structure des mécanismes en robotique. Conférence *á Í Ecole centrale d'arts et manufactures*, Paris.

Manolescu, N., Tudosie, I., Balanescu, I., Birciu, D. and Lonescu, T., 1987. Structural and kinematic synthesis of planar kinematic chain (PKC) and mechanisms (PM) with variable structure during the work. *Proc. 7 th World Congress*, *The Theory Mach. & Mech.*, Sevilia, Spain, 45-48.

Martins D. and Guenther R., 2003. Hierarchical kinematic analysis of robots. *Mechanism and Machine Theory* 38:497-518.

Merlet, J. P., 1990. *Les robots paralléles*, Hérmes, Paris.

Merlet J. P., 2006. *Parallel Robots*, Dorecht, Netherland, Springer.

Mitrouchev, P., 2001. Symbolic structural synthesis and a description method for planar kinematic chains in robotics. *European Journal of Mechanics A/Solids* 20:777-794.

Mruthyunjaya, T. S., 1979. Structural synthesis by transformation of binary chains. *Mechanism and Machine Theory* 14:221-238.

Mruthyunjaya, T. S., 1984. A computerized methodology for structural synthesis of kinematic chains: Part 1 – Formulation. *Mechanism and Machine Theory* 19(6): 487-495.

Mruthyunjaya, T. S., 1984. A computerized methodology for structural synthesis of kinematic chains: Part 2 - Application to several fully or partially known cases. *Mechanism and Machine Theory* 19(6):497-505.

Mruthyunjaya, T. S., 2003. Kinematic structure of mechanisms revisited. *Mechanism and Machine Theory*, 38:279–320.

Nie, X. and Krovi, V., 2005. Fourier Methods for Kinematic Synthesis of Coupled Serial Chain Mechanisms. *Journal of Mechanical Design* 127:232-241.

Perez, A. and McCarthy, J. M., 2003. Dimensional Synthesis of Bennett Linkages, *Journal of Mechanical Design* 125:98-104.

Press, H. W., Flannery, B. P., Teukolsky and S. A. and Vetterling, W. T., 1993. *Numerical Recipes in Fortran 77: The Art of Scientific Computing*. Cambridge University Press.

Rao, A. C., Deshmukh P. B., 2001. Computer aided structural synthesis of planar kinematic chains obviating the test for isomorphism. *Mechanism and Machine Theory* 36:489-506.

Rao, N. M. and Rao, K. M., 2006. Multi-position Dimensional Synthesis of a Spatial 3-RPS Parallel Manipulator, *Journal of Mechanical Design*, 128:815-819.

Reifschneider, L. G., 2005. Teaching Kinematic Synthesis of Linkages Without Complex Mathematics, *Journal of Industrial Technology*, 21(4):1-16.

Roth B., 1975. Performance evaluation of manipulators from a kinematic viewpoint. *NBS Special Publications*. 459:39–61.

Russell, K. and Sodhi, R. S., 2001. Kinematic synthesis of adjustable RRSS mechanisms for multi-phase motion generation. *Mechanism and Machine Theory* 36:939-952.

Sancibrian, R., Garcia, P., Viadero, F. and Fernandez, A., 2006, A general procedure based on exact gradient determination in dimensional synthesis of planar mechanisms, *Mechanism and Machine Theory*, 41:212-229.

Sheth, N. P. and Uicker, J. J., 1971, A generalized symbolic notation for mechanism, *Journal of Eng. Ind-T ASME*, 93:102-112.

Simaan N., July 1999, Analysis and Synthesis of Parallel Robots for Medical Applications. *Master Research Thesis*, Israel Institute of Technology, Hafia.

Simionescu, P. A. and Smith, M. R., 2000. Applications of Watt II function generator cognates. *Mechanism and Machine Theory*, 35:1535-1549.

Stewart, D., 1965-66, A platform with six degrees of freedom. *Proceedings of the IMechE*, 180(1.15):371-385.

Su, H.-J. and McCharty, J. M., 2005. The synthesis of an RPS serial chain to reach a given set of task positions. *Mechanism and Machine Theory* 40:757-775.

Tanev T. K, 2000. Kinematics of a hybrid (parallel-serial) robot manipulator. *Mechanism and Machine Theory* 35:1183-1196.

Tsai, K. Y. and Lin, J. C., 2006. Determining the compatible orientation workspace of Stewart–Gough parallel manipulators. Mechanism *and Machine Theory*, 41:1168-1184.

Vasiliu, A. and Yannou, B., 1997. Dimensional synthesis of planar mechanisms using neural networks: application to path generator linkages. *Mechanism and Machine Theory* 36:299-310.

Wang, J., Liu, X., Ye, P. and Duan, G. (Beijing, China), United States Patent No: 6575676.

Wang Y.-X. and Wang Y.-M., 2005. Inverse kinematics of variable geometry parallel manipulator. *Mechanism and Machine Theory* 40:141-155.

Woo L. S., 1967. Type synthesis of plane linkages. *Journal of Eng. Ind-T ASME* B-89: 159-172.

Wu, T.-M. and Chen, C.-K., 1997. Closed form synthesis of planar and spatial linkages function generation with symbolic representation. *Mathematics and Computers in Simulation* 44:155-162.

Yao, J. and Angeles, J., 2000. Computation of all optimum dyads in the approximate synthesis of planar linkages for rigid body guidance, *Mechanism and Machine Theory*, 35:1065-1078.

Zhanga, D., Wangb, L. and Esmailzadeha, E., 2006. PKM capabilities and applications exploration in a collaborative virtual environment, *Robotics and Computer-Integrated Manufacturing* 22:384-395.

Zhao, J.-S., Zhou, K. and Feng, Z.-J., 2004. A theory of degrees of freedom for mechanism. *Mechanism and Machine Theory* 39:621-643.

Zhao, J.-S., Chen M., Zhou K., Dong J.-X. and Feng Z.-J., 2006. Workspace of parallel manipulators with symmetric identical kinematic chains. *Mechanism and Machine Theory*, 41:632-645.

APPENDIX A

INVERSE OF SQUARE MATRIX IN SYNTHESIS OF SPHERICAL SEVEN LINK MECHANISM

$M_1 = (-N_{10}\ N_{14}\ N_{18} + N_9\ N_{15}\ N_{18} + N_{10}\ N_{13}\ N_{19} - N_8\ N_{15}\ N_{19} - N_9\ N_{13}\ N_{20} + N_8\ N_{14}\ N_{20}) / (N_5\ N_9\ N_{13}\ N_{17} - N_4\ N_{10}\ N_{13}\ N_{17} - N_5\ N_8\ N_{14}\ N_{17} + N_3\ N_{10}\ N_{14}\ N_{17} + N_4\ N_8\ N_{15}\ N_{17} - N_3\ N_9\ N_{15}\ N_{17} - N_5\ N_9\ N_{12}\ N_{18} + N_4\ N_{10}\ N_{12}\ N_{18} + N_5\ N_7\ N_{14}\ N_{18} - N_2\ N_{10}\ N_{14}\ N_{18} - N_4\ N_7\ N_{15}\ N_{18} + N_2\ N_9\ N_{15}\ N_{18} + N_5\ N_8\ N_{12}\ N_{19} - N_3\ N_{10}\ N_{12}\ N_{19} - N_5\ N_7\ N_{13}\ N_{19} + N_2\ N_{10}\ N_{13}\ N_{19} + N_3\ N_7\ N_{15}\ N_{19} - N_2\ N_8\ N_{15}\ N_{19} - N_4\ N_8\ N_{12}\ N_{20} + N_3\ N_9\ N_{12}\ N_{20} + N_4\ N_7\ N_{13}\ N_{20} - N_2\ N_9\ N_{13}\ N_{20} - N_3\ N_7\ N_{14}\ N_{20} + N_2\ N_8\ N_{14}\ N_{20})$

$M_2 = (N_5\ N_{14}\ N_{18} - N_4\ N_{15}\ N_{18} - N_5\ N_{13}\ N_{19} + N_3\ N_{15}\ N_{19} + N_4\ N_{13}\ N_{20} - N_3\ N_{14}\ N_{20}) / (N_5\ N_9\ N_{13}\ N_{17} - N_4\ N_{10}\ N_{13}\ N_{17} - N_5\ N_8\ N_{14}\ N_{17} + N_3\ N_{10}\ N_{14}\ N_{17} + N_4\ N_8\ N_{15}\ N_{17} - N_3\ N_9\ N_{15}\ N_{17} - N_5\ N_9\ N_{12}\ N_{18} + N_4\ N_{10}\ N_{12}\ N_{18} + N_5\ N_7\ N_{14}\ N_{18} - N_2\ N_{10}\ N_{14}\ N_{18} - N_4\ N_7\ N_{15}\ N_{18} + N_2\ N_9\ N_{15}\ N_{18} + N_5\ N_8\ N_{12}\ N_{19} - N_3\ N_{10}\ N_{12}\ N_{19} - N_5\ N_7\ N_{13}\ N_{19} + N_2\ N_{10}\ N_{13}\ N_{19} + N_3\ N_7\ N_{15}\ N_{19} - N_2\ N_8\ N_{15}\ N_{19} - N_4\ N_8\ N_{12}\ N_{20} + N_3\ N_9\ N_{12}\ N_{20} + N_4\ N_7\ N_{13}\ N_{20} - N_2\ N_9\ N_{13}\ N_{20} - N_3\ N_7\ N_{14}\ N_{20} + N_2\ N_8\ N_{14}\ N_{20})$

$M_3 = (-N_5\ N_9\ N_{18} + N_4\ N_{10}\ N_{18} + N_5\ N_8\ N_{19} - N_3\ N_{10}\ N_{19} - N_4\ N_8\ N_{20} - N_3\ N_9\ N_{20}) / (N_5\ N_9\ N_{13}\ N_{17} - N_4\ N_{10}\ N_{13}\ N_{17} - N_5\ N_8\ N_{14}\ N_{17} + N_3\ N_{10}\ N_{14}\ N_{17} + N_4\ N_8\ N_{15}\ N_{17} - N_3\ N_9\ N_{15}\ N_{17} - N_5\ N_9\ N_{12}\ N_{18} + N_4\ N_{10}\ N_{12}\ N_{18} + N_5\ N_7\ N_{14}\ N_{18} - N_2\ N_{10}\ N_{14}\ N_{18} - N_4\ N_7\ N_{15}\ N_{18} + N_2\ N_9\ N_{15}\ N_{18} + N_5\ N_8\ N_{12}\ N_{19} - N_3\ N_{10}\ N_{12}\ N_{19} - N_5\ N_7\ N_{13}\ N_{19} + N_2\ N_{10}\ N_{13}\ N_{19} + N_3\ N_7\ N_{15}\ N_{19} - N_2\ N_8\ N_{15}\ N_{19} - N_4\ N_8\ N_{12}\ N_{20} + N_3\ N_9\ N_{12}\ N_{20} + N_4\ N_7\ N_{13}\ N_{20} - N_2\ N_9\ N_{13}\ N_{20} - N_3\ N_7\ N_{14}\ N_{20} + N_2\ N_8\ N_{14}\ N_{20})$

$M_4 = (N_5\ N_9\ N_{13} - N_4\ N_{10}\ N_{13} - N_5\ N_8\ N_{14} + N_3\ N_{10}\ N_{14} + N_4\ N_8\ N_{15} - N_3\ N_9\ N_{15}) / (N_5\ N_9\ N_{13}\ N_{17} - N_4\ N_{10}\ N_{13}\ N_{17} - N_5\ N_8\ N_{14}\ N_{17} + N_3\ N_{10}\ N_{14}\ N_{17} + N_4\ N_8\ N_{15}\ N_{17} - N_3\ N_9\ N_{15}\ N_{17} - N_5\ N_9\ N_{12}\ N_{18} + N_4\ N_{10}\ N_{12}\ N_{18} + N_5\ N_7\ N_{14}\ N_{18} - N_2\ N_{10}\ N_{14}\ N_{18} - N_4\ N_7\ N_{15}\ N_{18} + N_2\ N_9\ N_{15}\ N_{18} + N_5\ N_8\ N_{12}\ N_{19} - N_3\ N_{10}\ N_{12}\ N_{19} - N_5\ N_7\ N_{13}\ N_{19} + N_2\ N_{10}\ N_{13}\ N_{19} + N_3\ N_7\ N_{15}\ N_{19} - N_2\ N_8\ N_{15}\ N_{19} - N_4\ N_8\ N_{12}\ N_{20} + N_3\ N_9\ N_{12}\ N_{20} + N_4\ N_7\ N_{13}\ N_{20} - N_2\ N_9\ N_{13}\ N_{20} - N_3\ N_7\ N_{14}\ N_{20} + N_2\ N_8\ N_{14}\ N_{20})$

$M_5 = (-N_5\ N_9\ N_{13}\ N_{16} + N_4\ N_{10}\ N_{13}\ N_{16} + N_5\ N_8\ N_{14}\ N_{16} - N_3\ N_{10}\ N_{14}\ N_{16} - N_4\ N_8\ N_{15}\ N_{16} + N_3\ N_9\ N_{15}\ N_{16} + N_5\ N_9\ N_{11}\ N_{18} - N_4\ N_{10}\ N_{11}\ N_{18} - N_5\ N_6\ N_{14}\ N_{18} + N_1\ N_{10}\ N_{14}\ N_{18} + N_4\ N_6\ N_{15}\ N_{18} - N_1\ N_9\ N_{15}\ N_{18} - N_5\ N_8\ N_{11}\ N_{19} - N_3\ N_{10}\ N_{11}\ N_{19} + N_5\ N_6\ N_{13}\ N_{19} - N_1\ N_{10}\ N_{13}\ N_{19} - N_3\ N_6\ N_{15}\ N_{19} + N_1\ N_8\ N_{15}\ N_{19} + N_4\ N_8$

$$N_{11}\ N_{20}-N_3\ N_9\ N_{11}\ N_{20}-N_4\ N_6\ N_{13}\ N_{20}+N_1\ N_9\ N_{13}\ N_{20}+N_3\ N_6\ N_{14}\ N_{20}-N_1$$
$$N_8\ N_{14}\ N_{20})\ /\ (N_5\ N_9\ N_{13}\ N_{17}-N_4\ N_{10}\ N_{13}\ N_{17}-N_5\ N_8\ N_{14}\ N_{17}+N_3\ N_{10}\ N_{14}$$
$$N_{17}+N_4\ N_8\ N_{15}\ N_{17}-N_3\ N_9\ N_{15}\ N_{17}-N_5\ N_9\ N_{12}\ N_{18}+N_4\ N_{10}\ N_{12}\ N_{18}+N_5\ N_7$$
$$N_{14}\ N_{18}-N_2\ N_{10}\ N_{14}\ N_{18}-N_4\ N_7\ N_{15}\ N_{18}+N_2\ N_9\ N_{15}\ N_{18}+N_5\ N_8\ N_{12}\ N_{19}-N_3$$
$$N_{10}\ N_{12}\ N_{19}-N_5\ N_7\ N_{13}\ N_{19}+N_2\ N_{10}\ N_{13}\ N_{19}+N_3\ N_7\ N_{15}\ N_{19}-N_2\ N_8\ N_{15}$$
$$N_{19}-N_4\ N_8\ N_{12}\ N_{20}+N_3\ N_9\ N_{12}\ N_{20}+N_4\ N_7\ N_{13}\ N_{20}-N_2\ N_9\ N_{13}\ N_{20}-N_3\ N_7$$
$$N_{14}\ N_{20}+N_2\ N_8\ N_{14}\ N_{20})$$

$$M_6=\ (N_{10}\ N_{14}\ N_{17}-N_9\ N_{15}\ N_{17}-N_{10}\ N_{12}\ N_{19}+N_7\ N_{15}\ N_{19}+N_9\ N_{12}\ N_{20}-N_7\ N_{14}$$
$$N_{20})\ /\ (N_5\ N_9\ N_{13}\ N_{17}-N_4\ N_{10}\ N_{13}\ N_{17}-N_5\ N_8\ N_{14}\ N_{17}+N_3\ N_{10}\ N_{14}\ N_{17}+N_4$$
$$N_8\ N_{15}\ N_{17}-N_3\ N_9\ N_{15}\ N_{17}-N_5\ N_9\ N_{12}\ N_{18}+N_4\ N_{10}\ N_{12}\ N_{18}+N_5\ N_7\ N_{14}$$
$$N_{18}-N_2\ N_{10}\ N_{14}\ N_{18}-N_4\ N_7\ N_{15}\ N_{18}+N_2\ N_9\ N_{15}\ N_{18}+N_5\ N_8\ N_{12}\ N_{19}-N_3\ N_{10}$$
$$N_{12}\ N_{19}-N_5\ N_7\ N_{13}\ N_{19}+N_2\ N_{10}\ N_{13}\ N_{19}+N_3\ N_7\ N_{15}\ N_{19}-N_2\ N_8\ N_{15}\ N_{19}-N_4$$
$$N_8\ N_{12}\ N_{20}+N_3\ N_9\ N_{12}\ N_{20}+N_4\ N_7\ N_{13}\ N_{20}-N_2\ N_9\ N_{13}\ N_{20}-N_3\ N_7\ N_{14}$$
$$N_{20}+N_2\ N_8\ N_{14}\ N_{20})$$

$$M_7=\ (-N_5\ N_{14}\ N_{17}+N_4\ N_{15}\ N_{17}+N_5\ N_{12}\ N_{19}-N_2\ N_{15}\ N_{19}-N_4\ N_{12}\ N_{20}+N_2\ N_{14}$$
$$N_{20})\ /\ (N_5\ N_9\ N_{13}\ N_{17}-N_4\ N_{10}\ N_{13}\ N_{17}-N_5\ N_8\ N_{14}\ N_{17}+N_3\ N_{10}\ N_{14}\ N_{17}+N_4$$
$$N_8\ N_{15}\ N_{17}-N_3\ N_9\ N_{15}\ N_{17}-N_5\ N_9\ N_{12}\ N_{18}+N_4\ N_{10}\ N_{12}\ N_{18}+N_5\ N_7\ N_{14}$$
$$N_{18}-N_2\ N_{10}\ N_{14}\ N_{18}-N_4\ N_7\ N_{15}\ N_{18}+N_2\ N_9\ N_{15}\ N_{18}+N_5\ N_8\ N_{12}\ N_{19}-N_3\ N_{10}$$
$$N_{12}\ N_{19}-N_5\ N_7\ N_{13}\ N_{19}+N_2\ N_{10}\ N_{13}\ N_{19}+N_3\ N_7\ N_{15}\ N_{19}-N_2\ N_8\ N_{15}\ N_{19}-N_4$$
$$N_8\ N_{12}\ N_{20}+N_3\ N_9\ N_{12}\ N_{20}+N_4\ N_7\ N_{13}\ N_{20}-N_2\ N_9\ N_{13}\ N_{20}-N_3\ N_7\ N_{14}$$
$$N_{20}+N_2\ N_8\ N_{14}\ N_{20})$$

$$M_8=\ (N_5\ N_9\ N_{17}-N_4\ N_{10}\ N_{17}-N_5\ N_7\ N_{19}+N_2\ N_{10}\ N_{19}+N_4\ N_{12}\ N_{20}-N_2\ N_9$$
$$N_{20})\ /\ (N_5\ N_9\ N_{13}\ N_{17}-N_4\ N_{10}\ N_{13}\ N_{17}-N_5\ N_8\ N_{14}\ N_{17}+N_3\ N_{10}\ N_{14}\ N_{17}+N_4$$
$$N_8\ N_{15}\ N_{17}-N_3\ N_9\ N_{15}\ N_{17}-N_5\ N_9\ N_{12}\ N_{18}+N_4\ N_{10}\ N_{12}\ N_{18}+N_5\ N_7\ N_{14}$$
$$N_{18}-N_2\ N_{10}\ N_{14}\ N_{18}-N_4\ N_7\ N_{15}\ N_{18}+N_2\ N_9\ N_{15}\ N_{18}+N_5\ N_8\ N_{12}\ N_{19}-N_3\ N_{10}$$
$$N_{12}\ N_{19}-N_5\ N_7\ N_{13}\ N_{19}+N_2\ N_{10}\ N_{13}\ N_{19}+N_3\ N_7\ N_{15}\ N_{19}-N_2\ N_8\ N_{15}\ N_{19}-N_4$$
$$N_8\ N_{12}\ N_{20}+N_3\ N_9\ N_{12}\ N_{20}+N_4\ N_7\ N_{13}\ N_{20}-N_2\ N_9\ N_{13}\ N_{20}-N_3\ N_7\ N_{14}$$
$$N_{20}+N_2\ N_8\ N_{14}\ N_{20})$$

$$M_9=\ (-N_5\ N_9\ N_{12}+N_4\ N_{10}\ N_{12}+N_5\ N_7\ N_{14}-N_2\ N_{10}\ N_{14}-N_4\ N_7\ N_{15}+N_2\ N_9$$
$$N_{15})\ /\ (N_5\ N_9\ N_{13}\ N_{17}-N_4\ N_{10}\ N_{13}\ N_{17}-N_5\ N_8\ N_{14}\ N_{17}+N_3\ N_{10}\ N_{14}\ N_{17}+N_4$$
$$N_8\ N_{15}\ N_{17}-N_3\ N_9\ N_{15}\ N_{17}-N_5\ N_9\ N_{12}\ N_{18}+N_4\ N_{10}\ N_{12}\ N_{18}+N_5\ N_7\ N_{14}$$
$$N_{18}-N_2\ N_{10}\ N_{14}\ N_{18}-N_4\ N_7\ N_{15}\ N_{18}+N_2\ N_9\ N_{15}\ N_{18}+N_5\ N_8\ N_{12}\ N_{19}-N_3\ N_{10}$$
$$N_{12}\ N_{19}-N_5\ N_7\ N_{13}\ N_{19}+N_2\ N_{10}\ N_{13}\ N_{19}+N_3\ N_7\ N_{15}\ N_{19}-N_2\ N_8\ N_{15}\ N_{19}-N_4$$
$$N_8\ N_{12}\ N_{20}+N_3\ N_9\ N_{12}\ N_{20}+N_4\ N_7\ N_{13}\ N_{20}-N_2\ N_9\ N_{13}\ N_{20}-N_3\ N_7\ N_{14}$$
$$N_{20}+N_2\ N_8\ N_{14}\ N_{20})$$

$$M_{10}=\ (N_5\ N_9\ N_{12}\ N_{16}-N_4\ N_{10}\ N_{12}\ N_{16}-N_5\ N_7\ N_{14}\ N_{16}+N_2\ N_{10}\ N_{14}\ N_{16}+N_4\ N_7$$
$$N_{15}\ N_{16}-N_2\ N_9\ N_{15}\ N_{16}-N_5\ N_9\ N_{11}\ N_{17}+N_4\ N_{10}\ N_{11}\ N_{17}+N_5\ N_6\ N_{14}\ N_{17}-N_1$$
$$N_{10}\ N_{14}\ N_{17}-N_4\ N_6\ N_{15}\ N_{17}+N_1\ N_9\ N_{15}\ N_{17}+N_5\ N_7\ N_{11}\ N_{19}-N_2\ N_{10}\ N_{11}$$
$$N_{19}-N_5\ N_6\ N_{12}\ N_{19}+N_1\ N_{10}\ N_{12}\ N_{19}+N_2\ N_6\ N_{15}\ N_{19}-N_1\ N_7\ N_{15}\ N_{19}-N_4\ N_7$$
$$N_{11}\ N_{20}+N_2\ N_9\ N_{11}\ N_{20}+N_4\ N_6\ N_{12}\ N_{20}-N_1\ N_9\ N_{12}\ N_{20}-N_2\ N_6\ N_{14}\ N_{20}+N_1$$
$$N_7\ N_{14}\ N_{20})\ /\ (N_5\ N_9\ N_{13}\ N_{17}-N_4\ N_{10}\ N_{13}\ N_{17}-N_5\ N_8\ N_{14}\ N_{17}+N_3\ N_{10}\ N_{14}$$

$N_{17}+N_4$ N_8 N_{15} $N_{17}-N_3$ N_9 N_{15} $N_{17}-N_5$ N_9 N_{12} $N_{18}+N_4$ N_{10} N_{12} $N_{18}+N_5$ N_7 N_{14} $N_{18}-N_2$ N_{10} N_{14} $N_{18}-N_4$ N_7 N_{15} $N_{18}+N_2$ N_9 N_{15} $N_{18}+N_5$ N_8 N_{12} $N_{19}-N_3$ N_{10} N_{12} $N_{19}-N_5$ N_7 N_{13} $N_{19}+N_2$ N_{10} N_{13} $N_{19}+N_3$ N_7 N_{15} $N_{19}-N_2$ N_8 N_{15} $N_{19}-N_4$ N_8 N_{12} $N_{20}+N_3$ N_9 N_{12} $N_{20}+N_4$ N_7 N_{13} $N_{20}-N_2$ N_9 N_{13} $N_{20}-N_3$ N_7 N_{14} $N_{20}+N_2$ N_8 N_{14} N_{20})

$M_{11}=$ $(-N_{10}$ N_{13} $N_{17}+N_8$ N_{15} $N_{17}+N_{10}$ N_{12} $N_{18}-N_7$ N_{15} $N_{18}-N_8$ N_{12} $N_{20}+N_7$ N_{13} $N_{20})/(N_5$ N_9 N_{13} $N_{17}-N_4$ N_{10} N_{13} $N_{17}-N_5$ N_8 N_{14} $N_{17}+N_3$ N_{10} N_{14} $N_{17}+N_4$ N_8 N_{15} $N_{17}-N_3$ N_9 N_{15} $N_{17}-N_5$ N_9 N_{12} $N_{18}+N_4$ N_{10} N_{12} $N_{18}+N_5$ N_7 N_{14} $N_{18}-N_2$ N_{10} N_{14} $N_{18}-N_4$ N_7 N_{15} $N_{18}+N_2$ N_9 N_{15} $N_{18}+N_5$ N_8 N_{12} $N_{19}-N_3$ N_{10} N_{12} $N_{19}-N_5$ N_7 N_{13} $N_{19}+N_2$ N_{10} N_{13} $N_{19}+N_3$ N_7 N_{15} $N_{19}-N_2$ N_8 N_{15} $N_{19}-N_4$ N_8 N_{12} $N_{20}+N_3$ N_9 N_{12} $N_{20}+N_4$ N_7 N_{13} $N_{20}-N_2$ N_9 N_{13} $N_{20}-N_3$ N_7 N_{14} $N_{20}+N_2$ N_8 N_{14} $N_{20})$

$M_{12}=$ $(N_5$ N_{13} $N_{17}-N_3$ N_{15} $N_{17}-N_5$ N_{12} $N_{18}+N_2$ N_{15} $N_{18}+N_3$ N_{12} $N_{20}-N_2$ N_{13} $N_{20})/(N_5$ N_9 N_{13} $N_{17}-N_4$ N_{10} N_{13} $N_{17}-N_5$ N_8 N_{14} $N_{17}+N_3$ N_{10} N_{14} $N_{17}+N_4$ N_8 N_{15} $N_{17}-N_3$ N_9 N_{15} $N_{17}-N_5$ N_9 N_{12} $N_{18}+N_4$ N_{10} N_{12} $N_{18}+N_5$ N_7 N_{14} $N_{18}-N_2$ N_{10} N_{14} $N_{18}-N_4$ N_7 N_{15} $N_{18}+N_2$ N_9 N_{15} $N_{18}+N_5$ N_8 N_{12} $N_{19}-N_3$ N_{10} N_{12} $N_{19}-N_5$ N_7 N_{13} $N_{19}+N_2$ N_{10} N_{13} $N_{19}+N_3$ N_7 N_{15} $N_{19}-N_2$ N_8 N_{15} $N_{19}-N_4$ N_8 N_{12} $N_{20}+N_3$ N_9 N_{12} $N_{20}+N_4$ N_7 N_{13} $N_{20}-N_2$ N_9 N_{13} $N_{20}-N_3$ N_7 N_{14} $N_{20}+N_2$ N_8 N_{14} $N_{20})$

$M_{13}=$ $(-N_5$ N_8 $N_{17}+N_3$ N_{10} $N_{17}+N_5$ N_7 $N_{18}-N_2$ N_{10} $N_{18}-N_3$ N_7 $N_{20}-N_2$ N_8 $N_{20})/(N_5$ N_9 N_{13} $N_{17}-N_4$ N_{10} N_{13} $N_{17}-N_5$ N_8 N_{14} $N_{17}+N_3$ N_{10} N_{14} $N_{17}+N_4$ N_8 N_{15} $N_{17}-N_3$ N_9 N_{15} $N_{17}-N_5$ N_9 N_{12} $N_{18}+N_4$ N_{10} N_{12} $N_{18}+N_5$ N_7 N_{14} $N_{18}-N_2$ N_{10} N_{14} $N_{18}-N_4$ N_7 N_{15} $N_{18}+N_2$ N_9 N_{15} $N_{18}+N_5$ N_8 N_{12} $N_{19}-N_3$ N_{10} N_{12} $N_{19}-N_5$ N_7 N_{13} $N_{19}+N_2$ N_{10} N_{13} $N_{19}+N_3$ N_7 N_{15} $N_{19}-N_2$ N_8 N_{15} $N_{19}-N_4$ N_8 N_{12} $N_{20}+N_3$ N_9 N_{12} $N_{20}+N_4$ N_7 N_{13} $N_{20}-N_2$ N_9 N_{13} $N_{20}-N_3$ N_7 N_{14} $N_{20}+N_2$ N_8 N_{14} $N_{20})$

$M_{14}=$ $(N_5$ N_8 $N_{12}-N_3$ N_{10} $N_{12}-N_5$ N_7 $N_{13}+N_2$ N_{10} $N_{13}+N_3$ N_7 $N_{15}-N_2$ N_8 $N_{15})/(N_5$ N_9 N_{13} $N_{17}-N_4$ N_{10} N_{13} $N_{17}-N_5$ N_8 N_{14} $N_{17}+N_3$ N_{10} N_{14} $N_{17}+N_4$ N_8 N_{15} $N_{17}-N_3$ N_9 N_{15} $N_{17}-N_5$ N_9 N_{12} $N_{18}+N_4$ N_{10} N_{12} $N_{18}+N_5$ N_7 N_{14} $N_{18}-N_2$ N_{10} N_{14} $N_{18}-N_4$ N_7 N_{15} $N_{18}+N_2$ N_9 N_{15} $N_{18}+N_5$ N_8 N_{12} $N_{19}-N_3$ N_{10} N_{12} $N_{19}-N_5$ N_7 N_{13} $N_{19}+N_2$ N_{10} N_{13} $N_{19}+N_3$ N_7 N_{15} $N_{19}-N_2$ N_8 N_{15} $N_{19}-N_4$ N_8 N_{12} $N_{20}+N_3$ N_9 N_{12} $N_{20}+N_4$ N_7 N_{13} $N_{20}-N_2$ N_9 N_{13} $N_{20}-N_3$ N_7 N_{14} $N_{20}+N_2$ N_8 N_{14} $N_{20})$

$M_{15}=$ $(-N_5$ N_8 N_{12} $N_{16}+N_3$ N_{10} N_{12} $N_{16}+N_5$ N_7 N_{13} $N_{16}-N_2$ N_{10} N_{13} $N_{16}-N_3$ N_7 N_{15} $N_{16}+N_2$ N_8 N_{15} $N_{16}+N_5$ N_8 N_{11} $N_{17}-N_3$ N_{10} N_{11} $N_{17}-N_5$ N_6 N_{13} $N_{17}+N_1$ N_{10} N_{13} $N_{17}+N_3$ N_6 N_{15} $N_{17}-N_1$ N_8 N_{15} $N_{17}-N_5$ N_7 N_{11} $N_{18}+N_2$ N_{10} N_{11} $N_{18}+N_5$ N_6 N_{12} $N_{18}-N_1$ N_{10} N_{12} $N_{18}-N_2$ N_6 N_{15} $N_{18}+N_1$ N_7 N_{15} $N_{18}+N_3$ N_7 N_{11} $N_{20}-N_2$ N_8 N_{11} $N_{20}-N_3$ N_6 N_{12} $N_{20}+N_1$ N_8 N_{12} $N_{20}+N_2$ N_6 N_{13} $N_{20}-N_1$ N_7 N_{13} $N_{20})/(N_5$ N_9 N_{13} $N_{17}-N_4$ N_{10} N_{13} $N_{17}-N_5$ N_8 N_{14} $N_{17}+N_3$ N_{10} N_{14} $N_{17}+N_4$ N_8 N_{15} $N_{17}-N_3$ N_9 N_{15} $N_{17}-N_5$ N_9 N_{12} $N_{18}+N_4$ N_{10} N_{12} $N_{18}+N_5$ N_7 N_{14} $N_{18}-N_2$ N_{10} N_{14} $N_{18}-N_4$ N_7 N_{15} $N_{18}+N_2$ N_9 N_{15} $N_{18}+N_5$ N_8 N_{12} $N_{19}-N_3$ N_{10} N_{12} $N_{19}-N_5$ N_7 N_{13} $N_{19}+N_2$ N_{10} N_{13} $N_{19}+N_3$ N_7 N_{15} $N_{19}-N_2$ N_8 N_{15}

$N_{19} - N_4 \ N_8 \ N_{12} \ N_{20} + N_3 \ N_9 \ N_{12} \ N_{20} + N_4 \ N_7 \ N_{13} \ N_{20} - N_2 \ N_9 \ N_{13} \ N_{20} - N_3 \ N_7$
$N_{14} \ N_{20} + N_2 \ N_8 \ N_{14} \ N_{20})$

$M_{16} = \ (N_9 \ N_{13} \ N_{17} - N_8 \ N_{14} \ N_{17} - N_9 \ N_{12} \ N_{18} + N_7 \ N_{14} \ N_{18} + N_8 \ N_{12} \ N_{19} - N_7 \ N_{13}$
$N_{19}) \ / \ (N_5 \ N_9 \ N_{13} \ N_{17} - N_4 \ N_{10} \ N_{13} \ N_{17} - N_5 \ N_8 \ N_{14} \ N_{17} + N_3 \ N_{10} \ N_{14} \ N_{17} + N_4$
$N_8 \ N_{15} \ N_{17} - N_3 \ N_9 \ N_{15} \ N_{17} - N_5 \ N_9 \ N_{12} \ N_{18} + N_4 \ N_{10} \ N_{12} \ N_{18} + N_5 \ N_7 \ N_{14}$
$N_{18} - N_2 \ N_{10} \ N_{14} \ N_{18} - N_4 \ N_7 \ N_{15} \ N_{18} + N_2 \ N_9 \ N_{15} \ N_{18} + N_5 \ N_8 \ N_{12} \ N_{19} - N_3 \ N_{10}$
$N_{12} \ N_{19} - N_5 \ N_7 \ N_{13} \ N_{19} + N_2 \ N_{10} \ N_{13} \ N_{19} + N_3 \ N_7 \ N_{15} \ N_{19} - N_2 \ N_8 \ N_{15} \ N_{19} - N_4$
$N_8 \ N_{12} \ N_{20} + N_3 \ N_9 \ N_{12} \ N_{20} + N_4 \ N_7 \ N_{13} \ N_{20} - N_2 \ N_9 \ N_{13} \ N_{20} - N_3 \ N_7 \ N_{14}$
$N_{20} + N_2 \ N_8 \ N_{14} \ N_{20})$

$M_{17} = \ (-N_4 \ N_{13} \ N_{17} + N_3 \ N_{14} \ N_{17} + N_4 \ N_{12} \ N_{18} - N_2 \ N_{14} \ N_{18} - N_3 \ N_{12} \ N_{19} + N_2 \ N_{13}$
$N_{19}) \ / \ (N_5 \ N_9 \ N_{13} \ N_{17} - N_4 \ N_{10} \ N_{13} \ N_{17} - N_5 \ N_8 \ N_{14} \ N_{17} + N_3 \ N_{10} \ N_{14} \ N_{17} + N_4$
$N_8 \ N_{15} \ N_{17} - N_3 \ N_9 \ N_{15} \ N_{17} - N_5 \ N_9 \ N_{12} \ N_{18} + N_4 \ N_{10} \ N_{12} \ N_{18} + N_5 \ N_7 \ N_{14}$
$N_{18} - N_2 \ N_{10} \ N_{14} \ N_{18} - N_4 \ N_7 \ N_{15} \ N_{18} + N_2 \ N_9 \ N_{15} \ N_{18} + N_5 \ N_8 \ N_{12} \ N_{19} - N_3 \ N_{10}$
$N_{12} \ N_{19} - N_5 \ N_7 \ N_{13} \ N_{19} + N_2 \ N_{10} \ N_{13} \ N_{19} + N_3 \ N_7 \ N_{15} \ N_{19} - N_2 \ N_8 \ N_{15} \ N_{19} - N_4$
$N_8 \ N_{12} \ N_{20} + N_3 \ N_9 \ N_{12} \ N_{20} + N_4 \ N_7 \ N_{13} \ N_{20} - N_2 \ N_9 \ N_{13} \ N_{20} - N_3 \ N_7 \ N_{14}$
$N_{20} + N_2 \ N_8 \ N_{14} \ N_{20})$

$M_{18} = \ (N_4 \ N_8 \ N_{17} - N_3 \ N_9 \ N_{17} - N_4 \ N_7 \ N_{18} + N_2 \ N_9 \ N_{18} + N_3 \ N_7 \ N_{19} - N_2 \ N_8 \ N_{19}) \ / \ (N_5$
$N_9 \ N_{13} \ N_{17} - N_4 \ N_{10} \ N_{13} \ N_{17} - N_5 \ N_8 \ N_{14} \ N_{17} + N_3 \ N_{10} \ N_{14} \ N_{17} + N_4 \ N_8 \ N_{15}$
$N_{17} - N_3 \ N_9 \ N_{15} \ N_{17} - N_5 \ N_9 \ N_{12} \ N_{18} + N_4 \ N_{10} \ N_{12} \ N_{18} + N_5 \ N_7 \ N_{14} \ N_{18} - N_2 \ N_{10}$
$N_{14} \ N_{18} - N_4 \ N_7 \ N_{15} \ N_{18} + N_2 \ N_9 \ N_{15} \ N_{18} + N_5 \ N_8 \ N_{12} \ N_{19} - N_3 \ N_{10} \ N_{12} \ N_{19} - N_5$
$N_7 \ N_{13} \ N_{19} + N_2 \ N_{10} \ N_{13} \ N_{19} + N_3 \ N_7 \ N_{15} \ N_{19} - N_2 \ N_8 \ N_{15} \ N_{19} - N_4 \ N_8 \ N_{12}$
$N_{20} + N_3 \ N_9 \ N_{12} \ N_{20} + N_4 \ N_7 \ N_{13} \ N_{20} - N_2 \ N_9 \ N_{13} \ N_{20} - N_3 \ N_7 \ N_{14} \ N_{20} + N_2 \ N_8$
$N_{14} \ N_{20})$

$M_{19} = \ (-N_4 \ N_8 \ N_{12} + N_3 \ N_9 \ N_{12} + N_4 \ N_7 \ N_{13} - N_2 \ N_9 \ N_{13} - N_3 \ N_7 \ N_{14} + N_2 \ N_8$
$N_{14}) \ / \ (N_5 \ N_9 \ N_{13} \ N_{17} - N_4 \ N_{10} \ N_{13} \ N_{17} - N_5 \ N_8 \ N_{14} \ N_{17} + N_3 \ N_{10} \ N_{14} \ N_{17} + N_4$
$N_8 \ N_{15} \ N_{17} - N_3 \ N_9 \ N_{15} \ N_{17} - N_5 \ N_9 \ N_{12} \ N_{18} + N_4 \ N_{10} \ N_{12} \ N_{18} + N_5 \ N_7 \ N_{14}$
$N_{18} - N_2 \ N_{10} \ N_{14} \ N_{18} - N_4 \ N_7 \ N_{15} \ N_{18} + N_2 \ N_9 \ N_{15} \ N_{18} + N_5 \ N_8 \ N_{12} \ N_{19} - N_3 \ N_{10}$
$N_{12} \ N_{19} - N_5 \ N_7 \ N_{13} \ N_{19} + N_2 \ N_{10} \ N_{13} \ N_{19} + N_3 \ N_7 \ N_{15} \ N_{19} - N_2 \ N_8 \ N_{15} \ N_{19} - N_4$
$N_8 \ N_{12} \ N_{20} + N_3 \ N_9 \ N_{12} \ N_{20} + N_4 \ N_7 \ N_{13} \ N_{20} - N_2 \ N_9 \ N_{13} \ N_{20} - N_3 \ N_7 \ N_{14}$
$N_{20} + N_2 \ N_8 \ N_{14} \ N_{20})$

$M_{20} = \ (N_4 \ N_8 \ N_{12} \ N_{16} - N_3 \ N_9 \ N_{12} \ N_{16} - N_4 \ N_7 \ N_{13} \ N_{16} + N_2 \ N_9 \ N_{13} \ N_{16} + N_3 \ N_7 \ N_{14}$
$N_{16} - N_2 \ N_8 \ N_{14} \ N_{16} - N_4 \ N_8 \ N_{11} \ N_{17} + N_3 \ N_9 \ N_{11} \ N_{17} + N_4 \ N_6 \ N_{13} \ N_{17} - N_1 \ N_9$
$N_{13} \ N_{17} - N_3 \ N_6 \ N_{14} \ N_{17} + N_1 \ N_8 \ N_{14} \ N_{17} + N_4 \ N_7 \ N_{11} \ N_{18} - N_2 \ N_9 \ N_{11} \ N_{18} - N_4$
$N_6 \ N_{12} \ N_{18} + N_1 \ N_9 \ N_{12} \ N_{18} + N_2 \ N_6 \ N_{14} \ N_{18} - N_1 \ N_7 \ N_{14} \ N_{18} - N_3 \ N_7 \ N_{11}$
$N_{19} + N_2 \ N_8 \ N_{11} \ N_{19} + N_3 \ N_6 \ N_{12} \ N_{19} - N_1 \ N_8 \ N_{12} \ N_{19} - N_2 \ N_6 \ N_{13} \ N_{19} + N_1 \ N_7$
$N_{13} \ N_{19}) \ / \ (N_5 \ N_9 \ N_{13} \ N_{17} - N_4 \ N_{10} \ N_{13} \ N_{17} - N_5 \ N_8 \ N_{14} \ N_{17} + N_3 \ N_{10} \ N_{14}$
$N_{17} + N_4 \ N_8 \ N_{15} \ N_{17} - N_3 \ N_9 \ N_{15} \ N_{17} - N_5 \ N_9 \ N_{12} \ N_{18} + N_4 \ N_{10} \ N_{12} \ N_{18} + N_5 \ N_7$
$N_{14} \ N_{18} - N_2 \ N_{10} \ N_{14} \ N_{18} - N_4 \ N_7 \ N_{15} \ N_{18} + N_2 \ N_9 \ N_{15} \ N_{18} + N_5 \ N_8 \ N_{12} \ N_{19} - N_3$
$N_{10} \ N_{12} \ N_{19} - N_5 \ N_7 \ N_{13} \ N_{19} + N_2 \ N_{10} \ N_{13} \ N_{19} + N_3 \ N_7 \ N_{15} \ N_{19} - N_2 \ N_8 \ N_{15}$
$N_{19} - N_4 \ N_8 \ N_{12} \ N_{20} + N_3 \ N_9 \ N_{12} \ N_{20} + N_4 \ N_7 \ N_{13} \ N_{20} - N_2 \ N_9 \ N_{13} \ N_{20} - N_3 \ N_7$
$N_{14} \ N_{20} + N_2 \ N_8 \ N_{14} \ N_{20}).$

CURRICULUM VITAE

Fatih Cemal Can was born in Denizli, on 10 November, 1977. He attended Pamukkale University from 1994 to 1998, and graduated with a Bachelor of Science degree in 1998. He began graduate studies in Mechanical Engineering Department of Middle East Technical University, in the fall of 2000. He pursued his research in Inertial Parameter Design of Spatial Mechanism under the direction of Professor Resit Soylu and received the Master of Science degree from the Middle East Technical University in 2003. Spring of 2004, he settled in İzmir and began doctoral studies in Mechanical Engineering Department of İzmir Institute of Technology. He presented his scientific investigations to PhD thesis committee five times during his research period. He continued his research with Analysis and Synthesis of Parallel Manipulators under the direction of Professor Rasim Alizade. During his research, he and his collogues published one journal paper whose title is "Structural synthesis of Euclidean platform robot manipulators with variable general constraints" presented to Mechanism and Machine Theory Journal (Science Citation Index). His other journal publication is "Forward and Inverse Kinematics of Serial Planar Manipulators by Using Quaternion Algebra" presented to Problems of Mechanics. He participated in 12 th IFToMM World Congress, Besancon, France, 2007, with the paper titled "Structural Synthesis of New Parallel and Serial Platform Manipulators". He also participated in International Conference on Artificial Intelligence (Emergent Research), Las Vegas, Nevada, USA, 2006, with the paper titled "Characterization of Swarm Behavior through Pair-Wise Interactions by Tsallis Entropy".